

**BIODIESEL PRODUCTION VIA
TRANSESTERIFICATION OF JATROPHA SEED OIL
USING POTASSIUM SUPPORTED ON NaY ZEOLITE
AND MCM-41 AS CATALYSTS**



Nuttinee Supamathanon

**A Thesis Submitted in Partial Fulfillment of the Requirements for the
Degree of Doctor of Philosophy in Chemistry
Suranaree University of Technology
Academic Year 2011**

การผลิตไบโอดีเซลด้วยปฏิกิริยาทรานส์เอสเทอริฟิเคชันของน้ำมันเมล็ดสบู่ดำ
โดยใช้โพแทสเซียมบนตัวรองรับซีโอไลต์วายเป็นรูปของโซเดียม
และบน MCM-41 เป็นตัวเร่งปฏิกิริยา

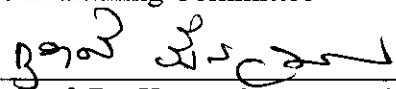


วิทยานิพนธ์นี้เป็นส่วนหนึ่งของการศึกษาตามหลักสูตรปริญญาวิทยาศาสตรดุษฎีบัณฑิต
สาขาวิชาเคมี
มหาวิทยาลัยเทคโนโลยีสุรนารี
ปีการศึกษา 2554

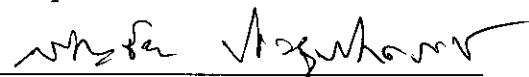
**BIODIESEL PRODUCTION VIA TRANSESTERIFICATION OF
JATROPHA SEED OIL USING POTASSIUM SUPPORTED
ON NaY ZEOLITE AND MCM-41 AS CATALYSTS**

Suranaree University of Technology has approved this thesis submitted in partial fulfillment of the requirements for the Degree of Doctor of Philosophy.

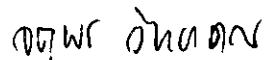
Thesis Examining Committee


(Asst. Prof. Dr. Kunwadee Rangriwatananon)

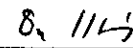
Chairperson


(Asst. Prof. Dr. Sanchai Prayoonpokarach)

Member (Thesis Advisor)


(Assoc. Prof. Dr. Jatuporn Wittayakun)

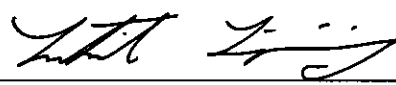
Member


(Asst. Prof. Dr. Thanaporn Manyum)

Member


(Asst. Prof. Dr. Chaiwat Raksakulpiwat)

Member


(Prof. Dr. Sukit Limpijumnong)

Vice Rector for Academic Affairs


(Assoc. Prof. Dr. Prapun Manyum)

Dean of Institute of Science

ณัฐฉิณี สุขเมธานนท์ : การผลิตไบโอดีเซลด้วยปฏิกิริยาทรานส์เอสเทอร์ฟิเคชันของน้ำมัน
เมล็ดสบู่ดำโดยใช้โพแทสเซียมบนตัวรองรับซีโอไลต์ด้วยในรูปของโซเดียมและบน
MCM-41 เป็นตัวเร่งปฏิกิริยา (BIODIESEL PRODUCTION VIA
TRANSESTERIFICATION OF JATROPHA SEED OIL USING POTASSIUM
SUPPORTED ON NaY ZEOLITE AND MCM-41 AS CATALYSTS)

อาจารย์ที่ปรึกษา : ผู้ช่วยศาสตราจารย์ ดร.สัญญา ประยูร โภคราช, 135 หน้า.

งานวิจัยนี้มุ่งเน้นการพัฒนาตัวเร่งปฏิกิริยาเบสวิธีพ่นที่ประกอบด้วยโพแทสเซียมบนตัว
รองรับซีโอไลต์ด้วยในรูปของโซเดียมและ MCM-41 สำหรับการผลิตไบโอดีเซลด้วย
ปฏิกิริยาทรานส์เอสเทอร์ฟิเคชันของน้ำมันจากเมล็ดสบู่ดำที่ปลูกในจังหวัดนครราชสีมา

น้ำมันเมล็ดสบู่ดำสกัดโดยการแช่เมล็ดสบู่ดำบดละเอียดในเฮกเซนเป็นเวลา 3 ชั่วโมง ที่
อุณหภูมิห้องให้ผลได้ของน้ำมัน 29.74% โดยน้ำหนัก น้ำมันที่สกัดได้ถูกนำไปวิเคราะห์สมบัติทาง
เคมีและทางกายภาพ องค์ประกอบกรดไขมันไม่อิ่มตัวและกรดไขมันอิ่มตัวมีค่า 77.70% และ
22.30% ตามลำดับ กรดโอเลอิก (44.60%) และกรดลิโนเลอิก (32.20%) เป็นองค์ประกอบหลักของ
กรดไขมันไม่อิ่มตัว ส่วนกรดปาล์มิติก (15.20%) เป็นองค์ประกอบหลักของกรดไขมันอิ่มตัว สมบัติ
ทางเคมีและทางกายภาพของน้ำมันชี้แนะว่าน้ำมันเมล็ดสบู่ดำสามารถนำไปใช้เป็นวัตถุดิบสำหรับ
การผลิตไบโอดีเซลด้วยปฏิกิริยาทรานส์เอสเทอร์ฟิเคชันได้

โพแทสเซียมบนตัวรองรับซีโอไลต์ด้วยในรูปของโซเดียม (xK/NaY) และบนตัวรองรับ
MCM-41 ($xK/MCM-41$) เมื่อ x คือเปอร์เซ็นต์น้ำหนักของโพแทสเซียมมีค่า 4 8 หรือ 12 เตรียมโดย
วิธีเอ็บซุ่มด้วยสารละลายบัฟเฟอร์ CH_3COOK/CH_3COOH ตัวเร่งปฏิกิริยา $12K/NaY-1$ และ
 $12K/NaY-2$ ซึ่งมีโพแทสเซียม 12% โดยน้ำหนักอยู่บนตัวรองรับซีโอไลต์ด้วยในรูปของโซเดียม
เตรียมโดยวิธีเอ็บซุ่มด้วย KNO_3 โดยตัวรองรับดังกล่าวสังเคราะห์จากซิลิกาจากแกลบข้าว ตัวเร่ง
ปฏิกิริยาเหล่านี้ถูกนำไปวิเคราะห์ลักษณะด้วยเทคนิคการเลี้ยวเบนของรังสีเอกซ์ (XRD) การดูดซับ-
การคายไนโตรเจน และฟูเรียร์ทรานส์ฟอร์มอินฟราเรดสเปกโทรสโกปี (FTIR) ผลการศึกษาแสดง
ให้เห็นว่าโครงสร้างของ NaY ยังคงสภาพอยู่หลังการใส่โพแทสเซียมเข้าไป ในขณะที่การพังของ
โครงสร้าง MCM-41 เกิดขึ้นเมื่อใส่โพแทสเซียมเข้าไป 8 และ 12% โดยน้ำหนัก

ตัวเร่งปฏิกิริยาทั้งหมดถูกนำมาศึกษาความสามารถในการเร่งปฏิกิริยาทรานส์เอสเทอร์ฟิเค
ชันของน้ำมันเมล็ดสบู่ดำกับเมทานอล ผลกระทบของตัวแปรในปฏิกิริยาที่ศึกษาได้แก่ อัตราส่วน
เมทานอลต่อน้ำมัน เวลาในการเกิดปฏิกิริยา และปริมาณโพแทสเซียมบนตัวรองรับ โดยติดตามการ
ดำเนินไปของปฏิกิริยาด้วยโครมาโทกราฟีฟิววบางและผลิตภัณฑ์ที่ได้จากสภาวะปฏิกิริยาที่
เหมาะสมที่สุดถูกนำไปวิเคราะห์ต่อด้วยโครมาโทกราฟีแก๊ส $12K/NaY$ ทำให้เกิดการแปลงผันอย่าง

สมบูรณ์ รองลงมาคือ 8K/NaY และ 4K/NaY ตามลำดับ 12K/NaY ให้ผลได้ไบโอดีเซลสูงสุดคือ 73.4% ภายในเวลาของปฏิกิริยา 3 ชั่วโมง อุณหภูมิของปฏิกิริยา 65 °C และอัตราส่วนโดยโมลของ เมทานอลต่อน้ำมัน 16:1 ได้มีการศึกษาการนำกลับมาใช้ใหม่ของ 12K/NaY และพบว่าไม่สามารถ ตัวเร่งปฏิกิริยาได้เนื่องจากมีการสูญเสียสปีชีส์ที่มีฤทธิ์ (สปีชีส์ K) ส่วน xK/MCM-41 12K/NaY-1 และ 12K/NaY-2 มีความสามารถในการเร่งปฏิกิริยาที่ต่ำมากภายใต้สภาวะที่ศึกษา

สมบัติความเป็นเบสของตัวเร่งปฏิกิริยาถูกศึกษาด้วยการคายตามอุณหภูมิโปรแกรมของ ไพร์โรลและการแปลงของ 2-เมทิล-3-บิวไทน์-2-ออล ผลการศึกษาบ่งบอกว่าปริมาณตำแหน่งเบส ของตัวเร่ง xK/NaY เพิ่มขึ้นตามลำดับดังนี้ 12K/NaY > 8K/NaY > 4K/NaY ซึ่งสอดคล้องกับผล การศึกษาการเร่งคือการแปลงผันเพิ่มขึ้นตามลำดับ เช่นเดียวกัน ส่วน xK/MCM-41 12K/NaY-1 และ 12K/NaY-2 มีปริมาณตำแหน่งเบสน้อยมากส่งผลให้มีความสามารถในการเร่งปฏิกิริยา ทรานเอสเทอร์ฟิเคชันต่ำ



สาขาวิชาเคมี

ปีการศึกษา 2554

ลายมือชื่อนักศึกษา _____

ลายมือชื่ออาจารย์ที่ปรึกษา _____

NUTTINEE SUPAMATHANON : BIODIESEL PRODUCTION VIA
TRANSESTERIFICATION OF JATROPHA SEED OIL USING POTASSIUM
SUPPORTED ON NaY ZEOLITE AND MCM-41 AS CATALYSTS. THESIS
ADVISOR : ASST. PROF. SANCHAI PRAYOONPOKARACH, Ph.D. 135 PP.

NaY ZEOLITE/ MCM-41/ JATROPHA SEED OIL/ BIODIESEL/
TRANSESTERIFICATION/ HETEROGENEOUS CATALYST

This research focuses on the development of base heterogeneous catalysts consisting of potassium supported on NaY zeolite and MCM-41 for biodiesel production via transesterification of Jatropha seed oil. The oil was obtained from the seeds of *Jatropha curcas* cultivated in Nakhon Ratchasima.

Extraction of the seed oil by soaking the ground seed in hexane for 3 h at room temperature provided 29.74 wt% oil yield. The extracted oil was analyzed for its chemical and physical properties. The unsaturated and saturated fatty acid components were 77.70% and 22.30%, respectively. Oleic acid (44.60%) and linoleic acid (32.20%) were the major components of the unsaturated fatty acid, while palmitic acid (15.20%) was the main component of the saturated fatty acid. Physicochemical properties of the oil suggested that it could be used as a feedstock for biodiesel production via transesterification.

Potassium supported on NaY (xK/NaY) and on MCM-41 (xK/MCM-41), where x is 4, 8 or 12 wt% of K loading, were prepared by impregnation method using buffer solution of CH₃COOK/CH₃COOH. Potassium supported on NaY with 12% of K loading (12K/NaY-1 and 12K/NaY-2) were also prepared by impregnation with solution of KNO₃. The catalyst supports were synthesized from rice husk silica. These catalysts were characterized by X-ray diffraction (XRD), nitrogen adsorption-

desorption and Fourier transform infrared spectroscopy (FTIR). The results indicated that the structure of NaY was preserved after K loading, whereas the collapse of MCM-41 structure was observed with 8 and 12 wt% of K loading.

All catalysts were studied for their catalytic activities in transesterification of Jatropha seed oil with methanol. The effect of the reaction variables including the ratio of methanol to oil, the reaction time and the amount of potassium loading on the support were investigated. The progress of the reaction was primarily monitored by thin layer chromatography and the products from the most suitable reaction condition were further analyzed by gas chromatography. The 12K/NaY provided a complete conversion, followed by the 8K/NaY and 4K/NaY, respectively. The 12K/NaY gave the optimum biodiesel yield of 73.4% under the reaction time of 3 h, the reaction temperature of 65 °C and methanol to oil molar ratio of 16:1. Reusability of 12K/NaY was investigated and it was found that the catalyst was partially deactivated because of the loss of active species (K species). The xK/MCM-41, 12K/NaY-1 and 12K/NaY-2 had very low catalytic activity under the studied condition.

The basic properties of the catalysts were studied by temperature programmed desorption of pyrrole and transformation of 2-methyl-3-butyn-2-ol. The results indicated that the amount of basic sites of xK/NaY catalysts increased in the following order: 12K/NaY > 8K/NaY > 4K/NaY. The results are in agreement with the catalytic studies as the conversion increased with the same order. The xK/MCM-41 and the catalyst prepared with KNO₃ had relatively low amount of the basic sites resulting in poor catalytic activity for transesterification.

School of Chemistry

Student's Signature _____

Academic Year 2011

Advisor's Signature _____

ACKNOWLEDGEMENTS

I would like to express my gratitude and appreciation to all those who have helped me throughout my study. First of all, I would like to thank my advisor, Asst. Prof. Dr. Sanchai Prayoonpokarach and Assoc. Prof. Dr. Jatuporn Wittayakun for guidance and encouragement towards the completion of this work. I would like to thank Prof. Dr. Frank Roessner at Technische Chemie II, Carl von Ossietzky Universität, Oldenburg, for Pyrrole-TPD and MBOH test reaction facility and kind guidance and continual advice in part of my experiment.

I also thank the thesis examining committee including Asst. Prof. Dr. Kunwadee Rangriwatananon, Asst. Prof. Dr. Chaiwat Raksakulpiwat, Asst. Prof. Dr. Thanaporn Manyum and Assoc. Prof. Dr. Jatuporn Wittayakun for their helpful suggestions. I would also like to thank all the lecturers of the School of Chemistry for their good attitude and useful advice, all of the staff at the Center for Scientific and Technological Equipment for their assistance and suggestion for the use of instruments.

I am grateful to Nakhon Ratchasima Field Crops Research Center in Sikhio District, Nakhon Ratchasima for Jatropha seed samples.

Thank to all of my good friends in the School of Chemistry, Suranaree University of Technology (SUT) and in Technische Chemie II, Carl von Ossietzky Universität Oldenburg. Special thanks for Mr. Wojciech Supronowicz for assistance and suggestion on the use of the gas phase methyl butynol and Pyrrole-TPD apparatus and other friends for their friendship and all their help.

I am grateful to the Rajamangala University of Technology Isan (RMUTI),
Nakon Ratchasima for the full scholarship throughout my study.

Finally, I would like to thank my family for their love, understandings,
encouragement and the part of financial support during my education.

Nuttinee Supamathanon



CONTENTS

	Page
ABSTRACT IN THAI.....	I
ABSTRACT IN ENGLISH.....	III
ACKNOWLEDGEMENTS.....	V
CONTENTS.....	VII
LIST OF TABLES.....	XIII
LIST OF FIGURES.....	XIV
LIST OF SCHEMES.....	XX
LIST OF ABBREVIATIONS.....	XXI
CHAPTER	
I INTRODUCTION.....	1
1.1 Significant of the study.....	1
1.2 Outline of the thesis.....	2
1.3 References.....	3
II EXTRACTION AND CHARACTERIZATION OF JATROPHA	
SEED OIL CULTIVATED IN NAKHON RATCHASIMA.....	5
2.1 Introduction.....	5
2.2 Experimental.....	7
2.2.1 Extraction of Jatropha seed oil.....	7

CONTENTS (Continued)

	Page
2.2.2 Determination of fatty acid composition and physicochemical properties of the extracted oils.....	9
2.3 Results and discussion.....	9
2.3.1 Oil yields.....	9
2.3.2 Physicochemical properties of the Jatropha seed oils....	10
2.3.3 Fatty acid composition of the Jatropha seed oils.....	12
2.4 Conclusions.....	13
2.5 References.....	14
III CHARACTERIZATION OF POTASSIUM SUPPORTED ON NaY ZEOLITE AND UTILIZATION AS CATALYSTS IN TRANSESTERIFICATION OF JATROPHA SEED OIL.....	17
3.1 Introduction.....	17
3.2 Experimental.....	23
3.2.1 Synthesis of NaY zeolite.....	23
3.2.2 Preparation of the catalysts.....	24
3.2.3 Characterization of the synthesized NaY zeolite and the K/NaY catalysts.....	25
3.2.4 Catalytic testing for transesterification.....	25
3.2.5 Analysis of reaction mixture and determination of biodiesel yield.....	27

CONTENTS (Continued)

	Page
3.2.5.1 Preliminary determination of conversion of transesterification by TLC.....	27
3.2.5.2 Determination of biodiesel yield by GC.....	28
3.2.6 Investigation of catalyst stability.....	29
3.2.6.1 Catalyst performance of the spent catalyst.....	29
3.2.6.2 Catalyst leachate activity on transesterification of glycerol trioctanoate.....	29
3.3 Results and discussion.....	32
3.3.1 Characterization of NaY and K/NaY catalysts.....	32
3.3.1.1 XRD.....	32
3.3.1.2 Surface area analysis.....	33
3.3.1.3 Infrared spectroscopy.....	35
3.3.2 Catalytic testing for transesterification.....	38
3.3.2.1 Effect of wt% loading of potassium.....	38
3.3.2.2 Effect of reaction time on 12K/NaY catalyst.....	41
3.3.2.3 Effect of methanol to oil molar ratio.....	43
3.3.3 Catalyst leaching test in transesterification.....	45
3.3.3.1 Transesterification of Jatropha oil with the spent catalyst.....	45
3.3.3.2 Transesterification of glycerol trioctanoate.....	46

CONTENTS (Continued)

	Page
3.4 Conclusions.....	49
3.5 References.....	49
IV BASIC PROPERTIES OF POTASSIUM SUPPORTED ON NaY STUDIED BY PYRROLE-TPD AND MBOH DECOMPOSITION.....	55
4.1 Introduction.....	55
4.2 Experimental.....	58
4.2.1 Catalyst preparation.....	58
4.2.2 Pyrrole-TPD.....	59
4.2.3 MBOH decomposition.....	60
4.3 Results and discussion.....	62
4.3.1 Pyrrole-TPD of K/NaY prepared from CH ₃ COOK/CH ₃ COOH.....	62
4.3.2 Pyrrole-TPD of 12K/NaY-1 and 12K/NaY-2.....	67
4.3.3 MBOH decomposition.....	70
4.4 Conclusions.....	77
4.5 References.....	77
V TRANSESTERIFICATION OF JATROPHA SEED OIL USING POTASSIUM SUPPORTED ON MCM-41 AS HETEROGENEOUS CATALYSTS.....	81

CONTENTS (Continued)

	Page
5.1 Introduction.....	81
5.2 Experimental.....	83
5.2.1 Synthesis of MCM-41.....	83
5.2.2 Preparation of catalysts.....	83
5.2.3 Characterization of catalysts.....	85
5.2.4 Transesterification of Jatropha seed oil.....	85
5.2.5 Characterization of basic properties.....	86
5.3 Results and discussion.....	86
5.3.1 Characterization of catalyst.....	89
5.3.2 Activities of the catalysts in transesterification.....	91
5.3.2.1 xK/MCM-41(A)-500 catalysts calcined at 500 °C.....	91
5.3.2.2 xK/MCM-41 catalysts calcined at 400 °C.....	94
5.3.3 Basic properties measurement.....	97
5.3.3.1 Pyrrole-TPD.....	97
5.3.3.2 Catalytic activity in conversion of MBOH.....	98
5.4 Conclusions.....	100
5.5 References.....	100
VI CONCLUSIONS.....	103
APPENDICES.....	105

CONTENTS (Continued)

	Page
APPENDIX A CATALYST PREPARATION BY IMPREGNATION METHOD.....	106
APPENDIX B DETERMINATION OF METHYL ESTER BY GAS CHROMATOGRAPHY.....	110
APPENDIX C CATALYTIC ACTIVITY IN CONVERSION OF 2-METHYL-3-BUTYN-2-OL.....	122
APPENDIX D TEMPERATURE PROGRAMMED DESORPTION OF PYRROLE (PYRROLE-TPD).....	131
CURRICULUM VITAE.....	135

LIST OF TABLES

Table		Page
2.1	The oil yields from three extraction methods.....	10
2.2	Chemical and physical characteristics of Jatrophaseed oil.....	11
2.3	Fatty acid composition of Jatropha seed oil.....	13
3.1	BET surface area of parent NaY zeolite, xK/NaY catalysts and relative percent decrease.....	35
3.2	Biodiesel yield from 12K/NaY catalyst at different methanol to oil molar ratios and from NaOH as homogeneous catalyst.....	45
4.1	Summary results for surface area, total peak area, amount of pyrrole and peak of desorption temperature from deconvolution and corresponding peak area of parent NaY and xK/NaY catalysts (x = 4, 8 and 12 wt% loading of K).....	65
4.2	Summary results of 12K/NaY-1 and 12K/NaY-2 catalysts for total peak area, amount of pyrrole and peak of desorption temperature from deconvolution of 12K/NaY-1 and 12K/NaY-2 catalysts.....	70

LIST OF FIGURES

Figure	Page
3.1 Apparatus set up for transesterification.....	26
3.2 Apparatus set up for catalyst leaching testing for transesterification of glycerol trioctanoate.....	30
3.3 XRD patterns of the parent NaY, xK/NaY (x = 4, 8 and 12 wt% loading of K), 12K/NaY-1 and 12K/NaY-2.....	33
3.4 Nitrogen adsorption isotherms of the parent NaY and xK/NaY catalysts (x = 4, 8 and 12 wt%).....	34
3.5 FTIR spectra of the parent NaY, calcined K/NaY catalysts with 4, 8 and 12 wt% loading of K and as-prepared K/NaY with 12 wt% loading of K (before calcination).....	37
3.6 Spots on the TLC plate of the mixture from transesterification of Jatropha seed oil over the parent NaY zeolite (b and c) compared to that of fatty acid methyl ester standard (a). Reaction condition: methanol to oil molar ratio of 16:1, reaction time of 3 h and temperature of 65 °C.....	38
3.7 Spots on the TLC plate of the mixtures from transesterification of Jatropha seed oil on 4K/NaY (c), 8K/NaY (d) and 12K/NaY (e) compared to that of fatty acid methyl ester standard (a) and crude Jatropha seed oil (b). Reaction condition: methanol to oil molar ratio of 16:1, reaction time of 3 h and temperature of 65 °C.....	39

LIST OF FIGURES (Continued)

Figure	Page
3.8 Spots on the TLC plate of the mixtures from transesterification of Jatropha seed oil over 12K/NaY-1 (b) and 12K/NaY-2 (c) compared to that of fatty acid methyl ester standard (a). Reaction condition: methanol to oil molar ratio of 16:1, reaction time of 3 h and temperature of 65 °C.....	40
3.9 Spots on the TLC plate of the mixtures from transesterification of Jatropha seed oil over 12K/NaY catalyst at various reaction times (b) 1 h, (c) 2 h and (d) 3 h compared to that of (a) fatty acid methyl ester standard. Reaction condition: methanol to oil molar ratio of 16:1 and temperature of 65 °C.....	42
3.10 Spots on the TLC plate of the mixtures from transesterification of Jatropha seed oil with NaOH catalyst at various reaction times (c) 1 h and (d) 3 h compared to that of (a) fatty acid methyl ester standard and (b) crude Jatropha seed oil. Reaction condition: methanol to oil molar ratio of 16:1 and temperature of 65 °C.....	43
3.11 Spots on the TLC plate of the mixtures from transesterification of Jatropha seed oil with 12K/NaY at methanol to oil molar ratio of (b) 9:1, (c) 16:1 and (d) 20:1 compared to that of (a) fatty acid methyl ester standard. Reaction condition: reaction time of 3 h and temperature of 65 °C.....	44

LIST OF FIGURES (Continued)

Figure	Page
3.12 Spots on the TLC plate of the mixtures from transesterification of Jatropha seed oil with the spent 12K/NaY (b and c) compared to that of fatty acid methyl ester standard (a). Reaction condition: methanol to oil molar ratio of 16:1, reaction time of 3 h and temperature of 65 °C.....	46
3.13 The composition of the reaction mixture for the consecutive transesterification of glycerol trioctanoate with methanol in the presence of 12K/NaY.....	47
3.14 The composition of the reaction mixture for the consecutive transesterification of glycerol trioctanoate with methanol in the absence of 12K/NaY.....	48
4.1 Diagram of instrument setup for the methylbutynol decomposition.....	60
4.2 Desorption profiles of pyrrole on the parent NaY (a) and the xK/NaY catalysts prepared by impregnation of CH ₃ COOK/CH ₃ COOH on NaY; (b) 4K/NaY, (c) 8K/NaY and (d) 12K/NaY.....	62
4.3 Experimental and deconvolution of TPD peaks of pyrrole desorption on parent NaY (a), 4K/NaY (b), 8K/NaY (c) and 12K/NaY catalyst (d).....	64
4.4 Scheme of the faujasite structure with oxygen types (○) and cation locations (●).....	66

LIST OF FIGURES (Continued)

Figure	Page	
4.5	Desorption profiles of pyrrole on the parent NaY, 12K/NaY, 12K/NaY-1 and 12K/NaY-2 catalysts.....	68
4.6	Experimental and deconvolution of TPD peaks of pyrrole on (a) 12K/NaY-1 and (b) 12K/NaY-2 catalysts.....	69
4.7	Selectivity of the product of MBOH test reaction over the parent NaY (a) and xK/NaY catalysts (b) 4K/NaY, (c) 8K/NaY and (d) 12K/NaY. Reaction temperature was 120 °C and amount of each sample was 20 mg.....	71
4.8	Conversion of MBOH test reaction over the parent NaY and xK/NaY catalysts with 4, 8 and 12 wt% loading, reaction temperature 120 °C, amount of catalyst was 20 mg.....	72
4.9	Conversion of MBOH test reaction over the 8K/NaY and 12K/NaY catalysts. Reaction temperature was 120 °C and amount of catalyst was 10 mg.....	73
4.10	Selectivity of the product of MBOH test reaction over (a) 8K/NaY and (b) 12K/NaY catalyst. Reaction temperature was 120 °C and amount of catalyst was 10 mg.....	74
4.11	Conversion of MBOH test reaction over the 12K/NaY, 12K/NaY-1 and 12K/NaY-2 catalysts. Reaction temperature was 120 °C and amount of catalyst was 20 mg.....	75

LIST OF FIGURES (Continued)

Figure	Page	
4.12	Selectivity of the product of MBOH test reaction over 12K/NaY-1. Reaction temperature was 120 °C and amount of catalyst was 20 mg.....	76
5.1	XRD patterns of the xK/MCM-41(A) and xK/MCM-41 with 4, 8 and 12 wt% loading; a) and b) xK/MCM-41(A) calcined at 300 °C and 500 °C, respectively, c) xK/MCM-41 calcined at 400 °C.....	88
5.2	XRD patterns of the parent RH-SiO ₂ and 12K/RH-SiO ₂	89
5.3	Transmission electron micrographs of the MCM-41, a); 8K/MCM-41, b) and 12K/MCM-41, c) catalysts.....	90
5.4	TLC plate showing spot a, methyl ester standard, spot b and c, liquid from transesterification of Jatropha seed oil with 4K/MCM-41(A)-500. Reaction condition: methanol to oil molar ratio, 40:1; reaction time, 6 h; temperature, 65 °C.....	91
5.5	TLC plate of liquid from transesterification of Jatropha seed oil with 4K/MCM-41(A)-500 under ultrasonic condition, spots b and c compared to methyl ester standard, spot a. Reaction condition: methanol to oil molar ratio, 40:1; reaction time, 2 h.....	92
5.6	TLC plate of liquid from transesterification of Jatropha seed oil with 8K/MCM-41(A)-500 under reflux condition, spot b compared to methyl ester standard, spot a. Reaction condition: methanol to oil molar ratio = 40:1, reaction time = 3 h, temperature = 65 °C.....	93

LIST OF FIGURES (Continued)

Figure	Page
5.7 TLC plate of liquid from transesterification of Jatropha seed oil with 8K/MCM-41(A)-500 under ultrasonic condition, spots b and c compared to methyl ester standard, spot a. Reaction condition: methanol to oil molar ratio = 40:1, reaction time = 2 h.....	94
5.8 TLC plate represent spot a, methyl ester standard; spots b, c, d and e, liquid from the reaction with 4-, 8- and 12K/MCM-41 catalysts, respectively. The reaction conditions were methanol to oil molar ratio of 16:1, reaction time of 3 h and reaction temperature of 65 °C.....	95
5.9 Result from transesterification over the 12K/RH-SiO ₂ catalyst. Spot a is a methyl ester standard. Spots b and c are liquid from the reaction condition was 16:1 methanol to oil molar ratio, 3 h reaction time and 65 °C temperature.....	96
5.10 Desorption profiles of pyrrole on the MCM-41, xK/MCM-41 with 4, 8 and 12 wt% loading of K and 12K/RH-SiO ₂	97
5.11 Conversion of MBOH over the parent MCM-41 and xK/MCM-41 catalysts. The reaction temperature was 120 °C and the amount of catalyst was 0.020 g.....	98
5.12 Conversion of MBOH test reaction over 12K/MCM-41, 12K/RH-SiO ₂ and 12K/NaY catalysts.....	99

LIST OF SCHEMES

Scheme	Page
3.1 Transesterification for biodiesel production.....	18
4.1 Overall reaction of MBOH.....	57



LIST OF ABBREVIATIONS

Å	Angstrom
°C	degree celcius
cm ⁻¹	wavenumber
et al	et alia (and other)
FTIR	Fourier transform infrared
g	gram
h	hour
kV	kilovolt
min	minute
m	meter
m ²	square meter
mm	milimeter
mL	milliliter
mg	milligram
µL	microliter
R	Alkyl group
RH	Rice husk
%T	percent transmittance
wt%	Weight percentage
TEM	Transmission electron microscope

LIST OF ABBREVIATIONS (Continued)

TPD	Temperature programmed desorption
XRD	X-ray diffraction
GC	Gas chromatography
MBOH	2-methyl-3-butyn-2-ol, methylbutynol



CHAPTER I

INTRODUCTION

1.1 Significance of the study

Environmental concerns about air pollution from the combustion of fossil fuels and the depletion of the world petroleum crude have led to the development of alternative fuels. Biodiesel is one of the alternative fuels that can be produced from renewable resources such as vegetable oil or animal fat by transesterification (Ma and Hanna, 1999; Srivastava and Prasad, 2000). In the reaction, triglycerides react with an alcohol in the presence of a catalyst to form a mixture of fatty acid methyl esters, which is referred to as biodiesel, and glycerol as a byproduct (Ma and Hanna, 1999; Van Gerpen, 2005; Meher, Vidya, and Naik, 2006).

Vegetable oils from many plants such as palm, soybean, sunflower, safflower, cotton, coconut, canola and rapeseed have been used for the production of biodiesel. However, the fact that edible oils are valuable as food supplies makes them less interesting as a feedstock for the biodiesel production. Consequently, oils from non-edible crops; for example, *Jatropha curcas* has become interesting for this purpose. *Jatropha curcas* is a drought resistant shrub grown well in Asia and Africa. The plant grows quickly with high-seed yield and high oil content and is therefore easy to establish as an oil source for biodiesel (Achten et al., 2008). Nakhon Ratchasima is one of the locations where the plant is cultivated; hence, *Jatropha* seeds were used as

an oil source for this research. The composition and properties of the oil were investigated before using as a reactant for transesterification.

Traditionally, homogeneous basic catalysts such as sodium hydroxide and potassium hydroxide are used for production of biodiesel via transesterification. These catalysts provided high yield of methyl esters in a relatively short reaction time, e.g. 1-3 h. However, formation of soap and removal of the catalyst after the reaction are major disadvantages of the process. A large amount of wastewater is produced from the process of catalyst separation and product cleaning (Narasimharao, Lee, and Wilson, 2007). To avoid the problems, it has been proposed to replace the homogeneous catalysts by heterogeneous ones. The heterogeneous catalyst offers a number of advantages such as simplification of the catalyst separation from the reaction mixture and reduction of pollutants and the production cost (Wallau and Schuchardt, 1995; Serio, Tesser, Pengmei, and Santacesaria, 2008). This research focused on developing of heterogeneous basic catalysts, based on NaY zeolite and MCM-41 as catalytic support for transesterification of Jatropha seed oil. The porous catalytic materials including NaY zeolite and MCM-41 have attracted attention for their applications in catalysis because of high surface area, small pore size distribution and adjustable acid/base strength. The base strength of NaY zeolite and MCM-41 can be increased by incorporating metal and metal oxide into their structures (Wallau and Schuchardt, 1995; Corma, Iborra, Miquel, and Primo, 1998).

1.2 Outline of the thesis

In this thesis, studies were directed towards developing heterogeneous basic catalyst for transesterification of Jatropha seed oil. Two catalyst supports were NaY

zeolite and MCM-41 which were synthesized from rice husk silica. The supports were loaded with potassium salt to adjust their basicity. The catalysts were characterized by various techniques before testing in the reaction.

The study of the oil extraction, chemical composition and characteristics of the oil obtained from *Jatropha* seeds provenance in Nakhon Ratchasima are presented in Chapter II. The results were compared with those from the literatures.

The extracted oil was used in the reaction catalyzed by developed catalysts which were prepared from two supports, NaY zeolite and MCM-41. In Chapter III, catalysts prepared from various amounts of potassium salt loaded on NaY zeolite were characterized by several techniques and investigated for their capability to catalyze transesterification. Reaction conditions were optimized for maximum biodiesel yield. Activity of the selected catalyst after being used once in the reaction was also tested. Similar studies were conducted with the catalysts based on MCM-41 and were discussed in Chapter V.

The basic property of the developed catalysts is of concern in Chapter IV. The catalytic activity in conversion of 2-methyl-3-butyn-2-ol (MBOH) and temperature programmed desorption of pyrrole (TPD-pyrrole) were employed to obtain the information on the basicity of the catalysts. Final conclusions and future work are presented in Chapter VI.

1.3 References

Achten, W. M. J., Verchot, L., Franken, Y. J., Mathijs, E., Singh, V. P., Aerts R. and Muys B. (2008). *Jatropha* bio-diesel production and use. **Biomass and Bioenergy**. 32: 1063-1084.

- Corma, A., Iborra, S., Miquel, S. and Primo, J. (1998). Catalysts for the production of fine chemicals. **Journal of Catalysis**. 173: 315-321.
- Ma, F. and Hanna, M. A. (1999). Biodiesel production: a review. **Bioresource Technology**. 70: 1-15.
- Meher, L. C., Vidya, S. D. and Naik, S. N. (2006). Technical aspects of biodiesel production by transesterification - a review. **Renewable and Sustainable Energy Reviews**. 10: 248-268.
- Narasimharao, K., Lee, A. and Wilson, K. (2007). Catalysts in production of biodiesel: A review. **Journal of Biobased materials and Bioenergy**. 1: 19-30.
- Serio, M. D., Tesser, R., Pengmei, L. and Santacesaria, E. (2008). Heterogeneous catalysts for biodiesel production. **Energy and Fuels**. 22: 207-217.
- Srivastava, A. and Prasad, R. (2000). Triglycerides-based diesel fuels. **Renewable and Sustainable Energy Reviews**. 4: 111-133.
- Van Gerpen, J. (2005). Biodiesel processing and production. **Fuel Processing Technology**. 86: 1097-1107.
- Wallau, M. and Schuchardt, U. (1995). Catalysis by metal containing zeolite. I: Basic sites. **Journal of the Brazilian Chemical Society**. 6: 393-403.

CHAPTER II

EXTRACTION AND CHARACTERIZATION OF JATROPHA SEED OIL CULTIVATED IN NAKHON RATCHASIMA

2.1 Introduction

Jatropha curcas Linn, commonly called physic or purging nut and locally known as “Sabudam” is a drought resistant shrub. Its genus belongs to tribe Joannesieae of Crotonoideae in the Euphorbiaceae family. The plant has approximately 170 known species (Heller, 1996) and is cultivated in Central and South America, South-east Asia, India and Africa. In Thailand, it can be grown in most regions, especially in the north-eastern area. The fruit seeds of this plant contain an oil that can be used as a source material for biodiesel production (Giibitz, Mittelbach, and Trabi, 1999; Augustus, Jayabalon, and Deiler, 2002).

Jatropha seed oil is regarded as a potential fuel substitute because it can be used as a renewable source for biodiesel. The oil is non-edible and therefore has gained more interest than those of consumable oils such as soybean and palm oil. Jatropha seed oil can be used directly with agricultural diesel engine (Agarwal and Agarwal, 2007). However, formation of carbon deposits in an engine and incomplete fuel combustion caused from the high viscosity of Jatropha seed oil could result in reduced shelf life of the engine. There are many ways to decrease the viscosity of the oil; for examples, preheating the oil, blending with other fuels, thermal cracking and

reacting with an alcohol in the presence of a catalyst, which is known as transesterification (Pramanik, 2003).

Transesterification was found to be an effective means to reduce the viscosity of the oil as the reaction transformed triglyceride to alkyl esters (Srivastava and Prasad, 2000). Foidl, Foidl, Sanchez, Mittelbach, and Hackel (1996) used *Jatropha* seed oil as a feedstock for biodiesel production. Methanol and ethanol were used as a reactant and potassium hydroxide (KOH) was used as a catalyst. The investigated crude and transesterified *Jatropha* seed oil showed properties and composition that were conformed to the American Society for Testing and Materials (ASTM) and European (EN) Standard. The methyl ester qualities of *Jatropha* seed oil met the American, German and European standards (Achten et al., 2008).

Two methods have been used for oil extraction, which are mechanical and chemical extraction. Expellers or ram presses are examples of mechanical extraction. Organic solvents such as *n*-hexane and petroleum ether are commonly used for chemical extraction. Mechanical extraction has limitation in terms of oil recovery because heat and high temperature generated from pressing could damage both the oil and meal (Adriaans, 2006). On the other hand, solvent extraction is more efficient to extract the oil than the mechanical extraction because it provides higher oil yield (Achten et al., 2008; El Kinawy, 2009). Solvent extraction is dependent on the type of solvent, particle size of the meal, solvent to meal ratio, extraction time and temperature of the process (El Kinawy, 2009; Sayyar, Yunus, and Muhammad, 2009). The oil content in weight percent of *Jatropha* seed ranges from 30 to 50% and that of the kernel ranges from 45 to 60% (Pramanik, 2003). In this work, solvent extraction using *n*-hexane and petroleum ether was employed.

The fatty acid composition of the *Jatropha* seed oil was reported in the literature (Achten et al., 2008). There are two main types of fatty acids which are saturated and unsaturated fatty acids. A symbol, C_n:_x, is given to represent different fatty acid molecules, where n and x are the number of carbon atoms and double bonds between carbon atoms in the acid molecule, respectively. For example, C18:2 represents the fatty acid with eighteen carbon atoms having two carbon-carbon double bonds in the molecule. *Jatropha* seed oil contains approximately > 75% of unsaturated fatty acids which consist mainly of oleic acid (C18:1) and linoleic acid (C18:2). Palmitic acid (C16:0) and stearic acid (C18:0) are the major components of the saturated fatty acids. Small amount of myristic acid (C14:0), palmitoleic acid (C16:1), linoleic acid (C18:3), arachidic acid (C20:0), eicosenoic acid (C20:1), eicosadienoic acid (C20:2) and behenic acid (C22:0) are also present. The variation in fatty acid composition could be attributed to the soil and climate conditions.

The properties of the crude *Jatropha* seed oils vary with their origins which affect the biodiesel production process. Thus, it is necessary to characterize the oil before it is used in transesterification.

2.2 Experimental

2.2.1 Extraction of *Jatropha* seed oil

The seeds were collected from test plantation in Chokchai District and Nakhon Ratchasima Field Crops Research Center in Sikhio District, Nakhon Ratchasima. The seeds were dried in an oven at 105 °C for 4 h and cooled down to room temperature before grinding with a grinder (Waring Commercial, Model

32BL79, USA). The oil from the ground seed was extracted by soaking, stirring and soxhlet method.

In soaking method, 100 g of the ground seed was placed in a 1-L erlenmeyer flask and 400 mL of hexane (C_6H_{14} , AR grade, LAB-SCAN) was added. The process was carried out for 3 h at room temperature and stirring the mixture with a glass rod was made every 20 min. At the end of the soaking period, the mixture was filtered through a filter paper (Whatman no. 1) placed in a Buchner funnel. Water in the filtrate was removed by using anhydrous sodium sulfate (Na_2SO_4 , AR grade, Carlo Erba) and the liquid was poured into a weighed 250-mL round bottom flask to remove hexane by a rotary evaporator (BUCHI, Rotavapor R-114, UK). The flask containing yellowish oil was weighed again. The weight of the oil was obtained by subtracting the weight of the flask from that of the flask with the oil. A percentage of oil yield was calculated according to the following equation:

$$\text{Oil yield (\% w/w)} = \frac{\text{weight of the seed oil (g)}}{\text{weight of the ground seed (g)}} \times 100 \quad (1)$$

For stirring method, 20 g of the ground seed was put into a 1-L erlenmeyer flask and 0.5 L of petroleum ether (J. T. Beaker) were added. The process was carried out for 8 h at room temperature under stirring with a magnetic stirrer (Velp Scientifica, ARE, Italy). After the stirring period, the extracted liquid was processed as that done in soaking method.

For Soxhlet method, 20 g of the ground seed was put into a thimble which was placed in the Soxhlet extraction apparatus. The extraction was conducted

for 8 h. Petroleum ether (J. T. Beaker) with the volume of 0.5 L was used as a solvent. The temperature of the extraction process was 70 ± 1.0 °C. After 8 h, the extracted liquid was poured into a 250-mL round bottom flask with the known weight and the solvent was removed with the rotary evaporator. The yellowish oil was weighed and the oil yield was calculated using equation (1). The extracted oils from the seeds collected from Chokchai and Sikhio Districts were notated JSO1 and JSO2, respectively.

2.2.2 Determination of fatty acid composition and physicochemical properties of the extracted oils

The Jatropha seed oils, JSO1 and JSO2, were characterized by Industrial Metrology and Testing Service Centre, Thailand Institute of Scientific and Technological Research (TISTR). The fatty acid composition was determined according to the method of Association of Official Analytical Chemists (AOAC, 969.33, 2005). The physicochemical properties including iodine value, free fatty acid, acid value, peroxide value, saponification value, unspionifiable matter, specific gravity, refractive index and viscosity were determined according to Thai Industrial Standards (44-2516).

2.3 Results and discussion

2.3.1 Oil yields

The oil yields of three extraction methods are presented in Table 2.1. The obtained yields are in the range of 25-35% which are similar to those reported in

Table 2.1 The oil yields from three extraction methods.

Extraction method	Oil yield (% w/w)	
	JSO1	JSO2
Soaking method	29.74	25.90
Stirring method	32.71	-
Soxhlet method	34.62	-

the literature (Jindal, Nandwana, and Rathore, 2010). The oil yield from Soxhlet extraction was slightly higher than that from the soaking method and stirring method, but the soxhlet extraction took 5 h longer. Therefore, the soaking method was used in the further study.

2.3.2 Physicochemical properties of the *Jatropha* seed oils

Chemical and physical characteristics of *Jatropha* seed oils are given in Table 2.2. The values agree well with those reported in literature (Achten et al., 2008). Acid value is a measure of the amount of free fatty acid present in fat or oil. The acid value is a good measure of the breakdown of the triglyceride in the oil or fat into the free fatty acid. The JSO1 oil has about a factor of 2 higher acid value than that of JSO2 oil. The acid values were converted to free fatty acid contents of 2.06 and 0.92 wt% for JSO1 and JSO2, respectively. In transesterification of vegetable oils or animal fats using base catalyst, the fats or oils should contain fewer than 2 wt% of free fatty acids (FFA) to obtain high yield of biodiesel. FFA could react with the catalyst to form soap; consequently, the amount of active catalyst was decreased. The soap formed in the reaction mixture could also lead to the difficulty in product

separation. The extracted oils in this work were therefore used in transesterification without FFA pretreatment. It is worth noting that the FFA content in the oil could be increased as a result of hydrolysis of triglycerides in the presence of moisture with an inappropriate storage of the oil.

Table 2.2 Chemical and physical characteristics of Jatropha seed oil.

Properties	JSO1	JSO2
Acid value (mg KOH/g sample)	4.11	1.83
Free fatty acid (wt%)	2.06	0.92
Iodine value (g I ₂ / 100 g sample)	59.60	60.50
Saponification value (mg KOH/g sample)	189.77	187.58
Unsaponifiable matter (wt%)	0.38	0.34
Viscosity at 30 °C (centistokes)	38.47	32.84
Specific gravity at 20 °C	0.91	0.91
Refractive index at 20 °C	1.47	1.47

The iodine value (IV) is a measure of the degree of unsaturation of fat and oil. The higher the IV in oil or fat, the more the double bonds is present and the higher the potential for polymerization of glycerides in the oil. This reaction can cause engine failure with the gummed-up oil (Emil, Yaakob, Satheesh, Jahim and Salimon, 2009). The IVs of JSO1 and JSO2 oils were 59.60 and 60.50 g I₂/100 g oil, respectively. The IVs of the oils are within the limit value of 120 for EN14214 specification (Knothe, 2003). The oil with the IV in the range of 50-100 could be used

directly with an unmodified diesel engine (Calais and Clark, 2006). However, the lifetime of the engine, the fuel pump and the injector might decrease (Verma and Gaur, 2009).

Saponification values of JSO1 and JSO2 oil were 189.77 and 187.58 mg KOH/g oil, respectively. Both oils have unsaponifiable matter < 0.4 wt%. The high saponification value and low unsaponifiable matter in the oils indicate that the oils are normal triglycerides (Akintayo, 2004) and therefore the oil can be used as a feedstock for biodiesel production. The viscosity of JSO1 is slightly higher than that of JSO2. The specific gravity and refractive index of both oils were the same. Physicochemical properties of crude *Jatropha* seed oil in this work were similar to those reported in the literatures (Akintayo, 2004; Achten et al., 2008; Emil, Yaakob, Satheesh Kumar, Jahim, and Salimon, 2010).

2.3.3 Fatty acid composition of the *Jatropha* seed oils

The fatty acid composition of the *Jatropha* seed oils is presented in Table 2.3 Both oils have the same fatty acid composition. Unsaturated fatty acids including oleic acid (C18:1) and linoleic acid (C18:2) are the major components in the oil. Saturated fatty acid composition which is combined to be < 23 wt% consisted of palmitic acid (C16:0), stearic acid (C18:0), arachidic acid (C20:0) and heptadecanoic acid (C17:0). The composition was in agreement with those reported in the literatures (Achten et al., 2008; Emil et al., 2010). The slightly difference in fatty acid contents could be attributed to variation in the cultivation condition such as climate, soil and seed variety (Achten et al., 2008).

Table 2.3 Fatty acid composition of Jatropha seed oil.

Fatty acid	wt%	
	JSO1	JSO2
Palmitic acid (C16:0)	15.20	15.00
Palmitoleic acid (C16:1)	0.70	0.90
Heptadecanoic acid (C17:0)	0.10	0.10
Stearic acid (C18:0)	6.80	6.00
Oleic acid (C18:1)	44.60	40.90
Linoleic acid (C18:2)	32.20	36.70
α -Linolenic acid (C18:3)	0.20	0.20
Arachidic acid (C20:0)	0.20	0.20
Total saturated fatty acids	22.3	21.3
Total unsaturated fatty acids	77.7	78.7

2.4 Conclusions

Chemical extraction was used to obtain the oil from Jatropha seed of Chokchai and Shikchio provenance. Slightly lower oil yield was obtained by soaking the ground seeds in hexane compared to that by the Soxhlet method. However, the extraction time was much shorter for the soaking method. The extracted oils from the seeds with different cultivation origins contained similar fatty acid composition with > 77 wt% of unsaturated fatty acids, mainly oleic acid and linoleic acid and > 21 wt% of saturated fatty acids, predominantly palmitic acid. The physicochemical properties of

the oils were characterized and the obtained information suggested that the oil had high potential as a feedstock for biodiesel production via transesterification.

2.5 References

- Achten, W. M J., Verchot, L., Franken, Y. J., Mathijs, E., Singh, V. P., Aerts R. and Muys B. (2008). *Jatropha* bio-diesel production and use. **Biomass and Bioenergy**. 32: 1063-1084.
- Adriaana, T. (2006). **Suitability of solvent extraction for *Jatropha curcas***. [Online]. Available: <http://www.fact-foundation.com/en/FACT/Publications>.
- Agarwal, D. and Agarwal, A. K. (2007). Performance and emissions characteristics of *Jatropha* oil (preheated and blends) in a direct injection compression ignition engine. **Applied Thermal Engineering**. 27: 2314-2323.
- Akintayo, E. T. (2004). Characteristics and composition of *Parkia biglobbosa* and *Jatropha curcas* oils and cakes. **Bioresource Technology**. 92: 307-310.
- Augustus, G. D. P. S., Jayabalan, M. and Deiler, G. J. (2002). Evaluation and bioinduction of energy components of *Jatropha curcas*. **Biomass and Biotechnology**. 23: 161-164.
- AOAC (Association of Official Analytical Chemists) International. (2005). Official Methods of Analysis of AOAC International, 18th ed. Gaithersburg, Maryland, USA.
- Calais, P. and Clark Tony, A. R. (2006). **Waste vegetable oil as a diesel replacement fuel**. [Online]. Available: <http://www.shortcircuit.com.au/warfa/paper/paper.htm>.
- El Kinawy, O. S. (2009). Technological aspects of *Jatropha* oil extraction. **Energy Sources, Part A**. 31: 1089-1098.

- Emil, A., Yaakob, Z., Kamarudin, S. K., Ismail, M. and Salimon, J. (2009). Characteristic and composition of *Jatropha curcas* oil seed from Malaysia and its potential as biodiesel feedstock. **European Journal of Scientific Research**. 29: 396-403.
- Emil, A., Yaakob, Z., Satheesh Kumar, M. N., Jahim, J. M. and Salimon, J. (2010). Comparative evaluation of physicochemical properties of *Jatropha* seed oil from Malaysia, Indonesia and Thailand. **Journal of the American Oil Chemists Society**. 87: 689-695.
- Foidl, N., Foidl, G., Sanchez, M., Mittelbach, M. and Hackel, S. (1996). *Jatropha curcas* L. as a source for the production of biofuel in Nicaragua. **Bioresource Technology**. 58: 77-82.
- Giibitz, G. M., Mittelbach, M. and Trabi, M. (1999). Exploitation of the tropical oil seed plant *Jatropha curcas* L. **Bioresource Technology**. 67: 73-82.
- Heller, J. (1996). **Physic nut. *Jatropha curcas* L.** Promoting the conservation and use of underutilized and neglected crops. 1. Institute of Plant Genetics and Crop Plant Research, Gatersleben, Germany and International Plant Genetic Resources Institute, Rome, Italy. [Online]. Available: <http://www.bionica.info/biblioteca/Heller1996Jatropha.pdf>.
- Jindal, S., Nandwana P. B. and Rathore, S. N. (2010). Comparative evaluation of combustion, performance and emissions of *Jatropha* methyl ester and Karanj methyl ester in a direct injection diesel engine. **Energy and Fuels**. 24: 1565-1572.
- Knothe, G. (2003). Analyzing biodiesel: Standards and other methods. **Journal of the American Oil Chemists Society**. 83: 823-833.

- Pramanik, K. (2003). Properties and use of *Jatropha curcas* oil and diesel fuel blends in compression ignition engine. **Renewable Energy**. 28: 239-248.
- Sayyar, S., Abidin, Z. Z., Yunus, R. and Muhammad, A. (2009). Extraction of oil from *Jatropha* seeds-optimization and kinetics. **American Journal of Applied Sciences**. 6: 1390-1395.
- Srivastava, A. and Prasad, R. (2000). Triglycerides-based diesel fuels. **Renewable and Sustainable Energy Reviews**. 4: 111-133.
- Verma, K. C. and Gaur, A. K. (2009) *Jatropha curcas* L.: Substitute for conventional energy. **World Journal of Agricultural Sciences**. 5: 552-556.



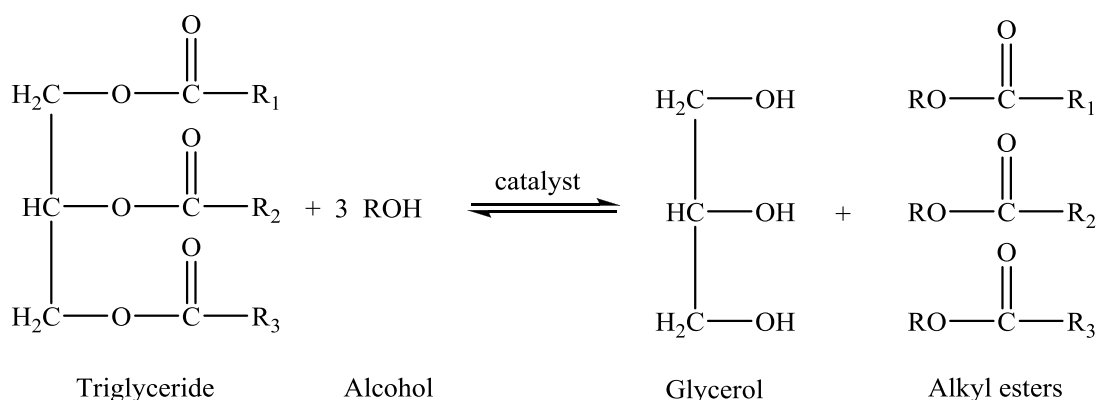
CHAPTER III

CHARACTERIZATION OF POTASSIUM SUPPORTED ON NaY ZEOLITE AND UTILIZATION AS CATALYSTS IN TRANSESTERIFICATION OF JATROPHA SEED OIL

3.1 Introduction

Biodiesel is interesting as an alternative fuel because it is renewable, environmental benign, non-toxic and biodegradable. Comparing with combustion of conventional diesel, biodiesel generates lower emission gases such as CO₂, NO_x and hydrocarbon particles (Ma and Hanna, 1999; Srivastava and Prasad, 2000; Demirbas, 2007). Biodiesel can be produced from renewable sources such as vegetable oils, animal fats and waste cooking oils by transesterification (Ma and Hanna, 1999; Srivastava and Prasad, 2000). The transesterification or alcoholysis is a reaction between triglyceride from oils and alcohol in the presence of a catalyst (Scheme 3.1). The products from the reaction are alkyl esters (biodiesel) and glycerol (Meher, Vidya, and Naik, 2006).

The overall transesterification reaction is believed to consist of three consecutive and reversible reactions as shown in equations (3.1)-(3.3) (Gerpen, 2005; Demirbas, 2007). The first step is a conversion of triglyceride to diglyceride, which is then converted to monoglyceride. Finally, the monoglyceride is changed to glycerol. Each step produces one methyl ester molecule.



Scheme 3.1 Transesterification for biodiesel production.



Type of catalysts plays an important role in the production of biodiesel. Catalysts can be classified, based on their phases into two groups, homogeneous when a solution of acid or base is used and heterogeneous when a solid acid or alkali or enzyme is used (Marchetti, Miguela, and Errazua, 2007; Narasimharao, Lee, and Wilson, 2007). Examples of the homogeneous acid catalysts are sulfuric (H_2SO_4), phosphoric (H_3PO_4), hydrochloric (HCl) and organic sulfonic acid ($\text{RS}(=\text{O})_2\text{-OH}$, where R is alkyl or aryl). With the acid catalysts, the transesterification is slower than that with the base catalysts. An advantage of the acid catalyst is that the reaction can be carried out with the oil that contains high content of free fatty acids and water.

Alkaline homogeneous catalysts generally used are sodium hydroxide (NaOH) and potassium hydroxide (KOH). They provide good catalytic activity but a large

amount of water is required to wash out the catalysts, generating a large amount of wastewater. Therefore, alkaline heterogeneous catalysts are studied because the catalyst separation from the biodiesel product is simple and washing water is not required (Marchetti et al., 2007; Narasimharao et al., 2007).

In this chapter biodiesel was produced from *Jatropha* seed oil over alkaline heterogeneous catalysts containing potassium supported on NaY zeolite, one of aluminosilicate materials with faujasite (FAU) structure. The catalyst symbols xK/NaY (x = loading by wt%) will be used throughout this chapter.

Zeolites have gained interest as catalyst supports because of their large surface areas and unique shape selectivity. The micropore structures of zeolites are stable and can be well preserved even under a vigorous condition. Many researchers studied zeolites as support materials for transesterification catalysts (Suppes, Dasari, Daskocil, Mankidy, and Goff, 2004; Xie, Huang, and Li, 2007; Noiroj, Intarapong, Luengnaruemitchai, and Jai-In, 2009) and as catalysts for esterification - a reaction between organic acid and alcohol in the presence of an acid catalyst (Chung and Park, 2009).

Suppes et al. (2004) compared K- and Cs-exchanged NaX, also in the FAU family, with NaO_x/NaX obtained by impregnation of sodium acetate (CH₃COONa) or sodium azide (NaN₃) on NaX and calcination at 500 °C. For transesterification of soybean oil at 60 °C for 24 h, the K- and Cs-exchanged NaX gave methyl ester yields of 10.3% and 7.3%, respectively. The methyl ester yields were much lower than that from the NaO_x/NaX which was more than 80%. Thus, different methods of catalyst preparation can affect the yield. The higher yield of methyl ester was achieved by catalyst prepared by impregnation method because the sodium oxide species were

incorporated into NaX zeolites. As the result, the base strength and number of basic sites were increased compared to the parent one. While ion exchange method was used weak basic site could be generated on the catalyst.

Xie et al. (2007) studied the transesterification of soybean oil with methanol to methyl ester using NaX loaded with KOH. The catalyst with 10 wt% KOH showed a good catalytic activity with a conversion of 85.6% under optimum condition: a 10:1 molar ratio of methanol to oil, a reaction time of 8 h, a catalyst amount of 3 wt% and a temperature of 65 °C. However, leaching of the KOH species from the supported catalyst caused a decline in the conversion to methyl esters from 85.2% to 48.7%.

Stability of zeolite depends on the type of structure and the Si/Al ratio (Xu, Rotunno, Bordiga, Prins, and van Bokhoven, 2006). In general, the zeolite stability increases with the Si/Al ratio (Saceda, de Leon, Rintramee, Prayoonpokarach, and Wittayakun, 2011). Because the Si/Al ratio of NaY (in the range of 2-4) is higher than that of NaX (in the range of 1-1.5), NaY is expected to be more stable. Consequently, NaY was used as a catalyst support in this work. Noiroj et al. (2009) loaded KOH on Al₂O₃ and NaY zeolite and used them as catalysts for transesterification of palm oil with methanol. The KOH/Al₂O₃ and KOH/NaY with KOH loading of 25 and 10 wt%, respectively, showed a good performance at temperature below 70 °C within 2-3 h giving the biodiesel yield of 91.07%. However, high loading of KOH (8-15 wt%) caused collapse of the crystalline structure of NaY due to the strong basicity of the solution. For heterogeneous catalysis, it is necessary to maintain the pore structure of the support after loading with metal. Consequently, other precursor which could preserve the zeolite structure is needed. In this work, a solution containing CH₃COOK and CH₃COOH with pH ~5 was chosen as a catalyst precursor instead of KOH.

There are two techniques to generate basic site on zeolite: ion exchange and impregnation. In the first method, the basic strength increases with increasing electropositive nature of the exchanged cation. In the second method, an increase in basicity is from the occlusion of alkali metal oxide cluster in zeolite cage happened through the decomposition of the impregnated alkali metal salt (Wallau and Schuchardt, 1995). With impregnation, the basic strength is higher than that with ion exchange owing not only to neutralization of surface acid site but also to the creation of new surface basic site (Barthomeuf, 1996; Hattori, 1995). As a result, in this work the precursor solution was impregnated on NaY zeolite.

For comparison, potassium nitrate (KNO_3) was also used as a catalyst precursor in this work. Xie, Peng, and Chen (2006) reported that $\text{KNO}_3/\text{Al}_2\text{O}_3$ with 35 wt% of KNO_3 loading showed a good catalytic activity with the highest conversion of 87% for transesterification of soybean oil with methanol. Because Al_2O_3 has low surface area, NaY should be a better support for this precursor. In the catalyst preparation, calcination temperature was also studied to find the suitable value for the decomposition of KNO_3 to generate K_2O .

With heterogeneous process, the change in catalyst stability by leaching of active species has been studied (Alonso, Mariscal, Moreno-Tost, Zafra Poves, and Granados, 2007; MacLeod, Harvey, Lee, and Wilson, 2008; Noiroj et al., 2009). MacLeod et al. (2008) evaluated the stability of alkali-doped metal oxide catalysts (LiNO_3/CaO , NaNO_3/CaO , KNO_3/CaO and LiNO_3/MgO) by comparing the performance of fresh and spent catalysts on transesterification under a similar condition. The reaction of oil with the catalyst leachate was investigated. The amount of alkali and alkaline earth metal leached into the reaction mixture was determined by

flame photometry and atomic absorption spectroscopy. The reuse of these catalysts showed good performance on transesterification with the conversion unchanged after 5 cycles.

Another method to check the stability is to test the catalytic activity with the catalyst leachate. Some degree of leaching could create some homogeneous catalytic activity. The residue alkali metal concentration in the reaction mixture is also the evidence that there is the metal leaching from the catalyst. Without calcination, Noiroj et al. (2009) determined the amount of K leaching from the KOH/Al₂O₃ and the KOH/NaY with X-ray fluorescence spectrometry (XRF) to compare the amount of active species on the prepared and spent catalysts. The results showed that 48.74% of the K was leached from the KOH/Al₂O₃ with 25 wt% of KOH loading. Thus, it was possible that the activity obtained was from catalyst in homogeneous phase. For the KOH/NaY catalyst with 10 wt% of KOH loading, it was found that only 3.18% of the K was leached. Although both catalysts could produce the same biodiesel yield (91.07%), the 10 wt% KOH/NaY had smaller amount of K leaching than that of 25 wt% of KOH/Al₂O₃. Thus, the 10 wt% KOH/NaY catalyst was expected to be a more appropriate catalyst than the 25 wt% KOH/Al₂O₃. Alonso et al. (2007) reported that the K leaches from K/γ-Al₂O₃ catalyst determined by inductively coupled plasma atomic emission spectroscopy (ICP-AES) were 65.81 and 84.93% after the first and the fourth run, respectively. The leaching was responsible for the loss of catalytic activity and, consequently, caused the decrease in biodiesel yield from the spent catalyst. Because the reusability of the catalyst depended on the active species on the surface, the study on leaching was investigated in this work.

The objective of the study in this chapter was to produce potassium catalysts on NaY zeolite by a method that preserved the zeolite structure. These catalysts were analyzed by several techniques such as X-ray diffraction (XRD), nitrogen adsorption-desorption and Fourier transform infrared spectroscopy (FTIR). The catalytic efficiency in the production of biodiesel from Jatropha seed oils with methanol via transesterification was studied. The effect of the reaction variables including the molar ratio of methanol to oil, the reaction time and the amount of potassium loading on zeolite were also investigated. Finally, the stability of catalyst was investigated by comparison of the activity of fresh and spent catalyst on the transesterification of glycerol trioctanoate.

3.2 Experimental

3.2.1 Synthesis of NaY zeolite

Rice husk silica (SiO_2) used in the NaY synthesis was obtained by acid leaching with a method from literature (Wittayakun, Khemthong, and Prayoonpokarach, 2008). The NaY zeolite was synthesized by a two-step route (Ginter, 2001; Wittayakun et al., 2008). First, a seed gel with a molar ratio of $10.67\text{Na}_2\text{O} : \text{Al}_2\text{O}_3 : 10\text{SiO}_2 : 180\text{H}_2\text{O}$ was prepared by mixing 6.65 g of distilled water, 1.35 g of NaOH (BDH) and 0.69 g of sodium aluminate (NaAlO_2 , Riedel-de Haën) in a 50-mL polypropylene (PP) beaker. The mixture was added into a solution containing 7.57 g of 27 wt% of sodium silicate (Na_2SiO_3) prepared from dissolution of SiO_2 in NaOH solution. The resulting mixture was stirred until homogeneous and transferred into a 100-mL PP bottle, capped and aged at room temperature for 24 h. Second, a feed gel with a molar ratio of $4.30\text{Na}_2\text{O} : \text{Al}_2\text{O}_3 : 10\text{SiO}_2 : 180\text{H}_2\text{O}$ was

prepared by mixing 43.65 g of distilled water, 0.05 g of NaOH and 4.36 g of NaAlO₂ in a 250-mL PP beaker, and adding the resulting mixture into a solution containing 47.48 g of 27 wt% of Na₂SiO₃. The resulting viscous mixture was used immediately without further aging. In the final step, the seed gel was slowly added into the feed gel under stirring to provide a more viscous mixture. The mixture was transferred into a 125-mL PP bottle, capped and aged at room temperature for another 24 h and crystallized at 90 °C for 24 h. The product containing NaY was cooled, filtered, washed thoroughly with distilled water until pH of the filtrate was lower than 9.0 and dried at 110 °C.

3.2.2 Preparation of the catalysts

Potassium acetate (CH₃COOK, UNILAB) and potassium nitrate (KNO₃, Carlo Erba) were used as the K precursor. The first precursor was prepared by mixing acetic acid (CH₃COOH, J. T. Baker) and CH₃COOK with varied concentration of potassium. Details of the preparation can be found in Appendix A. The K/NaY catalysts with K loading of 4, 8 and 12 wt% were prepared by impregnation of NaY with the precursor solution. The resulting mixtures were dried at 30 °C for 4 h and at 80 °C overnight before calcination at 400 °C for 3 h. The obtained samples were notated xK/NaY (x = 4, 8 and 12 wt% of K).

For a comparison purpose, the catalyst with 12 wt% of K loading on NaY was prepared by impregnation of KNO₃ solution on NaY. The resulting mixture was dried at 30 °C for 4 h and at 80 °C overnight before calcination at 500 °C or 600 °C for 3 h. The samples obtained after the calcination at 500 °C and 600 °C were denoted as 12K/NaY-1 and 12K/NaY-2, respectively.

3.2.3 Characterization of the synthesized NaY zeolite and the K/NaY catalysts

The phases of NaY and xK/NaY were analyzed by XRD on a Bruker, D5005 using Ni-filtered Cu K α radiation at 40 kV and 40 mA. The data were collected from 5 to 50° with a step size of 0.02.

Surface areas of NaY and xK/NaY were determined by N₂ adsorption-desorption analysis on a Micromeritics ASAP 2010 using the Brunauer-Emmet-Teller (BET) method from the adsorption data in the relative pressure range of 0.02-0.2. Prior to the measurement, the samples were degassed at 300 °C for 10 h.

FTIR spectra of the samples were recorded on a Perkin-Elmer, GX spectrometer in the mid IR range (4000-400 cm⁻¹) with a resolution of 4 cm⁻¹. The samples were prepared by KBr pellet technique by grinding with KBr (a ratio of sample : KBr approximately 1:200) to very fine powder and pressing to form a transparent disk using a hydraulic press with an equivalent weight of ca. 10 tons for 1 min.

3.2.4 Catalytic testing for transesterification

In the catalytic testing for transesterification, the analytical grade methanol (CH₃OH, QR \ddot{C}) and Jatropha seed oil were used as the reactants. The parent NaY, 4K/NaY, 8K/NaY, 12K/NaY, 12K/NaY-1 and 12K/NaY-2 were used as catalysts. The condition of transesterification was as follows: a methanol to oil molar ratio of 16:1, a reaction temperature of 65 °C and catalyst to oil ratio of 4% w/w. The transesterification was performed in a 50-mL round bottom flask equipped with a water-cooled condenser as shown in Figure 3.1.

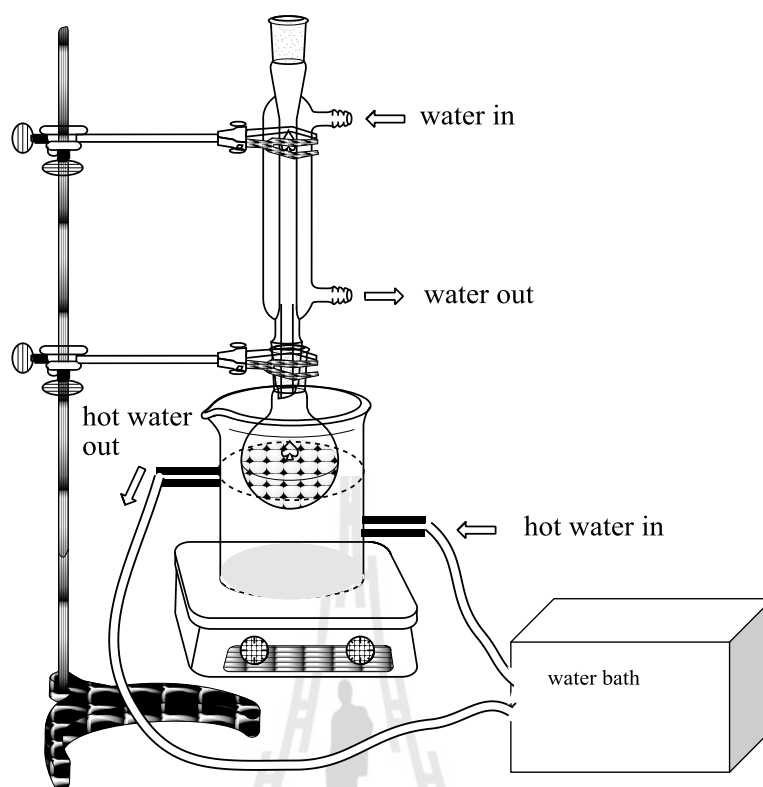


Figure 3.1 Apparatus set up for transesterification

A mixture of ca. 5.0 g Jatropha oil, ca. 0.2 g catalyst and ca. 2.9 g methanol was magnetically stirred and heated to 65 °C by using water bath (Heto Lab Equipment, AT110, Denmark) in which a constant temperature was maintained by hot water circulation. After the study period, the catalyst was separated by centrifugation (Heraeus Sepatech, Labofuge 200, Germany). The liquid mixture was separated in a separatory funnel and only the upper layer was taken to further analysis. The excess methanol was removed using a rotary evaporator. The remaining crude oil and methyl esters in the final mixture could be preliminarily identified by thin layer chromatography (TLC). A small drop of the sample was spotted on a TLC plate and developed in iodine vapor (as described in 3.2.5).

The performances of the heterogeneous catalysts were compared to that of a conventional NaOH homogeneous catalyst. The experiment was done according to a process described in literature (Berchmans and Hirata, 2008). NaOH (0.05 g with catalyst to oil ratio of 1% w/w) was dissolved in methanol before addition of ca. 5.0 g of Jatropha seed oil. After 3 h, when the reaction was complete, the reaction mixture was transferred into a separatory funnel, allowed to stand to separate into two phases; the upper layer contained methyl esters and the lower layer contained glycerol. The methyl esters were washed three times with ca. 2 mL of warm water (50 °C) to remove the catalyst, soap and trace of glycerol. Any remaining water was removed by anhydrous sodium sulphate (Na₂SO₄, CARLO ERBA).

The conversion was estimated by TLC with the procedure mentioned in section 3.2.5.

3.2.5 Analysis of reaction mixture and determination of biodiesel yield

3.2.5.1 Preliminary determination of conversion of transesterification by TLC

The progress of transesterification of all experiments was monitored by spotting the reaction mixture on TLC plates of size 5 cm × 2 cm and 5 cm × 3 cm (Silica Gel 60 F254; Merck, Darmstadt, Germany). A start line was drawn 1 cm from the bottom using a pencil. Fatty acid methyl ester standard (F.A.M.E. Mix, C8-C24, Supelco, 18918-1AMP) and Jatropha crude oil were also spotted on the TLC plate as references. After the spots were dried, the plate was developed in a solvent mixture of petroleum ether (Analytical grade (AR grade), J. T. Baker)/diethyl ether (AR grade, C₄H₁₀O, QRëC)/glacial acetic acid (AR grade, CH₃COOH, J. T. Baker) with a ratio of

85:15:1, v/v/v (Sukhawanit, Srinophakun, and Matsumura, 2004) and the dried plate was exposed to iodine vapor (UNICHROM) to determine the mobility of each component on the stationary phase.

3.2.5.2 Determination of biodiesel yield by GC

The solvents used in the experiments including hexane (C₆H₁₄, Lab Scan) and chloroform (CHCl₃, Mallinckrodt) were AR grade. Methyl esters in gas chromatography grade (GC grade) such as that of palmitic (C₁₇H₃₄O₂, Sigma, P5177), palmitoleic (C₁₇H₃₂O₂, Sigma, P9667), heptadecanoic (C₁₈H₃₆O₂, Sigma, H4515), stearic (C₁₉H₃₆O₂, Sigma, S5376), oleic (C₁₉H₃₆O₂, Sigma, O4754), linoleic (C₁₉H₃₄O₂, Sigma, L1876), linolenic (C₁₉H₃₂O₂, Sigma, L2626) and arachidic acids (C₂₁H₄₂O₂, Sigma, A3881) were used as standards. Methyl ester of nonadecanoic acid (C₂₀H₄₀O₂, Sigma, N5377) was used as an internal standard. The concentration (g/mL) of each methyl ester was obtained from a separate calibration curve. The preparation details of the stock solutions and calibration curves can be found in Appendix B.

The quantity of methyl esters was determined by a gas chromatograph (Hewlette Packard, GC-HP6890) equipped with a flame ionization detector (FID) and 30-meter HP-INNOWAX polyethylene glycol capillary column with 0.32 mm id and 0.15 μm film thickness. The initial column temperature was held at 140 °C for 3 min before ramping to 240 °C with a rate of 10 °C/min and held for 8 min. The biodiesel yield, the sum of all methyl esters, was calculated by a method from literature using equation 3.4 (Liu, Piao, Wang, Zhu, and He, 2008).

$$\% \text{ yield} = \frac{C_{\text{ester}} \times n}{\rho_{\text{oil}}} \times 100 \quad (3.4)$$

where C_{ester} is the concentration of methyl ester in g/mL; n is the diluted multiple of methyl ester, which can be calculated using the total volume of the n -hexane and the internal standard solution divided by the volume of methyl ester sample; ρ_{oil} is the density of *Jatropha* seed oil which was 0.91 g/mL.

3.2.6 Investigation of catalyst stability

In this work, the evaluation of the catalyst stability was studied by two methods: 1) comparing the performance of the fresh and spent catalysts on transesterification of *Jatropha* seed oil with methanol and 2) testing the catalyst leachate activity on transesterification of glycerol trioctanoate.

3.2.6.1 Catalyst performance of the spent catalyst

The stability of the spent catalyst providing the highest biodiesel yield, namely, 12K/NaY was investigated. The spent catalyst was separated from the reaction mixture by centrifugation, washed three times with hexane, dried at 60 °C and tested again for transesterification with a condition similar to the fresh catalyst (see section 3.2.4).

3.2.6.2 Catalyst leachate activity on transesterification of glycerol trioctanoate

The catalyst leachate prepared by soaking the fresh 12K/NaY in methanol at 90 °C for 1 h was used for the transesterification of glycerol trioctanoate by a procedure from Meyer, Roessner, Rakoczy, and Fischer (2010). The glycerol trioctanoate which is a single triglyceride was selected instead of native vegetable oils which are composed of several triglycerides. Thus, the progress of transesterification

through the intermediates to methyl ester and glycerol is easy to observe without any interference.

The catalytic testing was performed in a three-necked round-bottom flask fitted with a condenser, a thermometer and a septum (Figure 3.2). The reactants were mixed using a magnetic stirrer with speed of 1,200 rpm. The reaction condition included a methanol to glycerol trioctanoate molar ratio of 9:1, reaction temperature of 90 °C and catalyst to glycerol trioctanoate ratio of 10% w/w. In an initial test of the catalyst leachate, 3.0 g of activated 12K/NaY catalyst treated at 400 °C for 8 h in a tube furnace under nitrogen was added to 30.3 g of glycerol trioctanoate preheated to 90 °C under a vigorous stirring. The time of the reaction was recorded after an addition of 23.4 mL of anhydrous methanol. After 1 h, the catalyst was removed by filtration and the reaction of the catalyst leachate with glycerol trioctanoate was then proceeded.

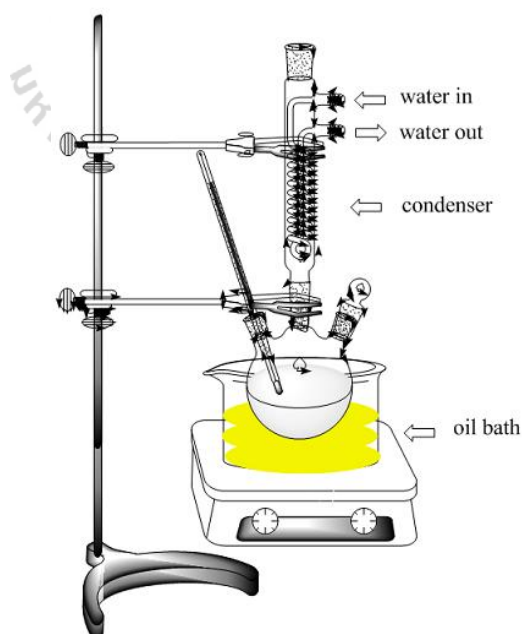


Figure 3.2 Apparatus set up for catalyst leaching testing for transesterification of glycerol trioctanoate.

During 1 h of reaction time, a 50 μL of sample was collected at the reaction time of 5, 10, 15, 20, 30, 45 and 60 min. Another 50 μL was collected at the reaction time of 90, 120, 160, 180 and 210 min. The reaction mixture was separated by filtration and its composition was determined by GC.

The reaction mixtures were derivatized to achieve a fast and complete analysis of the monoglycerides, the diglycerides and the glycerol in the presence of trioctanoate methyl ester before GC analysis (Plank and Lorbeer, 1995). The derivatization of the reaction mixture was carried out by adding 300 μL of bis(trimethylsilyl) trifluoroacetamide (BSTFA) as the silylating agent and 100 μL of pyridine to a sample of the reaction mixture in a 1-mL vial, heating at 75 $^{\circ}\text{C}$ for 15 min for the silylation and dissolving in 600 μL of hexane and the resulting mixture was analyzed by GC.

The GC analyses were performed with a HP 5890 gas chromatograph. The instrument was equipped with an Optima 5Accent fused silica column (15 m \times 0.25 mm, with a 0.25 mm film made up of 5% diphenylpolysiloxane and 95% dimethylpolysiloxane, Marcherey–Nagel) and flame ionization detector (FID). The data evaluation was performed using HP Chemstation software. The amount of products (given in mol%) was calculated according to Equation 3.5 on the basis of chromatogram peak area considering the corresponding response factors of both silylated and unsilylated compounds (Meyer et al., 2010).

$$\text{mol}\%_i = \frac{R_i A_i}{\sum_i R_i A_i} \quad (3.5)$$

The $\text{mol}\%_i$ represents the percentage of component i in the reaction mixture, A_i is the chromatogram area and R_i is the response factor including the correction for chemical structure and silylation.

3.3 Results and discussion

3.3.1 Characterization of NaY and K/NaY catalysts

3.3.1.1 XRD

XRD patterns of the parent NaY and xK/NaY ($x = \text{K loading of 4, 8 and 12 wt}\%$) are shown in Figure 3.3. Characteristic peaks of NaY similar to those in the literature (Wittayakun et al., 2008) were still observed in all catalysts indicating that impregnation of the zeolite with the mixture of $\text{CH}_3\text{COOH}/\text{CH}_3\text{COOK}$ did not cause an apparent impact on the NaY structure. The peak intensity decreased as the K loading increased probably because the crystallinity of zeolite decreased. Similar observation was also reported in the literature (Noiroj et al., 2009) that the characteristic peaks of NaY were still visible when loaded with 7-15 wt% KOH and the peak intensity decreased with KOH loading. Xie et al. (2007) also stated that KOH/NaX samples with KOH loading of 4-14 wt% gave similar XRD pattern to that of the parent NaX. Moreover, the peaks of new phases of K species such as K_2O ($2\theta = 31^\circ$ and 39°) were not observed after K loading, indicating the good dispersion of K on NaY. The results were similar to those in the literature (Xie and Li, 2006) in which the peaks of K_2O as new phase of K species were not observed when NaY was loaded with KI solution.

XRD patterns of 12K/NaY-1 and 12K/NaY-2 catalysts (Figure 3.3) also showed the characteristic peaks of NaY with lower intensities. The destruction of

NaY structure was not observed in 12K/NaY-2 which was calcined at 600 °C indicating high thermal stability. In addition, characteristic peaks of KNO_3 ($2\theta = 19.0$, 23.6 , 29.4 and 33.8°) (Zhu, Wang, Chun, and Wang, 1998) were not observed indicating that KNO_3 was well dispersed on zeolite. The loading of KNO_3 in this work was probably too low to form large aggregates.

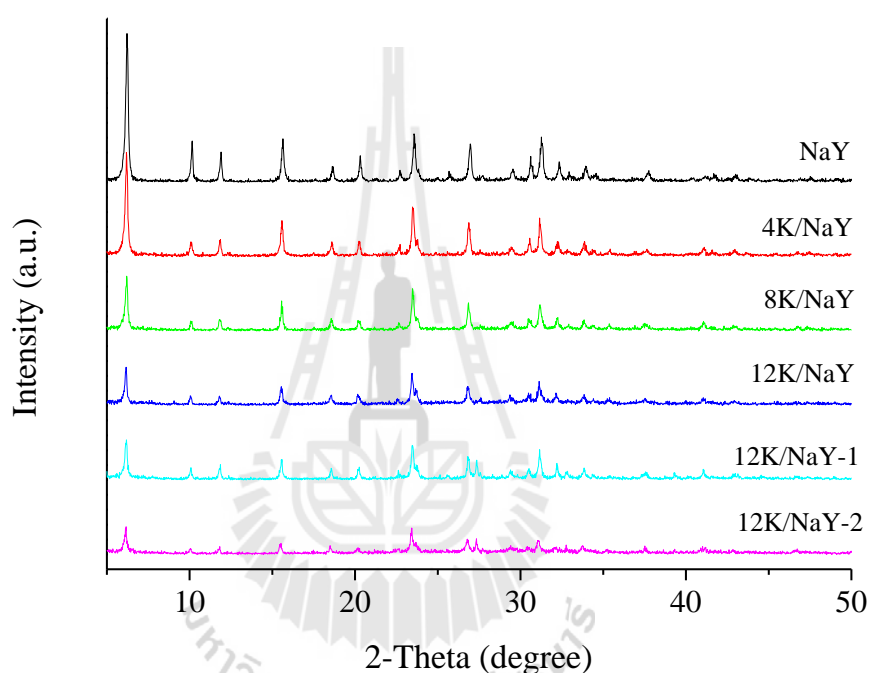


Figure 3.3 XRD patterns of the parent NaY, xK/NaY ($x = 4, 8$ and 12 wt% loading of K), 12K/NaY-1 and 12K/NaY-2.

3.3.1.2 Surface area analysis

N_2 adsorption/desorption isotherms of NaY and xK/NaY are shown in Figure 3.4. The isotherms of all samples were type I, characteristic of microporous materials such as zeolite. With increased K loading on NaY, the adsorbed volume decreased, suggesting the occupation of potassium species in the pore volume of NaY.

The BET surface areas of parent NaY and xK/NaY are shown in Table 3.1. All catalysts had lower surface areas than that of the parent NaY because K_2O generated after decomposition of CH_3COOK possibly located on both the surface and occluded in the zeolite. The decrease in surface areas of xK/NaY had a linear relationship with potassium loading (R^2 of 0.9938). However, these changes were less dramatic than those observed on NaY loaded with KOH whose decrease compared to that of the parent NaY with potassium loading of 7, 8, 9, 10 and 13 wt% were 62.4, 72.2, 78.1, 95.2 and 97.3%, respectively (Noiroj et al., 2009). The results indicated that changing potassium precursor from KOH to the mixture of CH_3COOH/CH_3COOK could preserve the zeolite structure. Moreover, the decrease of surface areas of xK/NaY catalysts was consistent with the decrease of the XRD intensity of NaY when the K loading was increased.

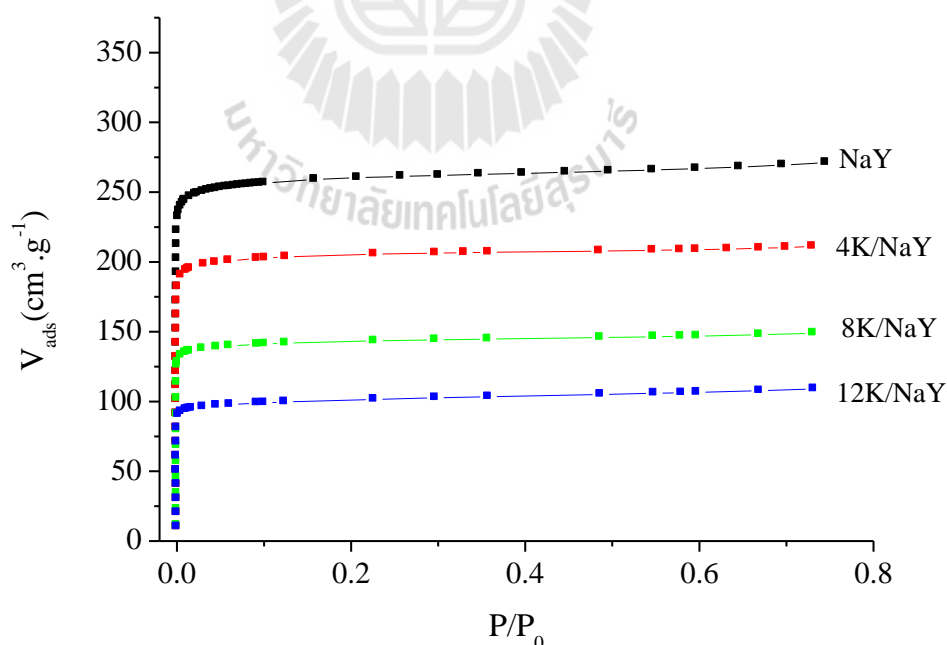


Figure 3.4 Nitrogen adsorption isotherms of the parent NaY and xK/NaY catalysts (x = 4, 8 and 12 wt%).

Table 3.1 BET surface areas of parent NaY zeolite, xK/NaY catalysts and relative percent decrease.

sample	BET surface area (m ² . g ⁻¹)	Percent decrease from NaY (%)
Parent NaY	934.72	-
4K/NaY	727.99	22.1
8K/NaY	506.10	45.9
12K/NaY	356.48	61.9

3.3.1.3 Infrared spectroscopy

FTIR spectra of NaY and xK/NaY catalysts are shown in Figure 3.5. From the parent NaY zeolite, peaks in the region 400-1200 cm⁻¹ were assigned to the fundamental vibrations of (Al,Si)O₄ tetrahedrals which were the primary building units of zeolite framework (Flanigen, Khatami, and Szymanski, 1971). The peak at 567 cm⁻¹ was attributed to double ring external linkage associated with the FAU structure (Ginter, Bell, and Radke, 1992). The peaks at 766 and 1000 cm⁻¹ were assigned to asymmetric and symmetric stretching vibration of external linkage (Flanigen et al., 1971). Moreover, the peaks at 464 and 691 cm⁻¹ were assigned to bending and symmetric stretching vibration of the internal tetrahedral (Rayalu, Udhoji, Meshram, Naidu, and Devotta, 2005). Absorption bands at 3468 and 1638 cm⁻¹ were assigned to stretching and bending vibration of hydroxyl groups of absorbed water (Xue et al., 2009).

After impregnating NaY with CH₃COOH/CH₃COOK with 12 wt% of K, all as-prepared samples (before calcination) still showed fundamental absorption

peaks of NaY. The new absorption peaks at 1567, 1416, 1345 and 646 cm^{-1} appeared attributing to the C=O antisymmetric stretching, C=O symmetric stretching, CH_3 deformation and OH translation modes, respectively (Frost, Locos, Kristof, and Kloprogge, 2001). The absorption peaks in the region 400-1200 cm^{-1} were still observed, indicating the existence of NaY structure. Furthermore, the absorption intensity at ~ 3468 and 1638 cm^{-1} decreased due to the exchange of potassium ions with proton on the OH groups (Rashtizadeh, Farzaneh, and Ghandi, 2010).

When the catalysts with 4, 8 and 12 wt% of K loading were calcined at 400 °C, the absorption peaks at 1567, 1416 and 646 cm^{-1} were not observed because acetate group was removed by oxidation and/or decomposition. However, the absorption peak of CH_3 deformation at 1345 cm^{-1} was still observed. The IR spectra of 4K/NaY, 8K/NaY and 12K/NaY catalysts also exhibited the absorption peaks at 1695, 1449, 1393 and 841 cm^{-1} , which suggested the formation of carbonate after activation (Sun et al., 2009). Moreover, IR spectra of the framework structure of NaY in the region 400-1200 cm^{-1} were clearly observable suggesting that the NaY structure was retained.

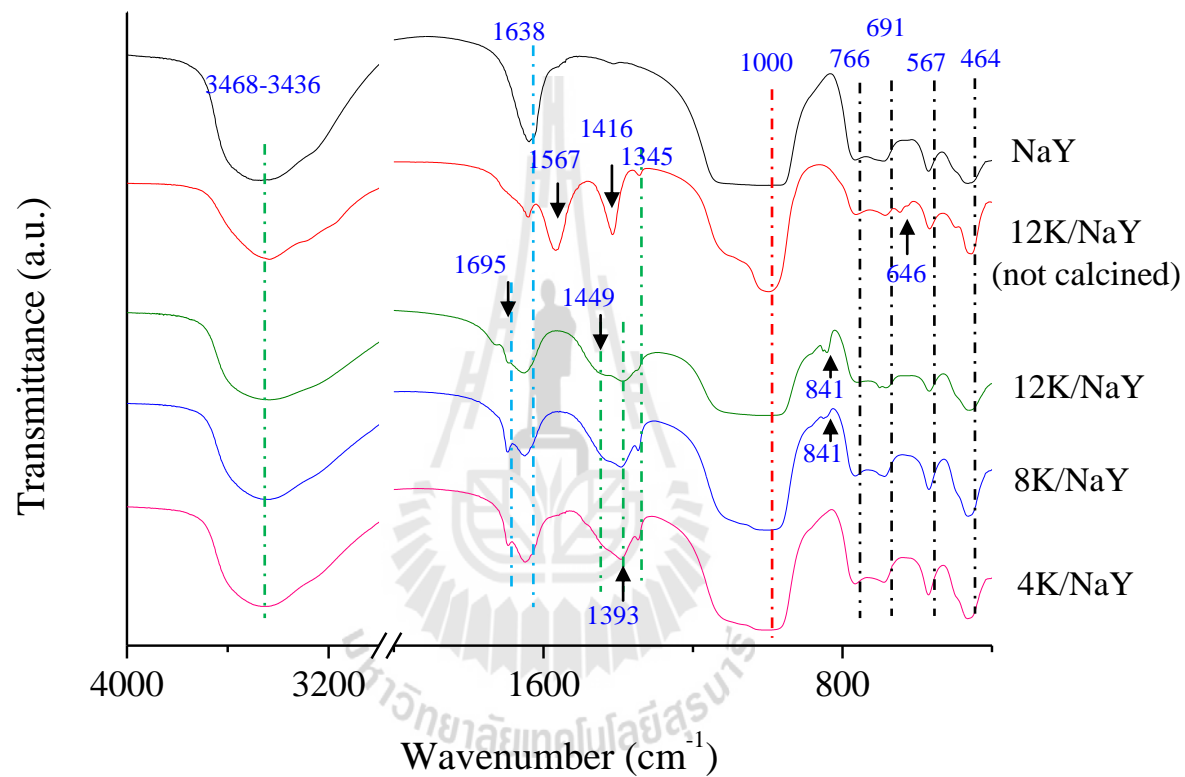


Figure 3.5 FTIR spectra of the parent NaY, calcined K/NaY catalysts with 4, 8 and 12 wt% loading of K and as-prepared K/NaY with 12 wt% loading of K (before calcination).

3.3.2 Catalytic testing for transesterification

3.3.2.1 Effect of wt% loading of potassium

Figure 3.6 shows spots on the TLC plate of the mixture from transesterification catalyzed by the parent NaY after 3 h of reaction. The spots of the reaction mixture from NaY were similar to that of the crude Jatropha seed oil, without any methyl ester. This result suggested that NaY was not active for transesterification and only served as a support for K.

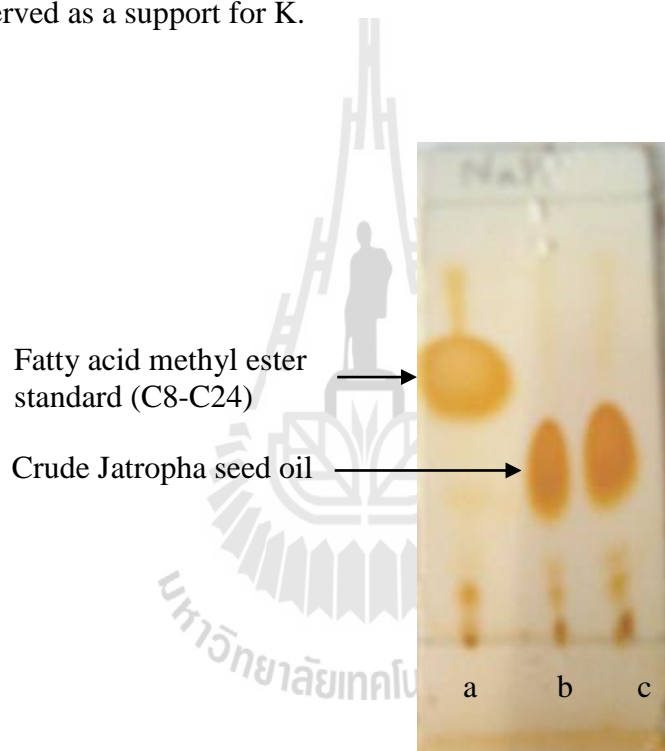


Figure 3.6 Spots on the TLC plate of the mixture from transesterification of Jatropha seed oil over the parent NaY zeolite (b and c) compared to that of fatty acid methyl ester standard (a). Reaction condition: methanol to oil molar ratio of 16:1, reaction time of 3 h and temperature of 65 °C.

Figure 3.7 shows spots on the TLC plate of the mixture from transesterification over $x\text{K}/\text{NaY}$ ($x = 4, 8$ and 12 wt%). Over the $4\text{K}/\text{NaY}$ catalyst, spots with similar position to that of the crude oil and methyl ester standard were observed indicating that the oil was partially converted to methyl esters. The separation of spots on the TLC plate exhibited that less than 50% of the oil according to the spot area was converted to methyl esters. The low conversion was probably attributed to its relatively low active sites. On the $8\text{K}/\text{NaY}$ catalyst, the conversion increased to about 70% according to the area of the spot of methyl esters on the TLC plate. Finally, the $12\text{K}/\text{NaY}$ catalyst provided the highest conversion of nearly 100% because only a spot of methyl esters was observed.

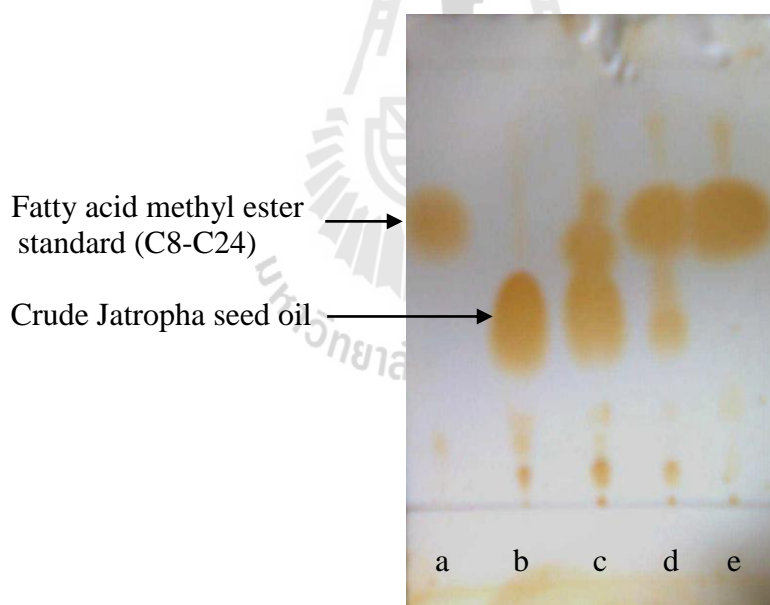


Figure 3.7 Spots on the TLC plate of the mixtures from transesterification of Jatropha seed oil on $4\text{K}/\text{NaY}$ (c), $8\text{K}/\text{NaY}$ (d) and $12\text{K}/\text{NaY}$ (e) compared to that of fatty acid methyl ester standard (a) and crude Jatropha seed oil (b). Reaction condition: methanol to oil molar ratio of 16:1, reaction time of 3 h and temperature of $65\text{ }^{\circ}\text{C}$.

It could be concluded that the conversion of Jatropha seed oil increased with increasing K loading on NaY and the loading of 12 wt% was suitable providing a complete conversion within 3 h. Thus, further studies on reaction parameters were only conducted on 12K/NaY.

Moreover, the performances of the catalyst with 12 wt% of K from KNO_3 precursor on NaY (12K/NaY-1 and 12K/NaY-2 catalysts) were studied. The TLC result from 12K/NaY-1 (Figure 3.8) showed only spots similar to that of the crude oil indicating that they could not catalyze the conversion of the Jatropha seed oil to methyl esters.

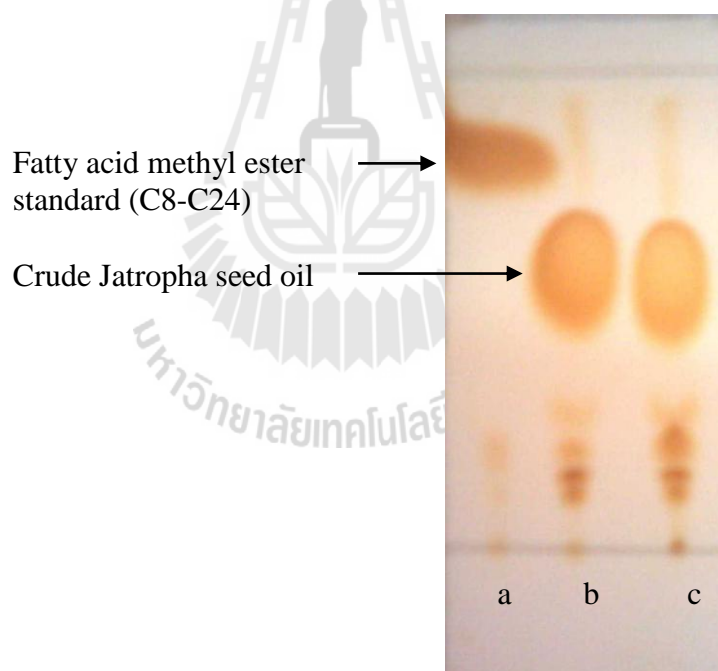


Figure 3.8 Spots on the TLC plate of the mixtures from transesterification of Jatropha seed oil over 12K/NaY-1 (b) and 12K/NaY-2 (c) compared to that of fatty acid methyl ester standard (a). Reaction condition: methanol to oil molar ratio of 16:1, reaction time of 3 h and temperature of 65 °C.

Because the products from the reaction over 12K/NaY-2 were similar to that from 12K/NaY-1. Changing calcination temperature from 500 to 600 °C did not improve the activity for transesterification. Consequently, the catalysts prepared from KNO_3 were not further investigated.

After the preliminary examination of the conversion of the Jatropha seed oil to methyl esters on xK/NaY prepared from the solution of $\text{CH}_3\text{COOH}/\text{CH}_3\text{COOK}$ with various loading and from KNO_3 , the most active catalyst was 12K/NaY. Therefore, only the products from this catalyst were analyzed to determine the total methyl ester yield by GC. This 12K/NaY was also used further to study effect of reaction time and methanol to oil molar ratio and its stability.

A correlation between the basicity and catalytic activity of xK/NaY towards the transesterification of Jatropha seed oil was reported in Chapter IV.

3.3.2.2 Effect of reaction time on 12K/NaY catalyst

Spots on the TLC plate of the mixtures from transesterification with 12K/NaY catalyst at 1, 2 and 3 h of the reaction time are shown in Figure 3.9. The spots similar to the crude Jatropha oil were still observed with the reaction time of 1 and 2 h indicating the incomplete reaction. With the 3 h reaction time, only a spot similar to that of methyl esters was observed suggesting the complete reaction. The conversion on the 12K/NaY clearly increased with time and 3 h was suitable to give a complete conversion of Jatropha seed oil to methyl esters. This reaction time was similar to that of KOH/NaY reported by Noiroj et al. (2009).

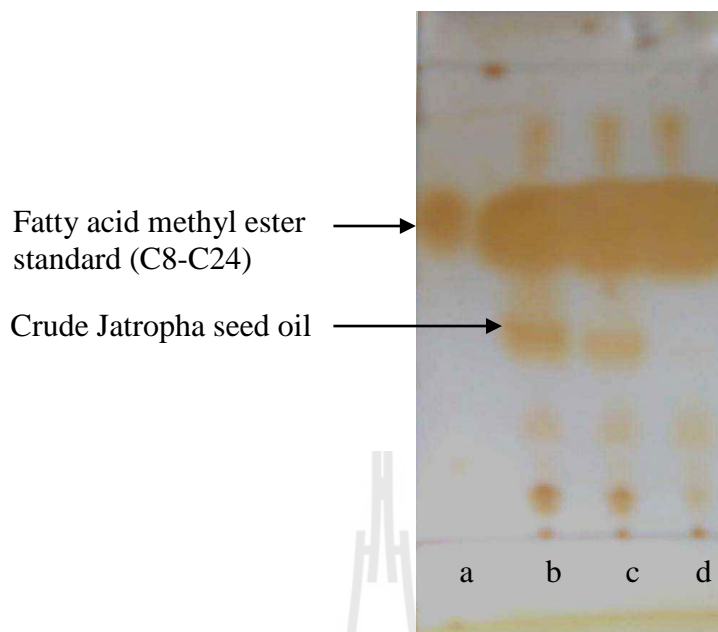


Figure 3.9 Spots on the TLC plate of the mixtures from transesterification of Jatropha seed oil over 12K/NaY catalyst at various reaction times (b) 1 h, (c) 2 h and (d) 3 h compared to that of (a) fatty acid methyl ester standard. Reaction condition: methanol to oil molar ratio of 16:1 and temperature of 65 °C.

For a comparison, the conversion of Jatropha seed oil was compared to that from the homogeneous catalyst. With NaOH, the reaction was carried out at 1 and 3 h and spots on the TLC of the reaction mixtures are shown in Figure 3.10. The complete conversion was observed from both durations.

It can be concluded that the conversion of Jatropha seed oil on 12K/NaY with reaction time of 3 h was similar to that with the NaOH catalyst. Because the reaction time for heterogeneous catalyst on transesterification was still longer than that of the homogeneous one, more development is needed to improve the reaction rate.

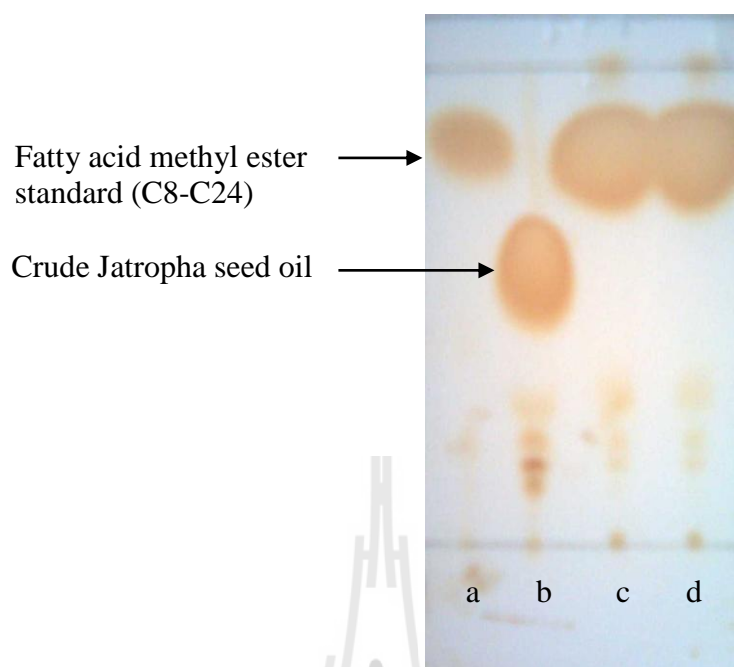


Figure 3.10 Spots on the TLC plate of the mixtures from transesterification of Jatropha seed oil with NaOH catalyst at various reaction times (c) 1 h and (d) 3 h compared to that of (a) fatty acid methyl ester standard and (b) crude Jatropha seed oil. Reaction condition: methanol to oil molar ratio of 16:1 and temperature of 65 °C.

3.3.3.3 Effect of methanol to oil molar ratio

According to Scheme 3.1, the theoretical mole ratio of methanol to triglyceride for transesterification is 3:1. Because this is an equilibrium reaction, an excess of methanol is required to shift the equilibrium to the product side to increase the conversion. The effect of methanol to oil molar ratio was studied on the ratio of 9:1, 16:1 and 20:1. The conversion from these ratios were studied by TLC. The results in Figure 3.11 showed that the reaction was not complete with the molar ratio of 9:1,

but complete with the other two molar ratios. Although the excess amount of methanol had no significant effect on the conversion, it caused difficulty on the glycerol separation due to the increase in its solubility, resulting in the decreased biodiesel yield (Kim et al., 2004; Meher et al., 2006).

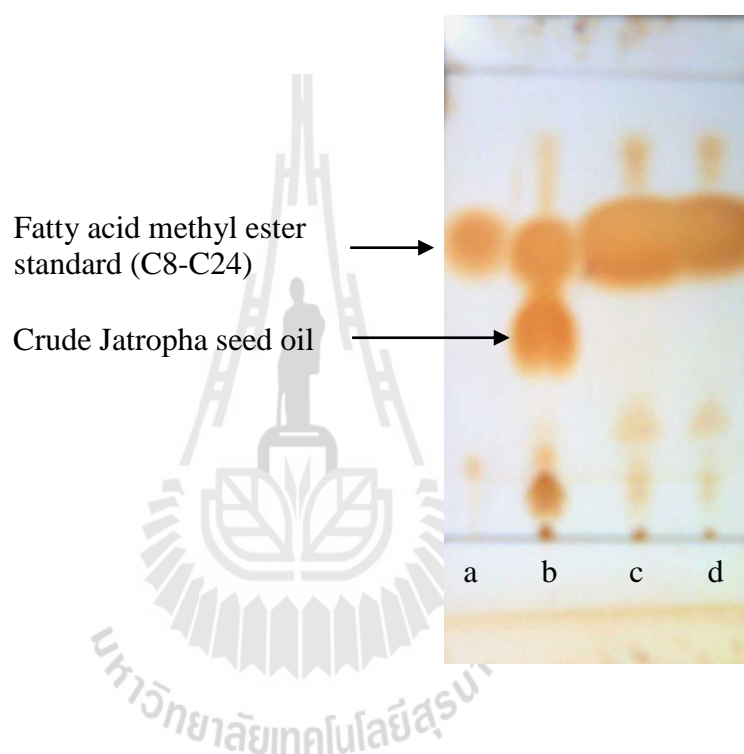


Figure 3.11 Spots on the TLC plate of the mixtures from transesterification of Jatropha seed oil with 12K/NaY at methanol to oil molar ratio of (b) 9:1, (c) 16:1 and (d) 20:1 compared to that of (a) fatty acid methyl ester standard. Reaction condition: reaction time of 3 h and temperature of 65 °C.

Table 3.2 compared the biodiesel yields from the reaction with various methanol to oil ratios. The highest yield was obtained when the molar ratio was 16:1. The high methanol to oil molar ratio is required to overcome the limitation of mass transfer. According to the results, the most suitable ratio was 16:1.

Moreover, yield from using NaOH as homogeneous catalyst was similar to that from using 12K/NaY catalyst. The high acid value of Jatropha seed oil could result in more soap formation, resulting in the decreased biodiesel yield.

Table 3.2 Biodiesel yield from 12K/NaY catalyst at different methanol to oil molar ratios and from NaOH as homogeneous catalyst.

Catalyst	Methanol to oil molar ratio	Biodiesel yield (%)
12K/NaY	9:1	42.6
	16:1	73.4
	20:1	71.6
NaOH	16:1	68.6

3.3.3 Catalyst leaching test in transesterification

3.3.3.1 Transesterification of Jatropha oil with the spent catalyst

Figure 3.12 shows spots on the TLC plate of the reaction mixture catalyzed by spent 12K/NaY. The mixture contained both crude Jatropha seed oil and methyl esters implying that the reaction was not complete. The conversion from the spent 12K/NaY catalyst was less than that from the fresh 12K/NaY catalyst. This

result suggested that the catalyst was partially deactivated and the cause of deactivation might be from loss of active species by leaching.

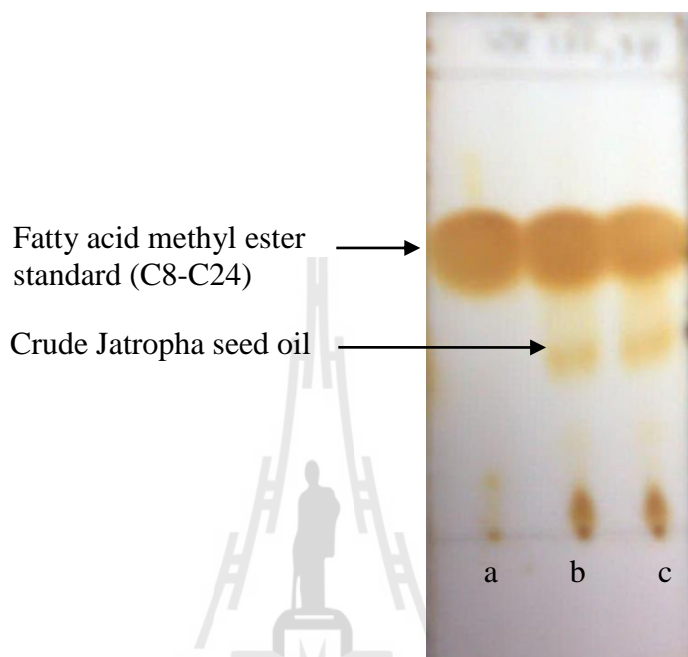


Figure 3.12 Spots on the TLC plate of the mixtures from transesterification of Jatropha seed oil with the spent 12K/NaY (b and c) compared to that of fatty acid methyl ester standard (a). Reaction condition: methanol to oil molar ratio of 16:1, reaction time of 3 h and temperature of 65 °C.

3.3.3.2 Transesterification of glycerol trioctanoate

There are three consecutive and reversible reactions in transesterification [Eq. (3.1)-(3.3)] and the reaction mixture composition contained monoglycerides, diglycerides, triglycerides, alkyl esters and glycerol. Such compositions were also observed in the transesterification of glycerol trioctanoate on 12K/NaY. As shown in Figure 3.13, glycerol trioctanoates was about 60 mol% at 5

min of reaction and afterward quickly decreased until about 5 mol% in a range of 5-30 min. After that, it gradually decreased and only 1-2 mol% was left after 60 min. Octanoic acid methyl ester was a major product with about 25 mol% at 5 min and rapidly increased to nearly constant value at 75 mol% within 30 min. The highest octanoic acid methyl ester of 75% was obtained at 60 min. Another product was glycerol which increased slowly and reached about 20 mol% in 60 min. For monoglycerides and diglycerides, the yield increased in the first 15 min and slowly decreased afterward. The results clearly indicated that octanoic acid methyl ester and glycerol increased because of the conversion of the glycerides to octanoic acid methyl ester and glycerol.

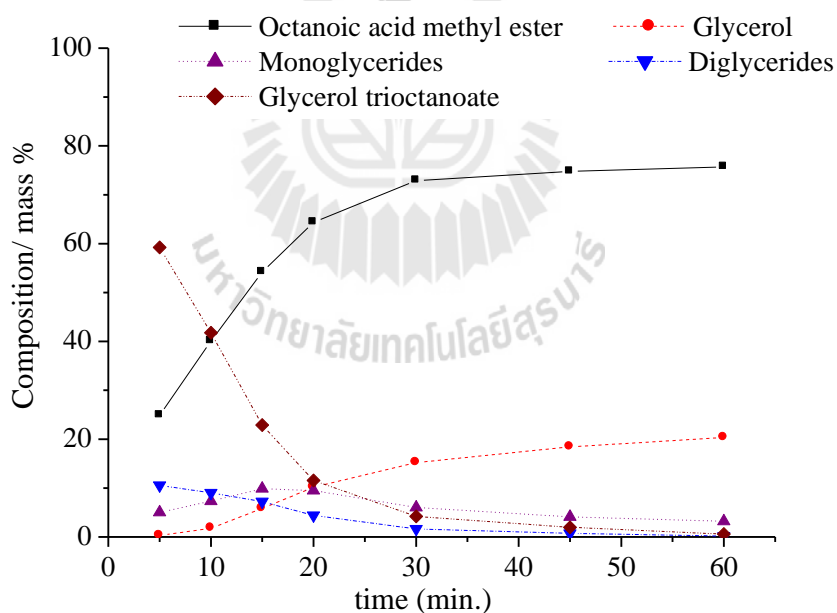


Figure 3.13 The composition of the reaction mixture for the consecutive transesterification of glycerol trioctanoate with methanol in the presence of 12K/NaY.

After 60 min, the 12K/NaY catalyst was removed and samples of the reaction mixture, without the catalyst, were collected at 90, 120, 160, 180 and 210 min for the determination of the yield of octanoic acid methyl ester. The results are shown in Figure 3.14. The increased of octanoic acid methyl ester yield was still observed even though the tranesterification was run without catalyst. If the catalyst was completely absent, the yield octanoic acid methyl ester should remain the constant. The result implied that active species was still present and it could be from the K species was leached into reaction mixture. The leachate from 12K/NaY could serve as a homogeneous catalyst in the tranesterification. This result was consistent with the decrease of activity of the spent 12K/NaY.

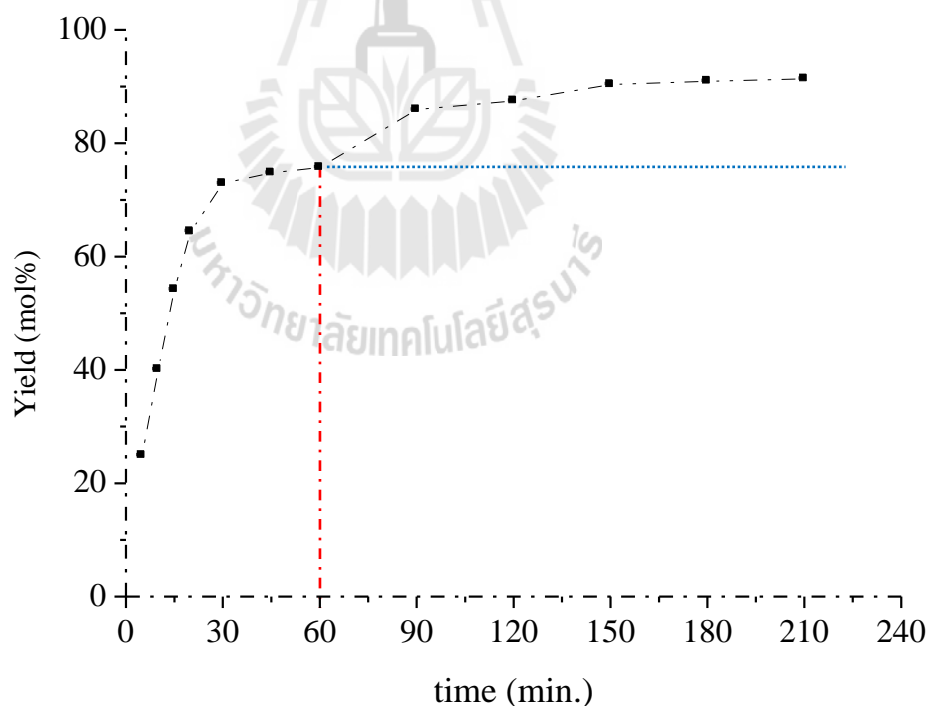


Figure 3.14 The composition of the reaction mixture for the consecutive tranesterification of glycerol trioctanoate with methanol in the absence of 12K/NaY.

3.4 Conclusions

The extracted oil from seeds of *Jatropha Curcas* cultivated in Nakhon Ratchasima was used as a feedstock to produce biodiesel via transesterification over heterogeneous catalysts consisting of potassium supported on NaY (K/NaY) with potassium loading of 4, 8 and 12 wt%. The catalysts prepared by impregnation of NaY with a solution of CH₃COOK/CH₃COOH could prevent collapses of the zeolite structure. The 12K/NaY catalyst provided the highest biodiesel yield of 73.4% under the reaction time of 3 h, the reaction temperature of 65 °C and methanol to oil molar ratio of 16:1. This yield was higher than that from a reaction with homogeneous NaOH catalyst under the same condition which produced 68.6%. Other heterogeneous catalysts with 12 wt% of K from potassium nitrate precursor on NaY were not active for transesterification. However, the catalyst was partially deactivated because the active species leached out to the reaction mixture.

3.5 References

- Alonso, D. M., Mariscal, R., Moreno-Tost, R., Zafra Poves, M. D. and Granados, M. L. (2007). Potassium leaching during triglyceride transesterification using K/ γ -Al₂O₃ catalysts. **Catalysis Communications**. 8: 2074-2080.
- Barthomeuf, D. (1996). Basic Zeolites: Characterization and Uses in Adsorption and Catalysis. **Catalysis Reviews**. 38: 521-612.
- Berchmans, H. J. and Hirata, S. (2008). Biodiesel production from crude *Jatropha curcas* L. seed oil with a high content of free fatty acids. **Bioresource Technology**. 99: 1716-1721.

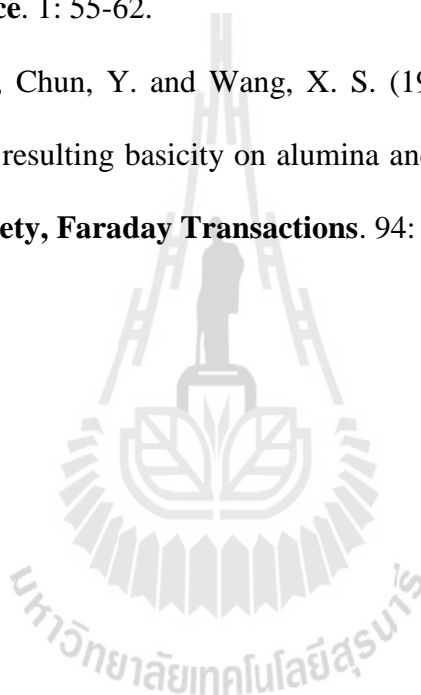
- Chung, K. -H. and Park, B. -G. (2009). Esterification of oleic acid in soybean oil on zeolite catalysts with different acidity. **Journal of Industrial and Engineering Chemistry**. 15: 388-392.
- Demirbas, A. (2007). Importance of biodiesel as transesterification fuel. **Energy Policy**. 35: 4661-4670.
- Flanigen, E. M., Khatami, H. and Szymanski, A. H. (1971). Infrared Structural Studies of Zeolite Frameworks. In: **Molecular Sieve Zeolites-I, Advances in Chemistry**, Vol. 101: Flanigen, E. M. and Sand, L. B. (eds.). pp. 201-229. American Chemical Society, Washington DC.
- Frost, R. L., Locos, O. B., Kristof, J. and Kloprogge, J. T. (2001). Infrared spectroscopic study of potassium and cesium acetate-intercalated kaolinites. **Vibrational Spectroscopy**. 26: 33-42.
- Gerpen, J. V. (2005). Biodiesel processing and production. **Fuel Processing Technology**. 86: 1097-1107.
- Ginter, D. (2001). Linde type X. In: **Verified Syntheses of Zeolitic Materials**: Robson, H. (2nd ed.). pp. 156-158. Elsevier Science B. V., The Netherlands.
- Ginter, D. M., Bell, A. T. and Radke, C. J. (1992). The effects of gel aging on the synthesis of NaY zeolite from colloidal silica. **Zeolites**. 12: 742-749.
- Hattori, H. (1995). Heterogeneous Basic Catalysis. **Chemical Reviews**. 95: 537-558.
- Kim, H. -J., Kang, B. -S., Kim, M. -J., Park, Y. -M., Kim, D. -K., Lee, J. -S. and Lee, K. -Y. (2004). Transesterification of vegetable oil to biodiesel using heterogeneous base catalyst. **Catalysis Today**. 93-95: 315-320.

- Liu, X., Piao, X., Wang, Y., Zhu, S. and He, H. (2008). Calcium methoxide as a solid base catalyst for the transesterification of soybean oil to biodiesel with methanol. **Fuel**. 87: 1076-1082.
- Ma, F. and Hanna, M. A. (1999). Biodiesel production: a review. **Bioresource Technology**. 70: 1-15.
- MacLeod, C. S., Harvey, A. P., Lee, A. F. and Wilson, K. (2008). Evaluation of the activity and stability of alkali-doped metal oxide catalysts for application to an intensified method of biodiesel production. **Chemical Engineering Journal**. 135: 63-70.
- Marchetti, J. M., Miguela, V. U. and Errazua, A. F. (2007). Possible methods for biodiesel production. **Renewable and Sustainable Energy Reviews**. 11: 1300-1311.
- Meher, L. C., Vidya, S. D. and Naik, S. N. (2006). Technical aspects of biodiesel production by transesterification - a review. **Renewable and Sustainable Energy Reviews**. 10: 248-268.
- Meyer, O., Roessner, F., Rakoczy, R. A. and Fischer, R. W. (2010). Impact of organic interlayer anions in hydrotalcite precursor on the catalytic activity of hydrotalcite-derived mixed oxides. **Heterogeneous & Homogeneous & Bio-ChemCatChem Catalysis**. 2: 314-321.
- Narasimharao, K., Lee, A. and Wilson, K. (2007). Catalysts in production of biodiesel: A review. **Journal of Biobased Materials and Bioenergy**. 1: 19-30.

- Noiroj, K., Intarapong, P., Luengnaruemitchai, A. and Jai-In, S. (2009). A comparative study of KOH/Al₂O₃ and KOH/NaY catalysts for biodiesel production via transesterification from palm oil. **Renewable Energy**. 34: 1145-1150.
- Plank, C. and Lorbeer, E. (1995). Simultaneous determination of glycerol, and mono-, di- and triglycerides in vegetable oil methyl esters by capillary gas chromatography. **Journal of Chromatography A**. 697: 461-468.
- Rayalu, S. S., Udhoji, J. S., Meshram, S. U., Naidu, R. R. and Devotta, S. (2005). Estimation of crystallinity in flyash-based zeolite-A using XRD and IR spectroscopy. **Current Science**. 89: 2147-2151.
- Rashtizadeh, E., Farzaneh, F. and Ghandi, M. (2010). A comparative study of KOH loaded on double aluminosilicate layers, microporous and mesoporous materials as catalyst for biodiesel production via transesterification of soybean oil. **Fuel**. 89: 3393-3398.
- Saceda, J. -J. F., de Leon, R. L., Rintramee, K., Prayoonpokarach, S. and Wittayakun, J. (2011). Properties of silica from rice husk and rice husk ash and their utilization for zeolite Y synthesis. **Quimica Nova**. 34: 1394-1397.
- Srivastava, A. and Prasad, R. (2000). Triglycerides-based diesel fuels. **Renewable and Sustainable Energy Reviews**. 4: 111-133.
- Suppes, G. J., Dasari, M. A., Doskocil, E. J., Mankidy, P. J. and Goff, M. J. (2004). Transesterification of soybean oil with zeolite and metal catalysts. **Applied Catalysis A: General**. 257: 213-223.

- Sukhawanit, C., Srinophakun, P. and Matsumura, M. (2004). Biodiesel production from crude sunflower oil. **Journal of Research in Engineering and Technology**. 1: 141-150.
- Sun, L. B., Gong, L., Liu, X. Q., Gu, F. N., Chun, Y. and Zhu, J. H. (2009). Generating basic sites on zeolite Y by potassium species modification: Effect of base precursor. **Catalysis Letters**. 132: 218-224.
- Van Gerpen, J. (2005). Biodiesel processing and production. **Fuel Processing Technology**. 86: 1097-1107.
- Wallau, M. and Schuchardt, U. (1995). Catalysis by metal containing zeolites. I: Basic sites. **Journal of the Brazilian Chemical Society**. 6: 393-403.
- Wittayakun, J., Khemthong, P. and Prayoonpokarach, S. (2008). Synthesis and characterization of zeolite NaY from rice husk silica. **Korean Journal of Chemical Engineering**. 25: 861-864.
- Xie, W. and Li, H. (2006). Alumina-supported potassium iodide as a heterogeneous catalyst for biodiesel production from soybean oil. **Journal of Molecular Catalysis A: Chemistry**. 255: 1-9.
- Xie, W., Peng, H. and Chen, L. (2006). Transesterification of soybean oil catalyzed by potassium loaded on alumina as a solid-base catalyst. **Applied Catalysis A: General**. 300: 67-74.
- Xie, W., Huang, X. and Li, H. (2007). Soybean oil methyl esters preparation using NaX zeolite loaded with KOH as a heterogeneous catalyst. **Bioresource Technology**. 98: 936-939.

- Xu, B., Rotunno, F., Bordiga, S., Prins, R. and van Bokhoven, J. A. (2006). Reversibility of structural collapse in zeolite Y: Alkane cracking and characterization. **Journal of Catalysis**. 241: 66-73.
- Xue, W., Zhou, Y. C., Song, B. A., Shi, X., Wang, J., Yin, S. T., Hu, D. Y., Jin, L. H. and Yang, S. (2009). Synthesis of biodiesel from *Jatropha curcas* L. seed oil using artificial zeolites loaded with CH₃COOK as a heterogeneous catalyst. **Natural Science**. 1: 55-62.
- Zhu, J. H., Wang, Y., Chun, Y. and Wang, X. S. (1998). Dispersion of potassium nitrate and the resulting basicity on alumina and zeolite NaY. **Journal of the Chemical Society, Faraday Transactions**. 94: 1163-1169.



CHAPTER IV

BASIC PROPERTIES OF POTASSIUM SUPPORTED ON NaY STUDIED BY PYRROLE-TPD AND MBOH DECOMPOSITION

4.1 Introduction

In Chapter III, the preparation of basic heterogeneous xK/NaY catalysts (x = 4, 8 and 12 %wt of K) by impregnation of a mixture CH₃COOK/CH₃COOH on zeolite NaY was reported. Such method could prevent the collapse of the zeolite structure and the obtained catalysts were effective for transesterification of Jatropha seed oil to produce biodiesel. With the potassium loading of 4, 8 and 12 wt%, the catalytic performance increased with the potassium loading and a complete conversion was observed on 12K/NaY. In contrast, the catalyst prepared with 12 wt% of K from KNO₃ precursor was much less active in transesterification. In this chapter, the basicity of K/NaY from both precursors was further investigated.

Typically, oxygen atom in the framework of zeolites is intrinsic Lewis basic sites which form an acid-base pair with the charge compensating cation (Barthomeuf, 1996). The basicity of zeolite can be further increased by impregnation with alkali metal salt which transformed to oxide after calcination. The occlusion of alkali metal oxide clusters in zeolite cages results in a further increase in the basicity of these materials (Dorskocil, Bordawekar, and Davis, 2000).

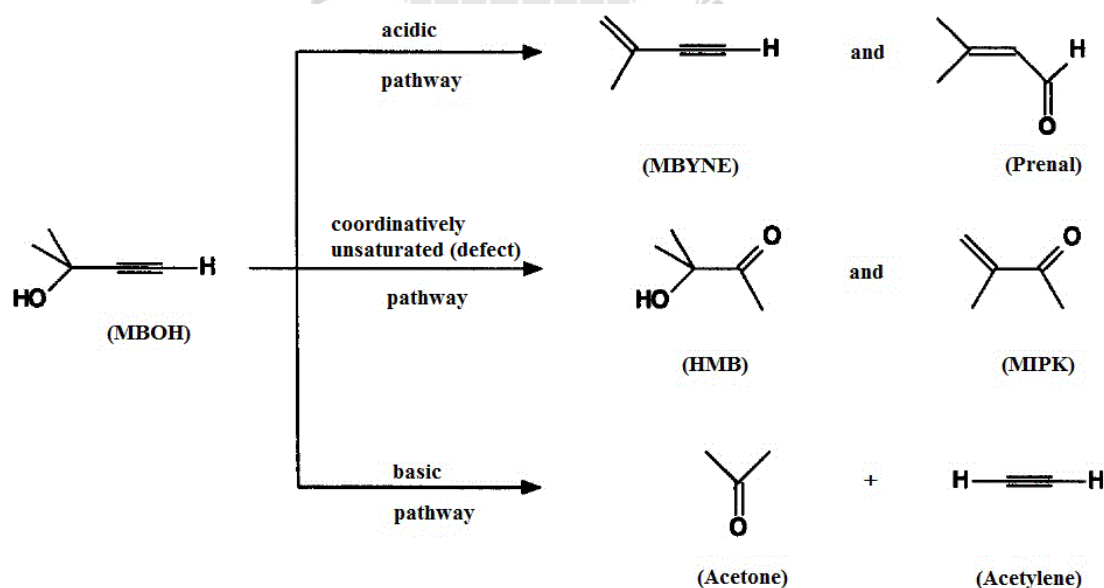
The basic properties of solids can be studied by temperature programmed desorption of carbon dioxide (CO₂-TPD). In a first approximation the desorption

temperature reflects the strength of CO₂ adsorption. The amount of desorbed carbon dioxide correlates with the amount of basic sites. Noiroj et al. (2009) used the CO₂-TPD to study the basic properties of NaY and KOH/NaY zeolites. The desorption temperature of both materials were 200 and 285°C, respectively and the basic strength increased with the KOH loading resulting in the catalytic activity for transesterification. Ramos, Casas, Rodríguez, and Pérez (2008) also used CO₂-TPD to study basicity of the catalysts prepared by loading sodium acetate solution on three different zeolites (mordenite, beta and X) to determine an influence of the zeolite type on the biodiesel production. The modified zeolite X provided a greater activity than those of the others because it contained a higher concentration of sodium oxide species which were expected to be super basic sites. Base on CO₂-TPD, the basicity of modified zeolite X was 250 μmol CO₂/g, while those of the samples based on beta and mordenite zeolite were 39 and 15 μmol CO₂/g, respectively.

However, a main drawback of CO₂-TPD is the strong interaction of CO₂ with the basic sites which does not allow the direct correlation between the desorption data and the number of basic sites (Barthomeuf, 1996). Consequently, an alternative probe molecule which adsorbs reversibly is desired for this purpose, pyrrole a five-membered ring heterocyclic aromatic compound with formula C₄H₄NH can be used because it is a weak acid molecule (Hattori, 1995; Barthomeuf, 1996; Förster et al., 1999; Doscocil et al., 2000). Pyrrole is an amphoteric molecule which can interact with either the Lewis basic oxygen of zeolite via its NH group by hydrogen bonding or with the Lewis acidic cation via the aromatic π-electrons interaction (Förster et al., 1999). In this work pyrrole-TPD was used to study the basicity of the NaY, xK/NaY

(prepared from $\text{CH}_3\text{COOK}/\text{CH}_3\text{COOH}$ solution), 12K/NaY-1 and 12K/NaY-2 (prepared from KNO_3 solution).

Furthermore, the basic properties of the xK/NaY catalysts were correlated with the catalytic conversion of 2-methyl-3-butyn-2-ol (MBOH) which can distinguish acidic and basic sites of solids. As shown in scheme 4.1, decomposition of MBOH precede through different reaction pathways on basic, acidic and coordinatively unsaturated (defect) sites providing different products (Lauron-Pernot, Luck, and Popa, 1991; Handa, Fu, Baba, and Ono, 1999; Brei, 2008). In the presence of weak acidic site, 3-methyl-3-buten-1-yne (MBYNE) is produced via the dehydration of MBOH. In the presence of strong acidic sites, 3-methyl-2-buten-1-al (Prenal) is formed via the isomerization of MBOH. The coordinatively unsaturated (defect) sites lead to formation of 3-hydroxy-3-methyl-2-butanone (HMB) and 3-methyl-3-buten-2-one (MIPK). Over the basic site, acetone and acetylene are produced from the decomposition of MBOH.



Scheme 4.1 Overall reaction of MBOH (Lauron-Pernot et al., 1991).

The MBOH reaction has been used to test basic zeolite catalyst. For instance, Meyer and Hoelderich (1999) investigated the basic properties of various basic NaX zeolite catalysts prepared by ion exchange or impregnation with aqueous solution of cesium acetate and methanolic solution of sodium azide. The basic sites were generated in the zeolite after loading alkali metals and alkaline metal oxides. They observed that both the conversion of MBOH and the selectivity to basic products correlated with the amount of cesium acetate decomposed on zeolite NaX.

The aim of this chapter was to study the basic properties of NaY and potassium supported on NaY zeolite (xK/NaY, 12K/NaY-1 and 12K/NaY-2), determined by temperature programmed desorption of pyrrole (Pyrrole-TPD) and the catalytic conversion of MBOH. The data from both methods were compared. The correlation between basicity properties and the catalytic in transesterification of Jathropa seed oil reported previously in Chapter III was made.

4.2 Experimental

4.2.1 Catalyst preparation

The catalysts studied in this chapter were the same ones reported in Chapter III. The NaY zeolite was impregnated with a various concentration of $\text{CH}_3\text{COOK}/\text{CH}_3\text{COOH}$ solution to give K loading of 4, 8 and 12 wt%. The resulting mixtures were dried in an oven at 30 °C for 4 h and at 80 °C overnight before calcination at 400 °C for 3 h. The obtained samples were notated xK/NaY (x = 4, 8 and 12). The catalysts (12K/NaY-1 and 12KNO₃/NaY-2 catalysts) were prepared by impregnation of NaY with aqueous solution of KNO₃ to give K loading of 12 wt%.

Then the mixtures were dried at 30 °C for 4 h and at 80 °C overnight before calcination at 500 °C and 600 °C for 3 h, respectively.

4.2.2 Pyrrole-TPD

The pyrrole-TPD analysis was performed in an apparatus constructed from Raczek Analyse Technic GmbH, Hannover (Germany) with a procedure derived from Kuśtrowski, Chmielarz, Bożek, Sawalha, and Roessner (2004). The 0.1 g sample with a particle size of 200-315 µm was placed in a flow type quartz reactor of flow type coupled to a thermal conductivity detector (TCD). Then the prepared catalysts was conditioned in helium flow (45 mL/min) to 350 °C at a heating rate of 10 °C/min, held for 1 h. Afterward, pyrrole was fed with the flow rate of 59.3 mL/min over the conditioned catalyst at 55 °C for 45 min. The physically adsorbed pyrrole was removed by flushing with helium with flow rate of 45 mL/min. at 100 °C for 2 h. The temperature programmed desorption (TPD) of chemically adsorbed pyrrole was studied in the temperature range up to 600 °C with a heating rate of 10 °C/min using a helium as carrier gas. The pyrrole multiple-point calibration, the plot between peak area and amount of pyrrole, was carried out by direct injection of pyrrole (0.5, 0.8 and 1.0 µL) into the quartz reactor. The amount of injected pyrrole in mol was calculated with equation (4.1). The TCD signals were recorded isothermally at 110 °C.

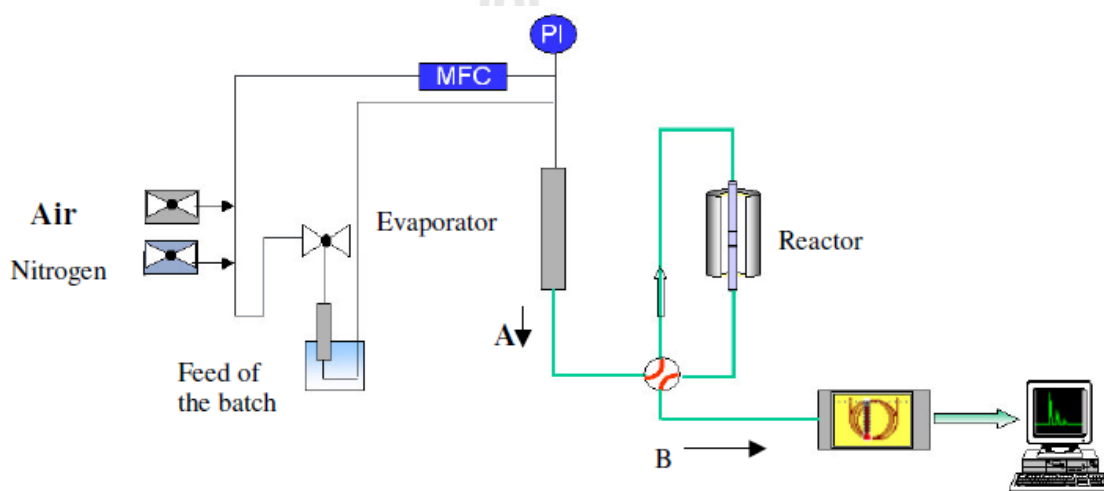
$$n_{\text{Pyr}} = \frac{\rho_{\text{Pyr}} V_{\text{Pyr}}}{M_{\text{Pyr}}} \quad (4.1)$$

where ρ_{Pyr} , V_{Pyr} and M_{Pyr} represent the density (0.966 g/mL), volume (µL) and molecular weight (67.09 g/mol) of pyrrole, respectively. The Gaussian deconvolution

of TPD curve that plotted TCD signal versus temperature ($^{\circ}\text{C}$) was done with Origin 6.0 to identify peak positions and to integrate the peak area.

4.2.3 MBOH decomposition

The conversion of MBOH was performed in a fixed bed reactor, automated bench unit as shown in the diagram in Figure 4.1 with a procedure modified from Kuśtrowski et al. (2004).



Temperature of transfer lines: A: $140\text{--}145\text{ }^{\circ}\text{C}$, B: $155\text{ }^{\circ}\text{C}$

PI: Pressure indicator

MFC: Mass flow controller

Figure 4.1 Diagram of instrument setup for the methylbutynol decomposition.

MBOH and toluene were obtained from Fluka with purity of 99% and used without further purification. A pre-experimental run was done with toluene which was not converted over the catalysts and used as an internal standard. A mixture of MBOH (95 vol%) and toluene (5 vol%) was placed in a storage vessel and cooled to 13 °C. The MBOH flow was adjusted to 0.02 mL/min through a capillary into an evaporator, in which a static nitrogen pressure of 2 bars as carrier gas was applied. Twenty mg of catalysts with a particle size of 200-315 µm was placed in the centre section of quartz tubular reactor, heated to 350 °C with a rate of 8 °C/min and kept at this temperature for 4 h under nitrogen flow (13.7 mL/min) to remove any adsorbed gases on the surface. After the catalyst activation, the reactor was cooled to 120 °C. The reaction products were analyzed on-line on a HP 8090 Series II gas chromatograph with a 60 m Optima Wax capillary column. The MBOH conversion (X_{MBOH}) is calculated from equation (4.2) from the difference between mole of MBOH injected ($n_{\text{MBOH,in}}$) and mole unreacted MBOH ($n_{\text{MBOH,out}}$). The yield (Y) is calculated from equation (4.3) where A_p and R_p represent the area and response factor of product compound, respectively. M_p is the corresponding molecular weight. A_k , R_k and M_k represent the area, response factor and mass of all components. The selectivity (S) is calculated in mol% from the yield of the product (Y_p) and the conversion of MBOH by equation (4.4).

$$X_{\text{MBOH}} (\%) = \frac{n_{\text{MBOH,in}} - n_{\text{MBOH,out}}}{n_{\text{MBOH,in}}} \times 100 \quad (4.2)$$

$$Y_p (\%) = \frac{A_p R_p / M_p}{\sum_k A_k R_k / M_k} \times 100 \quad (4.3)$$

$$S_p (\%) = \frac{Y_p}{X_{\text{MBOH}}} \times 100 \quad (4.4)$$

4.3 Results and discussion

4.3.1 Pyrrole-TPD of K/NaY prepared from $\text{CH}_3\text{COOK}/\text{CH}_3\text{COOH}$

The pyrrole-TPD profiles of the parent NaY and xK/NaY catalysts are shown in Figure 4.2. With the similar procedure on each sample, the parent NaY gave the most intense TCD signal. On the xK/NaY, the curve intensity decreased as the K loading was increased. The total peak area of each curve and the corresponding amount of pyrrole per gram of the catalyst, calculated from the calibration curve, are listed in Table 4.1.

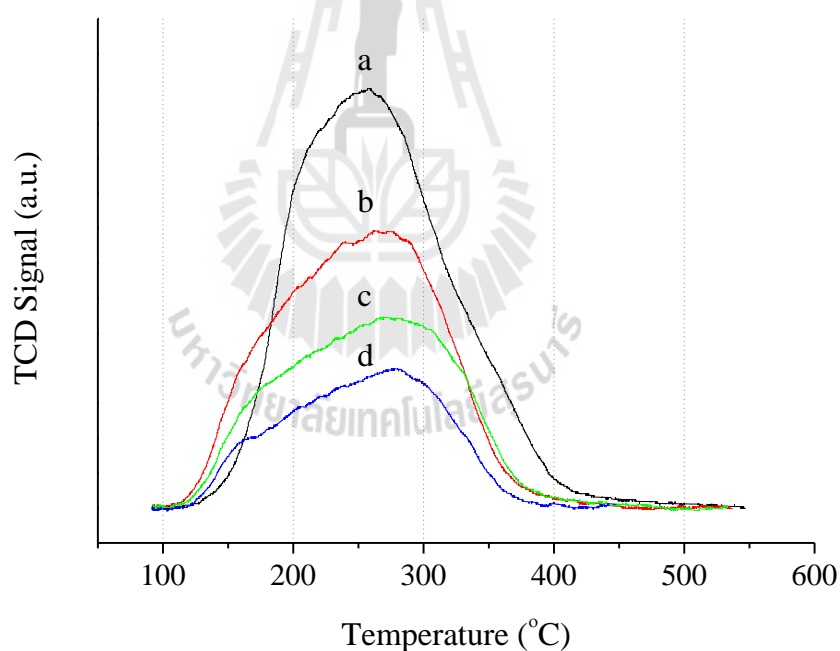


Figure 4.2 Desorption profiles of pyrrole on the parent NaY (a) and the xK/NaY catalysts prepared by impregnation of $\text{CH}_3\text{COOK}/\text{CH}_3\text{COOH}$ on NaY; (b) 4K/NaY, (c) 8K/NaY and (d) 12K/NaY.

As mentioned in Chapter III, the surface area of xK/NaY decreased linearly as the K loading was increased. Similarly, the adsorbed amount of pyrrole also decreased linearly with the increase of K loading ($R^2 = 0.9898$). It was likely that the amount of adsorbed pyrrole related directly to the surface area. The K ions could occlude in the zeolite cavities, decrease their size and became less accessible from the pyrrole molecules (Heidler, Janssens, Mortier, and Schoonheydt, 1997; Sánchez and Blasco, 2002).

By comparing the TPD profiles of the xK/NaY samples with those of the parent NaY, an additional shoulder was observed at around 150 °C suggesting that loading the zeolite with potassium generated another adsorption site. According to Dorskocil et al. (2000) and Lavalley (1996) potassium can generate species such as K_2O which acts as the strong base and pyrrolate anion ($C_4H_4N^-$) which could interact with surface hydroxyl groups. Because the latter sites were less basic, the pyrrole desorption occurred at a lower temperature. This model could explain the decrease of the desorbed amount of pyrrole with the increase of potassium content because the formed pyrrolate cannot desorb under the given conditions (namely, with less amount of $-Si-OH$).

Pyrrole molecule adsorbs on zeolite via: 1) hydrogen bond between the NH group and lattice oxygen - the Lewis basic sites; 2) interaction between pyrrole aromatic electrons with the cations (Na ions) - the Lewis acidic sites. With the K loading by impregnation, the cations could interact with the Lewis basic sites, hinder the adsorption of pyrrole and result in less hydrogen bonding. The K ion could also interact with the aromatic electrons. Moreover, some K cation could partially exchange with the Na cation, resulting in an enhancement of basicity. This

corresponds with a theory that the basicity is enhanced in the cation exchanged zeolite according to the cationic size, namely, $\text{Cs} > \text{Rb} > \text{K} > \text{Na} > \text{Li}$ (Heidler et al., 1997; Föster et al., 1999; Sánchez and Blasco, 2002).

Because the peak positions in all samples were not clearly resolved, the deconvolutions of the TPD profiles were generated and shown in Figure 4.3. The peak positions and areas are summarized in Table 4.1.

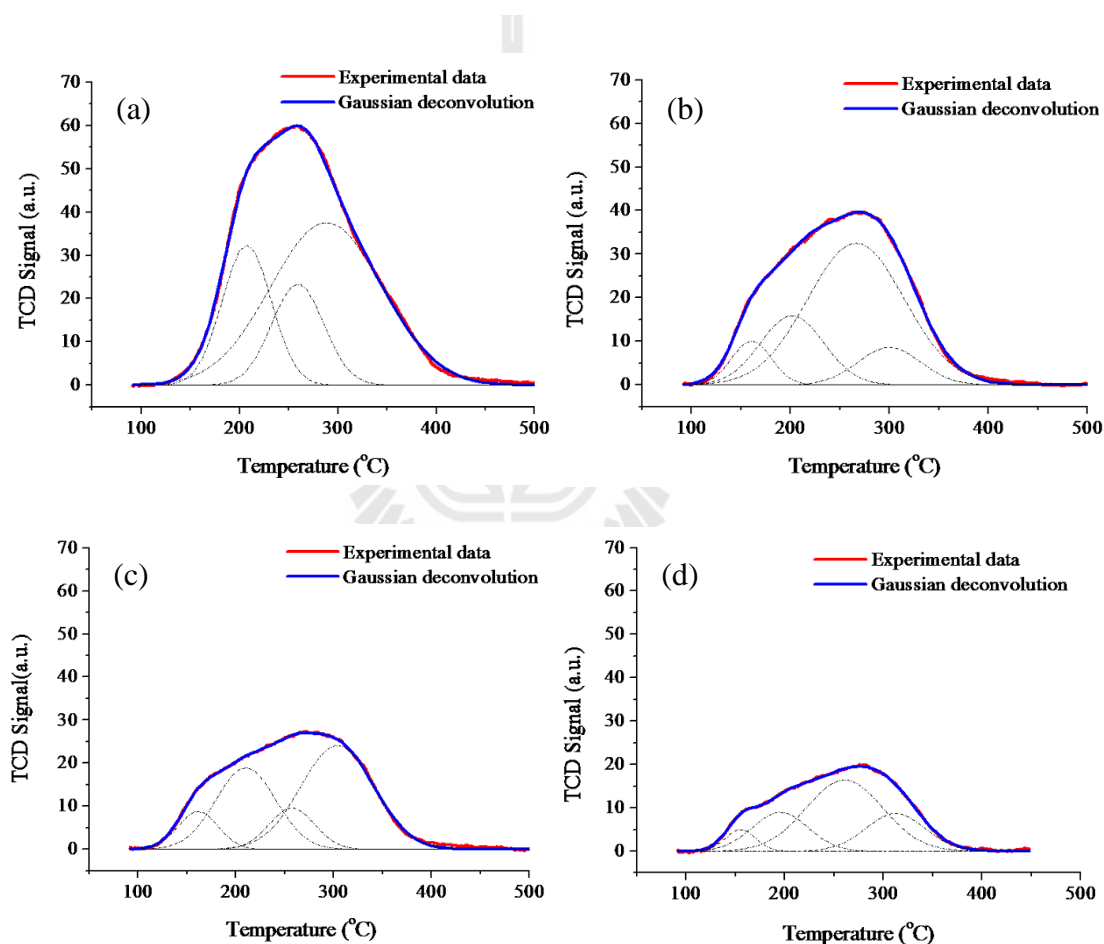


Figure 4.3 Experimental and deconvolution of TPD peaks of pyrrole desorption on parent NaY (a), 4K/NaY (b), 8K/NaY (c) and 12K/NaY catalyst (d).

Table 4.1 Summary results for surface area, total peak area, amount of pyrrole and peak of desorption temperature from deconvolution and corresponding peak area of parent NaY and xK/NaY catalysts (x = 4, 8 and 12 wt% loading of K).

Catalyst	Surface area ^a (m ² /g)	Total Peak area * (Unit area/g)	Amount of pyrrole (mmol/g)	Amount of pyrrole (mmol/m ²)	Peak of desorption temperature (°C) from deconvolution and corresponding peak area (%)			
parent NaY	934.72	89,133.7	19.90	0.0213	207 (22.64%)	259 (17.45%)	288 (59.90%)	
4K/NaY	727.99	64,498.8	14.40	0.0198	160 (7.85%)	210 (19.75%)	266 (61.77%)	299 (10.63%)
8K/NaY	506.10	47,108.9	10.52	0.0208	161 (9.51%)	210 (30.84%)	257 (11.78%)	303 (47.85%)
12K/NaY	356.48	30,750.4	6.86	0.0192	155 (6.09%)	195 (20.64%)	260 (52.04%)	312 (21.22%)

^a as reported in Chapter III

As shown in Figure 4.3, there were three peaks for NaY and four peaks for the xK/NaY. Component peaks with the different desorption temperature suggested the presence of various basic sites with different strengths. In NaY, three peaks can be assigned to the basic framework oxygens adjacent to Na cations at site I', I and II interacting with pyrrole molecule (Murphy, Massiani, Franck, and Barthomeuf, 1996; 1997). Normally, the cations of site I', I are linked to oxygen O(3) while the II cations are connected to O(2) oxygens (Figure 4.4). The extra-framework cation positions are sites I at the center of the hexagonal prisms, sites I' in the sodalite cages at the hexagonal prism six-ring, and sites II in the large cavities at the sodalite cage six-rings.

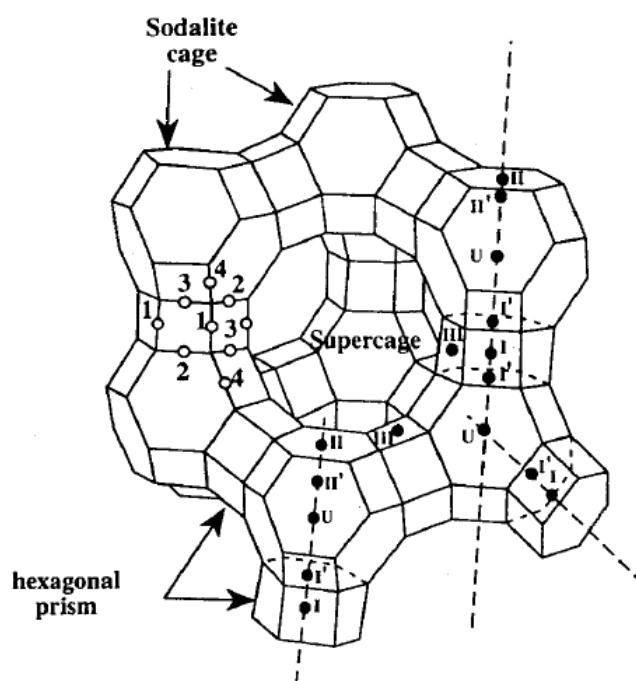


Figure 4.4 Scheme of the faujasite structure with oxygen types (○) and cation locations (●) (Scherzer, Bass, and Hunter, 1975).

In xK/NaY, three peaks are still present. However, the desorption temperature of the cation of sites II increased with the increased of K loading because the substitute of K cations in the supercage II of Na cations might occur. It is well known that the exchanged cations occupy site II, in other words, site II cations are more easily exchanged because this site is in the supercage such that some cation can easy enter to exchange with cation in the zeolite structure (Murphy et al., 1996; 1997). The higher desorption temperature with the increased K loading at 299, 303 and 312 °C of 4, 8 and 12 wt% K on NaY, respectively, relate to the increasing of basicity with the amount of exchanged K cation on zeolite. The new peak at the lower desorption temperature can be attributed to the interaction of pyrrolate anion ($C_4H_4N^-$) form pyrrole dissociation on the highly basic sites with OH species (Lavalley, 1996; Dorskocil et al., 2000).

4.3.2 Pyrrole-TPD of 12K/NaY-1 and 12K/NaY-2

In the case of catalysts prepared from KNO_3 precursor, the pyrrole-TPD profiles are shown in Figure 4.5. The curve intensity was decrease with increasing of calcination temperature. NaY zeolite has 3 times of intensity of 12K/NaY and about 5-6 times of intensity of 12K/NaY-1 and 12K/NaY-2. Based on KNO_3 precursor, 12K/NaY-1 showed higher intensity than 12K/NaY-2. It might be caused the calcination temperature. Moreover, the peak of desorption temperature of pyrrole of 12K/NaY-1 and 12K/NaY-1 appeared at the low temperature of 179 and 140 °C, respectively. It implied that the interaction of pyrrole on these surfaces exhibited the physisorption. After deconvolutions of the TPD profiles of 12K/NaY-1 and 12K/NaY-2 (Figure 4.6a and 4.6b), only one peak is showed. The amount of

pyrrole per gram of the catalyst is reported in Table 4.2. The 12K/NaY-1 with calcination of 500 °C has higher amount of pyrrole than 12K/NaY-1 with calcination of 600 °C. These results suggest that the interaction of CH₃COOK with NaY is stronger than that of KNO₃ with NaY because the conversion of CH₃COOK precursor to basic species is high. In the case of KNO₃ precursor, two factors mainly blocked the generation of a strong basicity are the difficult of KNO₃ decomposition-require the high temperature (more than 600 °C) and the collapse of NaY structure (Shen et al., 1999; Sun et al., 2008). Thus, the catalyst prepared with KNO₃ cannot help to increase basicity and the calcinations temperature had effected to the collapse of zeolite structure.

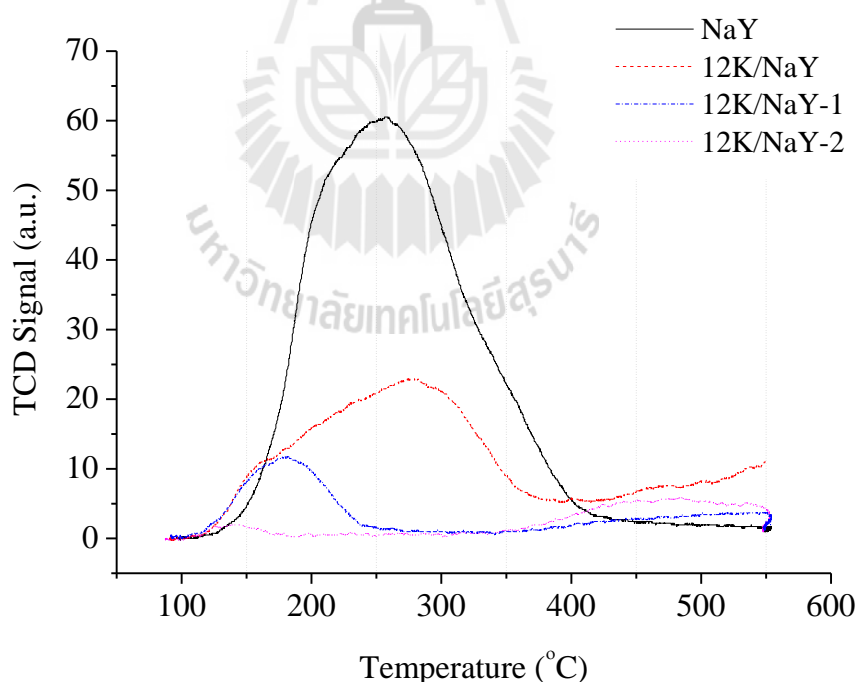


Figure 4.5 Desorption profiles of pyrrole on the parent NaY, 12K/NaY, 12K/NaY-1 and 12K/NaY-2 catalysts.

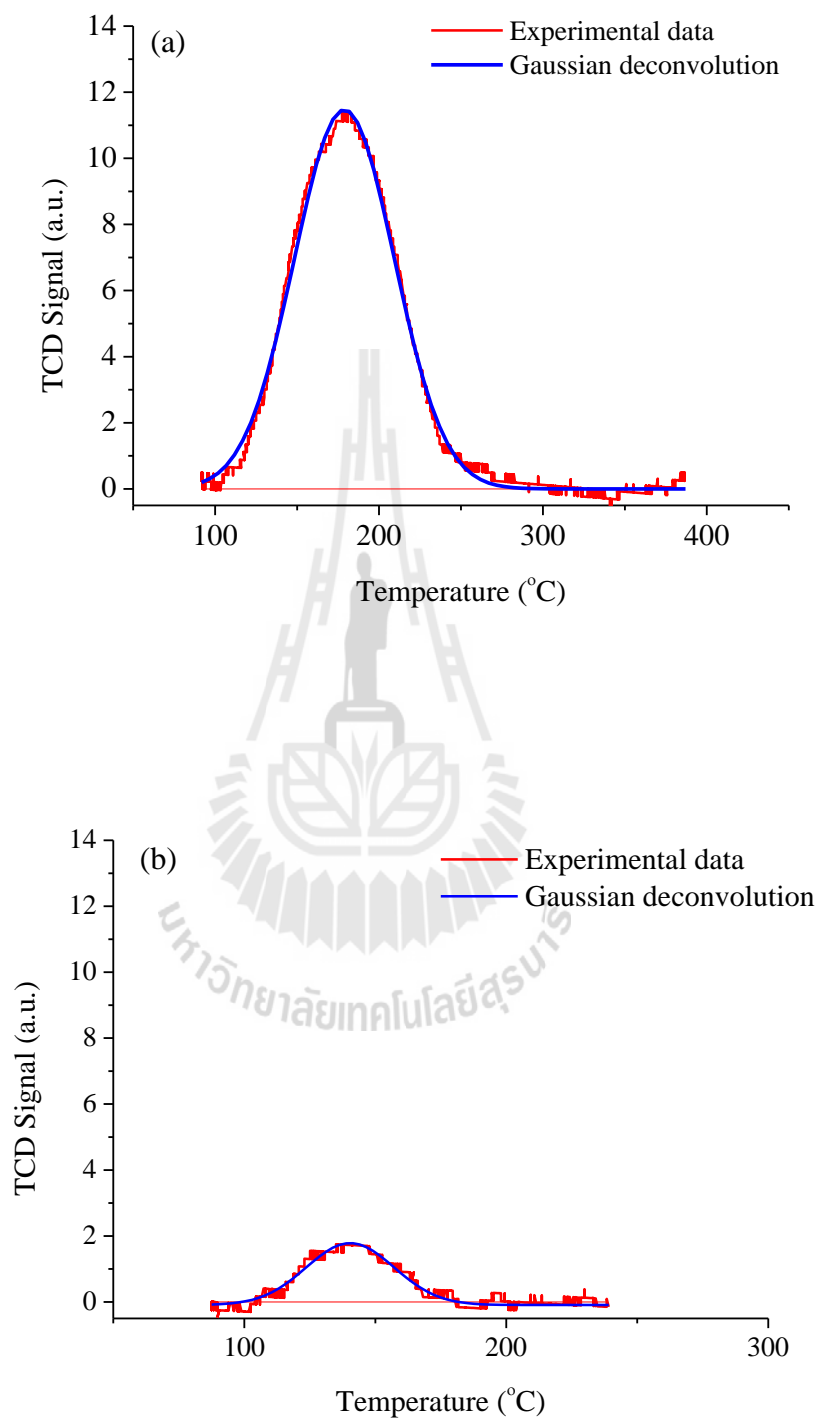


Figure 4.6 Experimental and deconvolution of TPD peaks of pyrrole on (a) 12K/NaY-1 and (b) 12K/NaY-2 catalysts.

Table 4.2 Summary results of 12K/NaY-1 and 12K/NaY-2 catalysts for total peak area, amount of pyrrole and peak of desorption temperature from deconvolution of 12K/NaY-1 and 12K/NaY-2 catalysts.

Catalyst	Total peak area (Unit area/g)	Amount of pyrrole (mmol/g)	Peak of desorption temperature (°C) from deconvolution
12K/NaY-1	1,959.6	1.96	179
12K/NaY-2	788.5	0.18	140

4.3.3 MBOH decomposition

The MBOH decomposition could distinguish acidic, basic and coordinatively unsaturated (defect) active sites of solids, the change in basicity can be compared directly from the product selectivity (Kuśtrowski et al., 2004). The selectivity over the parent NaY and xK/NaY catalysts are shown in Figure 4.7. The products from the defect sites (HMB and MIPK) were not significant in all catalysts. The reaction over the parent NaY zeolite catalyst generated products (~ 40 mol% each) from basic pathway (acetone and acetylene) and ~ 20 mol% with a significant amount of MBYNE which is a product from acidic pathway (Figure 4.7a). Thus, the surface of the parent NaY zeolite contained mainly the basic sites and a moderate amount of acidic sites. This observation was in a good agreement with that in literature (Huang and Kaliaguine, 1993). In contrast, all the xK/NaY catalysts generated only acetone and acetylene as the major products (Figure 4.7b-d). The amount of MBYNE was less than 0.9% for 4K/NaY and less than 0.3% for 8K/NaY

and 12K/NaY. These results indicated that impregnation with potassium suppressed the acidic sites of NaY zeolites and all the prepared catalysts were basic in nature. The molar ratio between acetone and acetylene (0.93, 0.90 and 0.85 of 4K/NaY, 8K/NaY and 12K/NaY catalyst, respectively) was less than the theoretical value which is one probably because of aldol condensation of acetone to produce products which adsorbed strongly on the surface (Aramendía et al., 1999; Corma and Iborra, 2006).

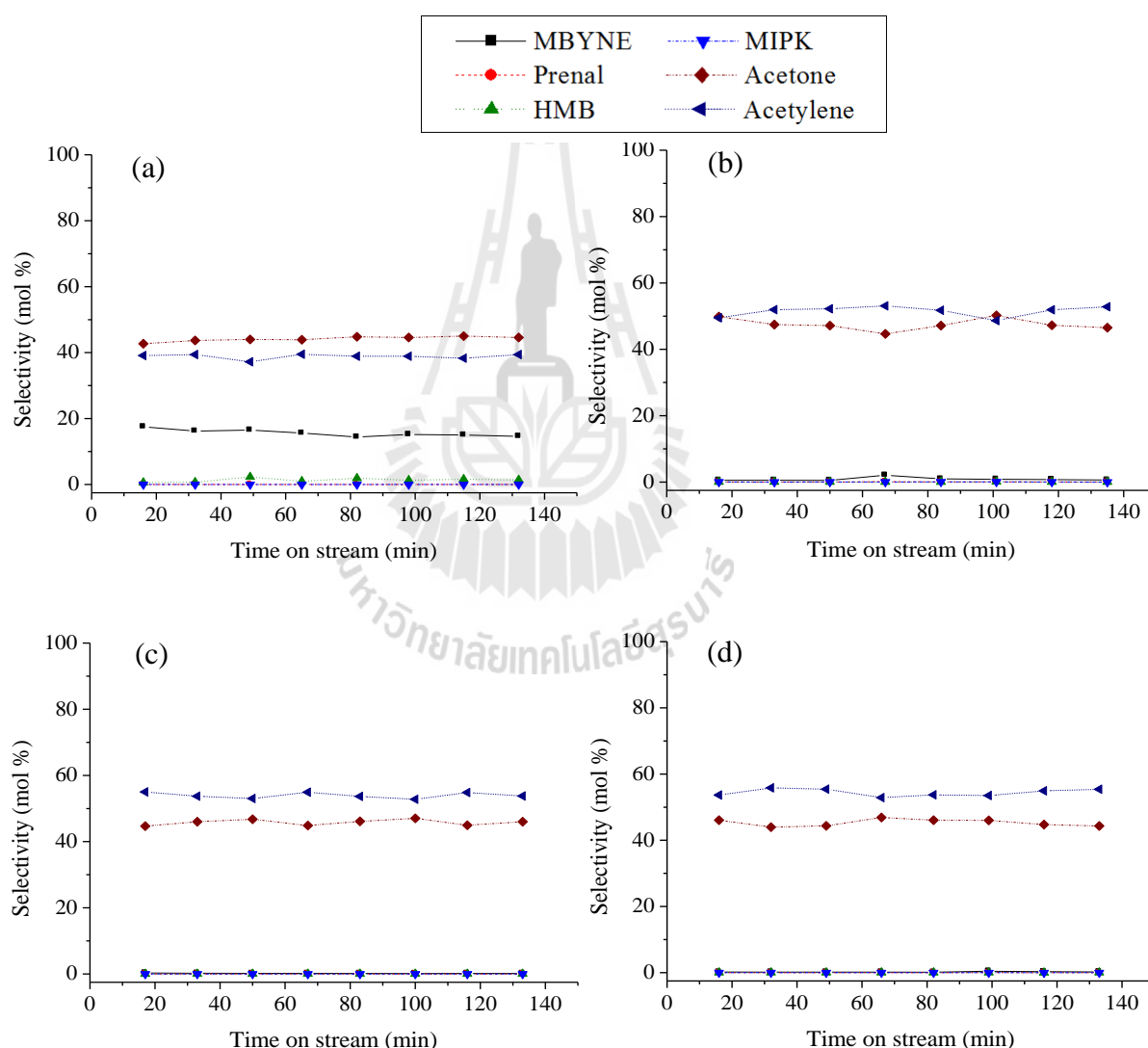


Figure 4.7 Selectivity of the product of MBOH test reaction over the parent NaY (a) and xK/NaY catalysts (b) 4K/NaY, (c) 8K/NaY and (d) 12K/NaY. Reaction temperature was 120 °C and amount of each sample was 20 mg.

The conversion of MBOH over the parent NaY and xK/NaY are shown in Figure 4.8. The conversion on NaY was significantly lower than those of the xK/NaY. The conversion on NaY was significantly lower than those of the xK/NaY. The conversion on of K/NaY increases with potassium loading. However, the conversion on 12K/NaY was only slightly higher than 8K/NaY and after 80 min and became nearly similar. This was probably caused by the high degree of conversion which does not allow differentiation between the two samples.

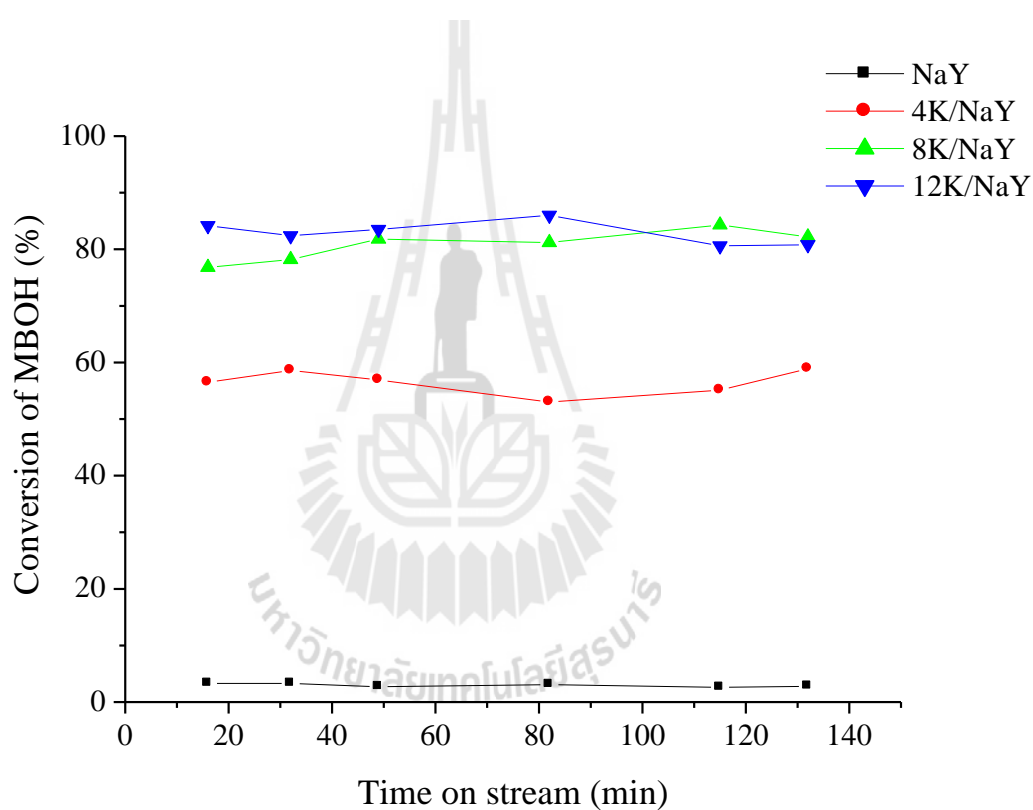


Figure 4.8 Conversion of MBOH test reaction over the parent NaY and xK/NaY catalysts with 4, 8 and 12 wt% loading, reaction temperature 120 °C, amount of catalyst was 20 mg.

To distinguish the conversion of these catalysts (8K/NaY and 12K/NaY) their amount for the MBOH test reaction was decreased from 20 mg to 10 mg. The conversion on 12K/NaY was higher than that on 8K/NaY (Figure 4.8) confirming the assumption that the amount of basic sites of xK/NaY increased with K loading. The products from the basic pathway (acetone and acetylene) were still predominant in both catalysts (Figure 4.10a and 4.10b). The information about basicity of these catalysts were in good agreement with their catalytic performance on transesterification of Jatropha seed oil in Chapter III in which the conversion and the biodiesel yield increased with K loading.

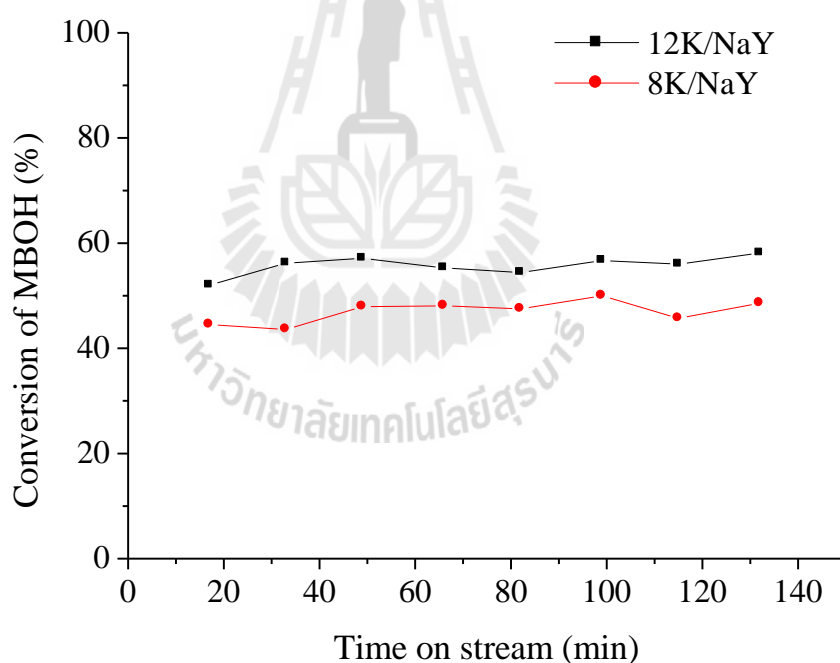


Figure 4.9 Conversion of MBOH test reaction over the 8K/NaY and 12K/NaY catalysts. Reaction temperature was 120 °C and amount of catalyst was 10 mg.

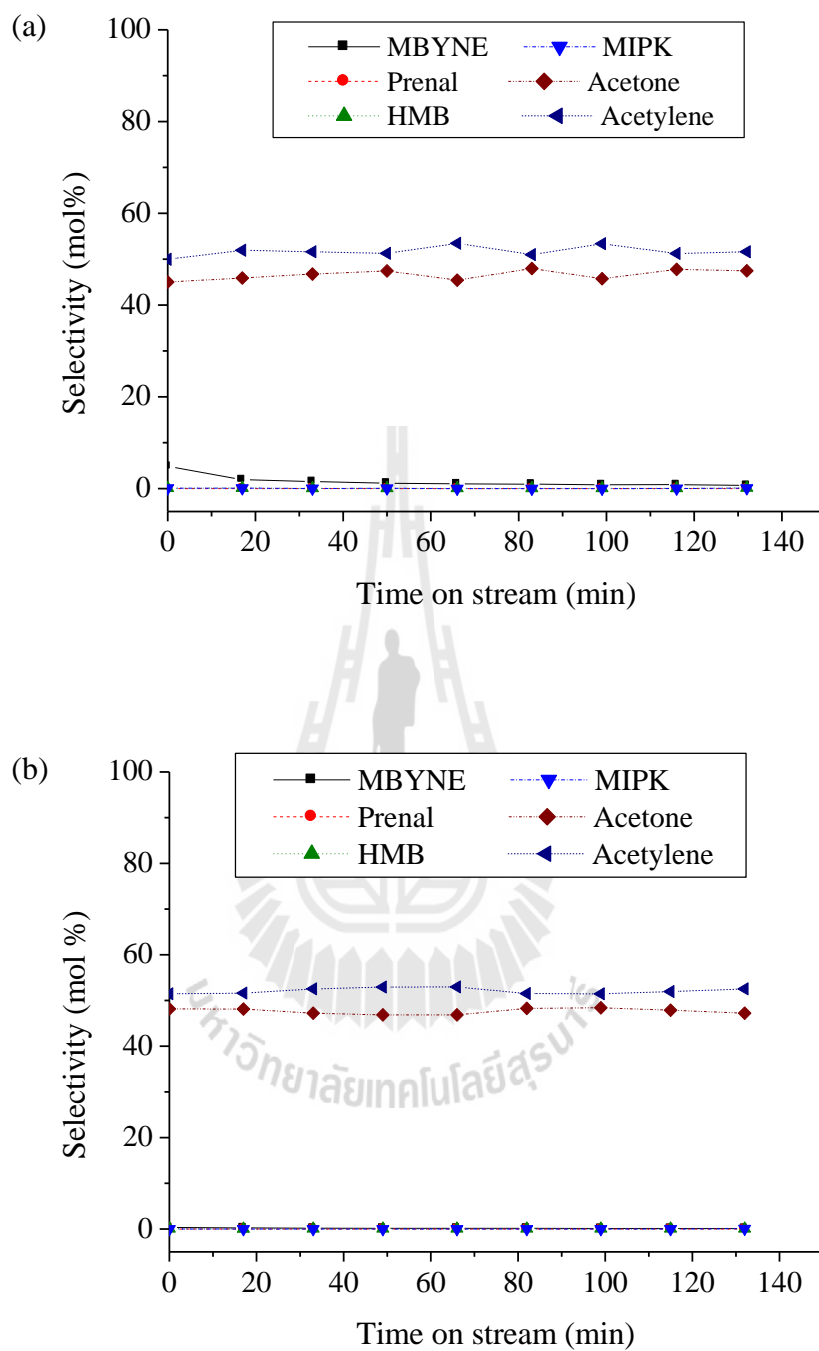


Figure 4.10 Selectivity of the product of MBOH test reaction over (a) 8K/NaY and (b) 12K/NaY catalyst. Reaction temperature was 120 °C and amount of catalyst was 10 mg.

The MBOH conversions over the 12K/NaY-1 and 12K/NaY-2 were investigated and compared with 12K/NaY prepared from the mixture $\text{CH}_3\text{COOK}/\text{CH}_3\text{COOH}$. As shown in Figure 4.11, the MBOH conversion of the 12K/NaY-1 was higher than that of 12K/NaY-2. Thus, the calcinations temperature of 500 °C produced a more active catalyst. However, both were much less active than the 12K/NaY from $\text{CH}_3\text{COOK}/\text{CH}_3\text{COOH}$. The activity from MBOH of these catalysts were in a good agreement with that from transesterification (mentioned in Chapter III).

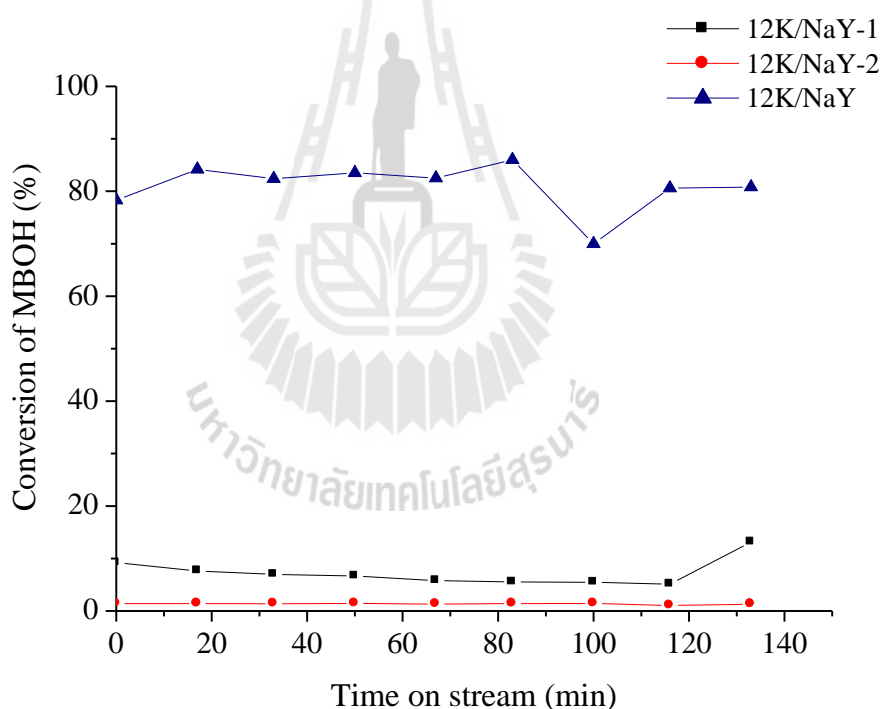


Figure 4.11 Conversion of MBOH test reaction over the 12K/NaY, 12K/NaY-1 and 12K/NaY-2 catalysts. Reaction temperature was 120 °C and amount of catalyst was 20 mg.

The selectivity over 12K/NaY-1 is shown in Figure 4.12. The catalysts showed acetone and acetylene that are the main products from basic pathway. The MBYNE from acidic pathway are produced. Similar product selectivity was observed from the parent NaY (Figure 4.7a). It implied that the catalyst prepared with KNO_3 cannot suppress the acid site on NaY. In conclusion, xK/NaY showed the best suppression of the acid site on NaY.

Among the sample investigated by MBOH, the catalysts were prepared with KNO_3 precursor has low basicity due to less generate basic site and suppress acid sites on NaY. While the catalysts were prepared with CH_3COOK has more basicity. The basicity properties of these catalysts are relation with catalytic activity for transesterification of Jatropha seed oil of their catalysts.

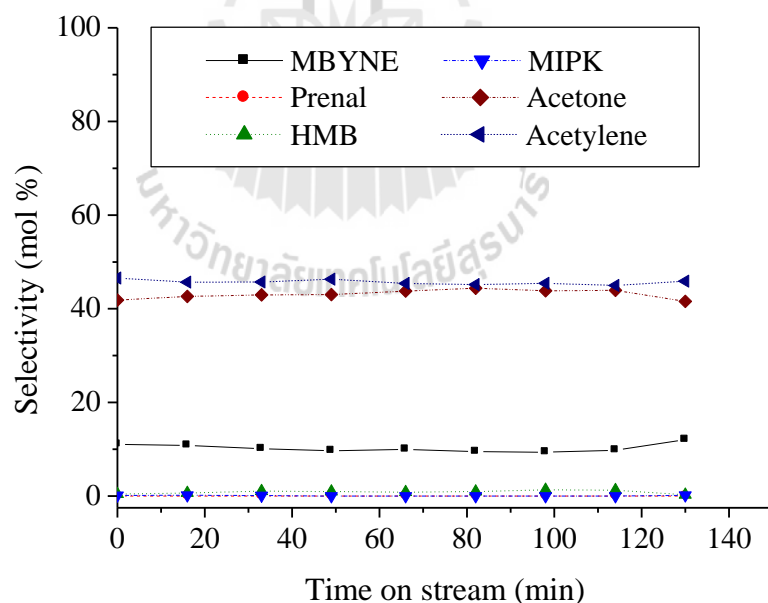


Figure 4.12 Selectivity of the product of MBOH test reaction over 12K/NaY-1.

Reaction temperature was 120 °C and amount of catalyst was 20 mg.

4.4 Conclusions

The basic properties of xK/NaY, heterogeneous base catalysts for transesterification of Jatropha seed oil were studied by pyrrole-TPD and MBOH test reaction. The pyrrole-TPD indicated the decrease of adsorption sites after impregnation of a solution of CH₃COOK/CH₃COOH on NaY in accordance with the decrease in surface area. The nature of pyrrole adsorption on the xK/NaY was different from that on NaY because K ions could hinder the intrinsic basic site (lattice oxygen) and possibly occluded in the zeolite cavities preventing the access of pyrrole. The K ions could also interact with the aromatic electrons of pyrrole. The difference in cation size between K and Na resulted in an additional adsorption sites. Further study by MBOH test reaction revealed that impregnation of potassium could suppress the acidic sites of NaY nearly completely and the basicity of xK/NaY increased with K loading.

4.5 References

- Aramendía, M. A., Boráu, V., García, I. M., Jiménez, C., Marinas, A., Marinas, J. M., Porras, A. and Urbano, F. J. (1999). Comparison of different organic test reactions over acid-base catalysts. **Applied Catalysis A: General**. 184: 115-125.
- Barthomeuf, D. (1996). Basic Zeolites: Characterization and uses in adsorption and catalysis. **Catalysis Reviews**. 38: 512-612.
- Brei, V.V. (2008). Correlation between the strength of the basic sites of catalysts and their activity in the decomposition of 2-methyl-3butyn-2-ol, as a test reaction. **Theoretical and Experimental Chemistry**. 44: 320-324.

- Corma, A. and Iborra, S. (2006). Optimization of alkaline earth metal oxide and hydroxide catalysts for base-catalyzed reactions. **Advances in Catalysis**. 49: 239-302.
- Doskocil, E. J., Bordawekar, S. and Davis, R. J. (2000). Chapter 2 Catalysis by solid bases. In: **Catalysis, Volume 15**: Spivey, J. J. (ed.), pp. 40-72. The Royal Society of Chemistry, UK.
- Förster, H., Fuess, H., Geidel, E., Hunger, B., Jobic, H., Kirschhock, C., Klepel, O. and Krause, K. (1999). Adsorption of pyrrole derivatives in alkali metal cation-exchanged faujasites: comparative studies by surface vibrational techniques, X-ray diffraction and temperature-programmed desorption augmented with theoretical studies Part I. Pyrrole as probe molecule. **Physical Chemistry Chemical Physics**. 1: 593-603.
- Handa, H., Fu, Y., Baba, T. and Ono, Y. (1999). Characterization of strong bases by test reaction. **Catalysis Letters**. 59: 195-200.
- Hattori, H. (1995). Heterogeneous basic catalysis. **Chemical Reviews**. 95: 537-558.
- Heidler, R., Janssens, G. O. A., Mortier, W. J. and Schoonheydt, R. A. (1997). Charge sensitivity analysis of the interaction of pyrrole with basic FAU-type zeolites using the electronegativity equalization method. **Microporous Materials**. 12: 1-11.
- Huang, M. and Kaliaguine, S. (1993). Reactions of methylbutynol on alkali-exchanged zeolites. A Lewis acid-base selectivity study. **Catalysis Letters**. 18: 373-389.

- Kuśtrowski, P., Chmielarz, L., Bożek, E., Sawalha, M. and Roessner, F. (2004). Acidity and basicity of hydrotacitederived mixed Mg-Al oxides studied by test reaction of MBOH conversion and temperature programmed desorption of NH_3 and CO_2 . **Materials Research Bulletin**. 39: 263-281.
- Lauron-Pernot, H., Luck, F. and Popa, J. M. (1991). Methylbutynol: a new and simple diagnostic tool for acidic and basic sites of solids. **Applied Catalysis**. 78: 213-225.
- Lavalley, J. C. (1996). Infrared spectrometric studies of the surface basicity of metal oxides and zeolites using adsorbed probe molecules. **Catalysis Today**. 27: 377-401.
- Meyer, U. and Hoelderich, W. F. (1999). Application of basic zeolites in the decomposition reaction of 2-methyl-3-butyn-2-ol and isomerization of 3-carene. **Journal of Molecular Catalysis**. 142: 213-222.
- Murphy, D. Massiani, P., Franck, R. and Barthomeuf, D. (1996). Basic site heterogeneity and location in alkali cation exchanged EMT zeolite. An IR study using adsorbed pyrrole. **Journal of Physical Chemistry**. 100: 6731-6738.
- Murphy, D. Massiani, P., Franck, R. and Barthomeuf, D. (1997). Determination of basic site location and strength in alkali exchanged zeolites. In: **Progress in Zeolite and Microporous Materials Studies in Surface Science and Catalysis**, Vol. 105: Chon, H. Ihm, S.-K. and Uh, Y. S. (eds.), pp. 639-646. Elsevier Science B. V., The Netherlands.
- Noiroj, K., Intarapong, P., Luengnaruemitchai, A. and Jai-In, S. (2009). A comparative study of $\text{KOH}/\text{Al}_2\text{O}_3$ and KOH/NaY catalysts for biodiesel

- production via transesterification from palm oil. **Renewable Energy**. 34: 1145-1150.
- Ramos, M. J., Casas, A., Rodríguez, L., Romero, R. and Pérez, A. (2008). Transesterification of sunflower oil over zeolites using different metal loading: A case of leaching and agglomeration studies. **Applied Catalysis A: General**. 346: 79-85.
- Sánchez, M. S. and Blasco, T. (2002). Investigation on the nature of the adsorption sites of pyrrole in alkali-exchanged zeolite Y by nuclear magnetic resonance in combination with infrared spectroscopy. **Journal of American Chemical Society**. 124: 3443-3456.
- Shen, B., Chun, Y., Zhu, J.H., Wang, Y., Wu, Z., Xia, X. J., and Xu, Q. H. (2009). Environmentally benign decomposition of potassium nitrate on zeolites. **PhysChemComm**. 2: 9-14
- Scherzer, J., Bass, J. L. and Hunter, F. B. (1975). Structural characterization of hydrothermally treated lanthanum Y zeolites. I. Framework vibrational spectra and crystal structure. **The Journal of Physical Chemistry**. 79: 1194-1199.
- Sun, L. B., Gu, F. N., Chun, Y., Kou, J. H., Yang, J., Wang, Y., Zhu, J. H. and Zou, Z. G. (2008). Adjusting the host-guest interaction to promote KNO_3 decomposition and strong basicity generation on zeolite NaY. **Microporous and Mesoporous Materials**. 116: 498-50.

CHAPTER V

TRANSESTERIFICATION OF JATROPHA SEED OIL USING POTASSIUM SUPPORTED ON MCM-41 AS HETEROGENEOUS CATALYSTS

5.1 Introduction

Mobil Crystalline Material-41, MCM-41, is a mesoporous material composed of silica framework with a hexagonal or honeycomb packing of uniform mesopore channels. Its physical properties such as high specific surface area, well defined regular pore diameter, narrow pore size distribution and excellent thermal and hydrothermal stability make it useful as an adsorbent and a catalytic support (Zhao, Lu Max, and Millar, 1996; Selvam, Bhatia, and Sonwane, 2001). In addition, highly ordered distribution of mesopores allows possibility of incorporating metals into the structures.

MCM-41 could be modified to improve hydrothermal stability and to produce active sites and the modification also broadens its application (Shylesh, Samuel, and Singh, 2007). The base strength of MCM-41 can be increased by incorporating metal and metal oxide into its structure. Corma, Iborra, Miquel, and Primo (1998) synthesized cesium supported on MCM-41 and used it as a catalyst for the production of monoglycerides by transesterification between glycerol and triglycerides. Jiménez-Morales, Santamaría-González, Maireles-Torres, and Jiménez-López (2011) studied

zirconium sulfate supported on MCM-41 as acid catalyst for transesterification of sunflower oil with ethanol. These acid catalysts have been used in the ethanolysis of sunflower oil at 200 °C. The use of 14.6 wt% of the catalyst containing 30 wt% zirconium sulfate provided biodiesel yield of 91.5 wt%. Sercheli, Vargas, and Schuchardt (1999) prepared heterogeneous basic catalysts by immobilization alkylguanidines-strong organic bases such as 1,5,7-Triazabicyclo[4.4.0]dec-5-ene (TBD) and 1,2,3-tricyclohexylguanidine (TCG) on MCM-41. The catalyst with TBD anchored onto MCM-41 showed good activity for transesterification than that of catalyst with TCG anchored onto MCM-41. The TBD-MCM-41 gave 92% yield in methyl ester at 70 °C for 5 h. Artkla, Grisdanurak, Neramittagapong, and Wittayakun (2008) used MCM-41 synthesized from rice husk silica, RH-MCM-41, as a catalytic support for potassium oxide (K_2O). Potassium acetate precursor was impregnated on the support to produce $K_2O/RH-MCM-41$ with K_2O loading of 4, 8 and 12%wt. These solid base catalysts were used in transesterification of palm olein oil and methanol at 50, 75 and 100 °C. Surface area of RH-MCM-41 was significantly reduced as K_2O loading was increased. It was suggested that high basicity of the potassium precursor caused the collapse of the mesoporous structure. The catalyst with 8% K_2O loading gave the highest conversion at all tested temperatures. At this loading, the activity increased with the temperature and the highest conversion was 84% at 100 °C in 7 h reaction time. Because of the promising catalytic performance, different precursor and milder treatment conditions were investigated to produce $K_2O/RH-MCM-41$ with preservation of the MCM-41 structure.

In this Chapter, the preparation of MCM-41 and the catalyst with K loading on MCM-41 with the CH_3COOK in buffer and characterization of the catalysts were

described. Basicities of these catalysts were investigated using temperature programmed desorption of pyrrole and catalytic conversion of 2-methyl-3-butyn-2-ol (MBOH). Comparison between the basicity of the catalyst with K loading on NaY zeolite and MCM-41 was also reported.

5.2 Experimental

5.2.1 Synthesis of MCM-41

The synthetic method for MCM-41 was adopted from that reported by Artkla et al. (2008). Sodium silicate solution was prepared by mixing 3.00 g rice husk silica, 3.00 g NaOH and 30 mL deionized water. The mixture was stirred for 12 h to obtain a clear solution. The solution was slowly poured into a template solution which composed of 4.50 g cetyltrimethylammonium bromide (CTAB) in 90 mL deionized water. The mixture pH was adjusted to 11.5 by slowly dropping 5 N H₂SO₄ until small particles started to form. The gel mixture was then transferred into a teflon-lined autoclave and annealed hydrothermally in an oven at 100 °C for 72 h. The white particles in the mixture were filtered out, dried at 100 °C, ground and calcined at 540 °C to remove the template.

5.2.2 Preparation of catalysts

Potassium supported MCM-41 catalysts were prepared by impregnation method. Potassium acetate/acetic acid (CH₃COOK/CH₃COOH) solutions with various amount of CH₃COOK and CH₃COOH were prepared and impregnated on MCM-41 to produce catalysts with 4, 8 and 12 wt% of K loading. To obtain a 4 wt% of K loading on MCM-41, 8 mL of CH₃COOK/CH₃COOH solution

which composed 0.6482 g CH_3COOK and 0.38 mL CH_3COOH in 50 mL aqueous solution, was added dropwise onto 1.03 g MCM-41. The impregnated supported was dried in an oven at 30 °C for 4 h and at 80 °C overnight before calcination at 400 °C for 3 h. Catalysts with 8 wt% and 12 wt% of K loading were prepared in similar fashion.

For 8K/MCM-41 catalysts, the $\text{CH}_3\text{COOK}/\text{CH}_3\text{COOH}$ solution used for impregnation composed of 1.2964 g CH_3COOK and 0.76 mL CH_3COOH in 50 mL solution and the solution composed of 1.9446 g CH_3COOK and 1.13 mL CH_3COOH was used for preparing 12K/MCM-41 catalyst. The obtained catalysts were notated xK/MCM-41, where x represents percent weight of potassium of 4, 8 and 12.

MCM-41 supplied by Artika was also used as the catalyst support and notated as MCM-41(A). Catalysts with 4, 8 and 12 wt% of K loading were prepared by impregnation method with various solutions of potassium acetate/acetic acid. With 4K/MCM-41 catalyst, the 0.8 g of MCM-41(A) was impregnated with $\text{CH}_3\text{COOK}/\text{CH}_3\text{COOH}$ solution which composed of 0.0753 g CH_3COOK and 43.8 μL CH_3COOH in 5 mL aqueous solution. The impregnated supported was placed in a fume hood at room temperature and afterwards dried in an oven at 80 °C before calcination at temperature of 300 °C or 500 °C for 3 h.

The solution of $\text{CH}_3\text{COOK}/\text{CH}_3\text{COOH}$ which composed of 0.1506 g CH_3COOK and 87.6 μL CH_3COOH in 5 mL aqueous solution was used for preparing 8K/MCM-41(A). With 12K/MCM-41(A), the solution composed of 0.2259 g of CH_3COOK and 131.4 μL CH_3COOH was impregnated onto 0.8000 g of MCM-41(A). These impregnated supports were dried and calcined as that of 4K/MCM-41(A). The

notations of these catalysts were xK/MCM-41(A)-300 and xK/MCM-41(A)-500 where x represents 4, 8 and 12 wt% of K loading and 300 or 500 represents the calcinations temperature.

Rice husk silica with 12 wt% of K loading designated as 12K/RH-SiO₂ was prepared and used for comparison study. The impregnated solution was 6.0248 g CH₃COOK and 3.51 mL CH₃COOH in 50 mL solution and 2 mL of this solution was slowly dropped onto 0.8000 g RH-SiO₂.

5.2.3 Characterization of catalysts

The crystalline phases of parent MCM-41, xK/MCM-41, xK/MCM-41(A) and 12K/RH-SiO₂ were examined by an X-ray diffractometer (Bruker AXS, D5005) using nickel-filtered Cu K α radiation. The X-ray was generated with a current of 40 mA and a potential of 40 kV. The measurements were made over a 2 θ range of 1 to 10° with a step size of 0.02° at a scanning speed of 1°/min.

The morphologies of MCM-41 and the prepared catalysts were investigated by a transmission electron microscope (JEOL JEM-2010). The samples were dispersed in an ethanol solution with the aid of a sonicator. Afterwards, the sample solution was dropped on a formvar-coated TEM grid (Copper 200 mesh grid) and dried in the air.

5.2.4 Transesterification of Jatropha seed oil

xK/MCM-41, xK/MCM-41(A)500 and 12K/SiO₂ catalysts were studied for their catalytic activity in transesterification of Jatropha seed oil. The apparatus for the reaction was described in Chapter III.

The reaction using 4K/MCM-41(A)-500 was carried out for 6 h with 40:1 methanol to oil molar ratio (2 mL of Jatropha seed oil and 3.3 mL of methanol), 2 wt% of catalyst based on the weight of the oil (0.1 g of catalyst) and 65 °C of reaction temperature. Moreover, with the same reaction mixture placed in 8-mL vial, the reaction was conducted in an ultrasonic bath (Model-575, Crest Ultrasonic Corp., NJ, USA) for 2 h.

For 8K/MCM-41(A)-500 catalyst tested under refluxing and under sonicating condition, the reaction condition was similar to that for 4K/MCM-41(A)-500, but the reaction time was 3 h for refluxing condition. The progress of the reaction was followed by thin layer chromatography (TLC). The detail of TLC procedure was explained in Chapter III.

5.2.5 Characterization of basic properties

Basic properties of the MCM-41, xK/MCM-41 and 12K/SiO₂ were investigated by temperature programmed desorption of pyrrole (pyrrole-TPD) and catalytic activity in conversion of 2-methyl-3-butyn-2-ol (MBOH). The samples were studied under the same experimental condition as those used for NaY samples described in the Chapter IV.

5.3 Results and discussion

5.3.1 Characterization of catalyst

Figure 5.1a and b show the XRD patterns of MCM-41(A), xK/MCM-41(A)-300 and xK/MCM-41(A)-500 (x = 4, 8, 12 wt% of K loading). The characteristic diffraction peaks of MCM-41 at 2.2, 3.8 and 4.4 degree are reflection of

the (100), (110) and (200) planes of hexagonal structure, respectively. The results are similar to those reported by Artkla et al. (2008) and Chen, Li, and Davis (1993). With 4 wt% of K loading on MCM-41(A), both of calcinations at 300 °C and 500 °C, the peak of the (100) plane shifted to higher 2θ value indicating the decreasing of d-spacing. With 8 wt% of K loading on MCM-41(A) calcined at 300 °C, the peak was still observed, but the intensity was very low. While no peak was observed for the 8K/MCM-41(A) catalyst calcined at 500 °C. With 12 wt% of K loading, the peak was not observed for catalysts calcined at 300 °C and 500 °C.

Figure 5.1c also shows the XRD patterns of MCM-41 and xK/MCM-41 ($x = 4, 8, 12$ wt% of K loading) calcined at 400 °C for 3 h. The trend of XRD patterns of these catalysts were similar as to those prepared with of MCM-41(A). The absence of the peaks suggested that the mesoporous structure of MCM-41 collapsed.

It can be concluded that impregnation of the MCM-41 with the potassium buffer solution cannot preserve the mesoporous structure of MCM-41. The collapse of MCM-41 structure might be attributed from the instability of mesoporous structure due to the hydrolysis of the Si-O-Si linkages with water molecules (Kawi and Shen, 2000). The other possible cause is the effect of new potassium species (K_2O) that could be formed after using high temperature for calcinations. K_2O with high basicity could dissolve the silica framework of MCM-41 (Xie et al., 2006; Artkla et al., 2008).

The XRD pattern of RH-SiO₂ in Figure 5.2 shows a broad peak at 22.5 degree which is a characteristic of amorphous silica. Similar diffraction pattern was observed with 12K/RH-SiO₂ and no diffraction peaks from K species were observed, indicating good dispersion of K on the surface of RH-SiO₂.

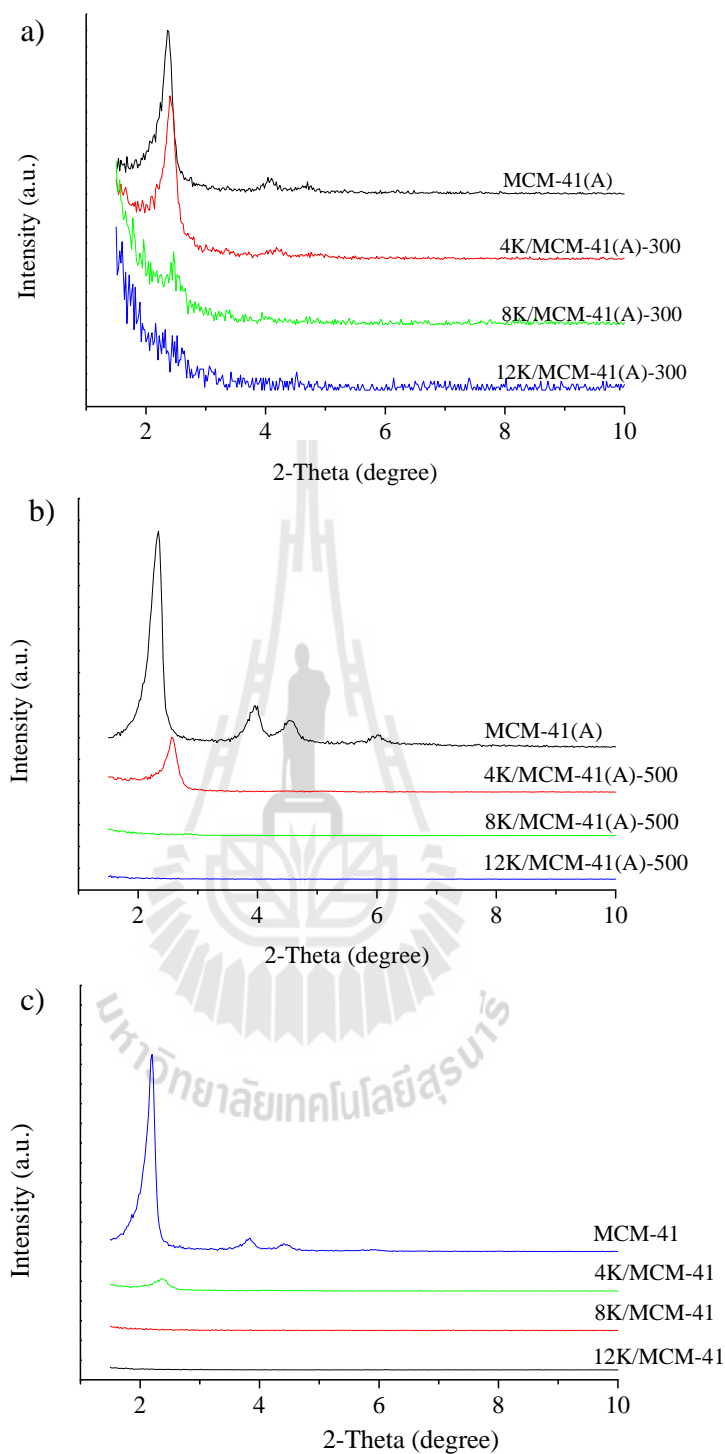


Figure 5.1 XRD patterns of the xK/MCM-41(A) and xK/MCM-41 with 4, 8 and 12 wt% loading; a) and b) xK/MCM-41(A) calcined at 300 °C and 500 °C, respectively, c) xK/MCM-41 calcined at 400 °C.

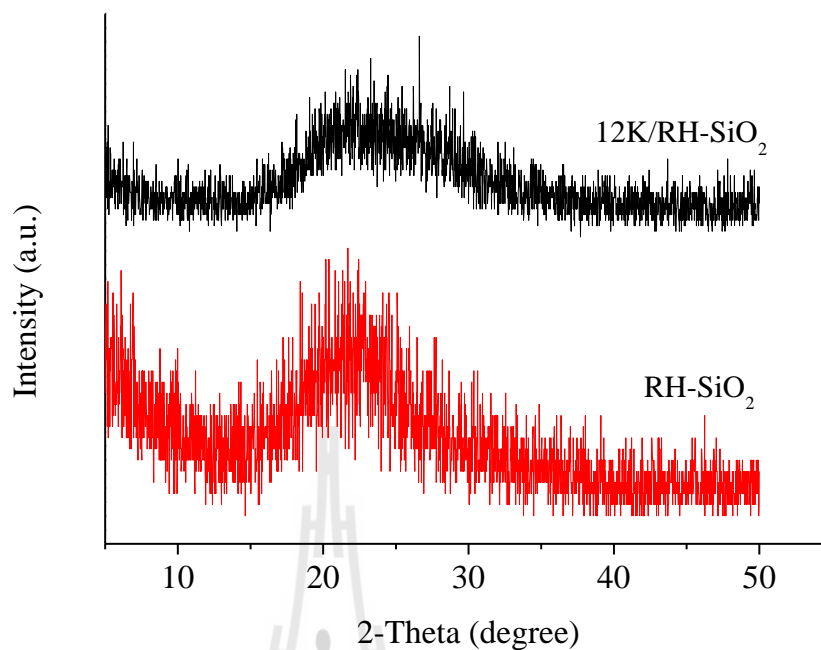


Figure 5.2 XRD patterns of the parent RH-SiO₂ and 12K/RH-SiO₂.

Transmission electron micrographs of MCM-41, 8K/MCM-41 and 12K/MCM-41 catalysts are shown in Figure 5.3. Figure 5.3a displays a honeycomb-like structure or hexagonal of uniform mesopores of MCM-41. The mesoporous structure was not observed for MCM-41 with 8 and 12wt% of K loading as shown in Figure 5.3b and c. These results agree with those obtained from XRD measurements.

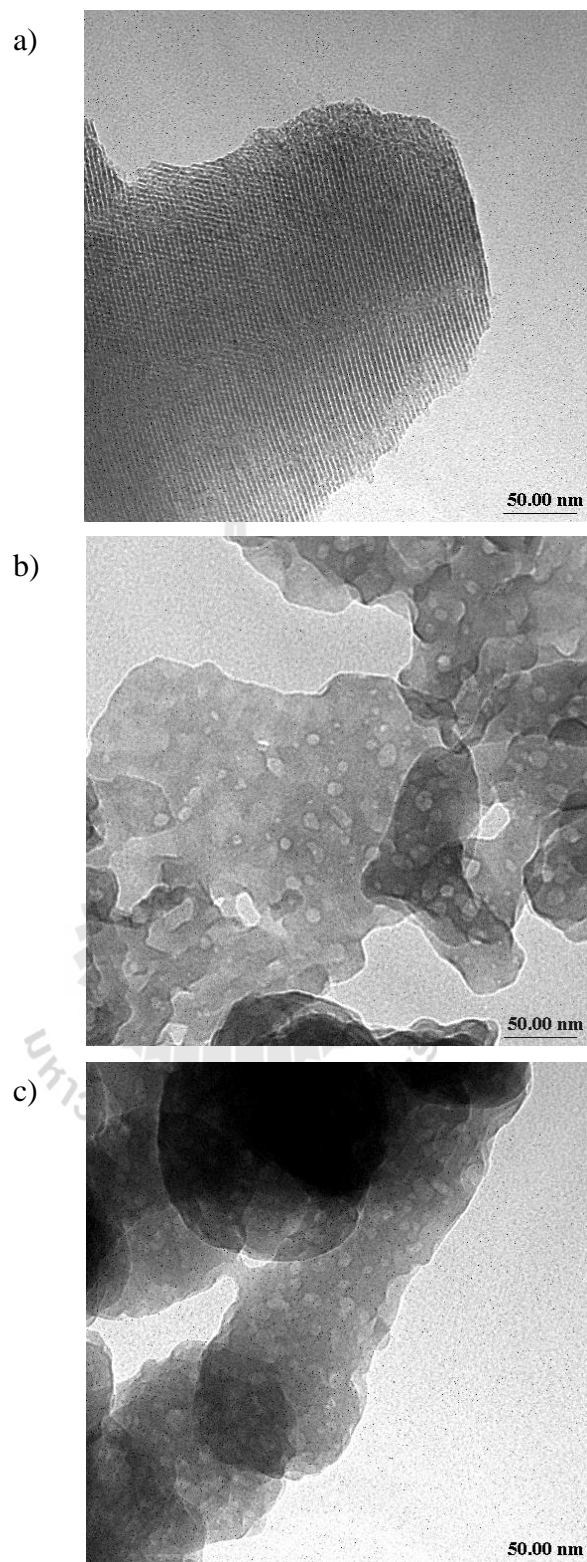


Figure 5.3 Transmission electron micrographs of the MCM-41, a); 8K/MCM-41, b) and 12K/MCM-41, c) catalysts.

5.3.2 Activities of the catalysts in transesterification

5.3.2.1 xK/MCM-41(A)-500 catalysts calcined at 500 °C

Figure 5.4 shows a TLC plate of a spot test from transesterification of Jatropha seed oil over 4K/MCM-41(A) under refluxing condition for 6 h. The results imply that the reaction was not complete because the spot of the crude oil was still present.

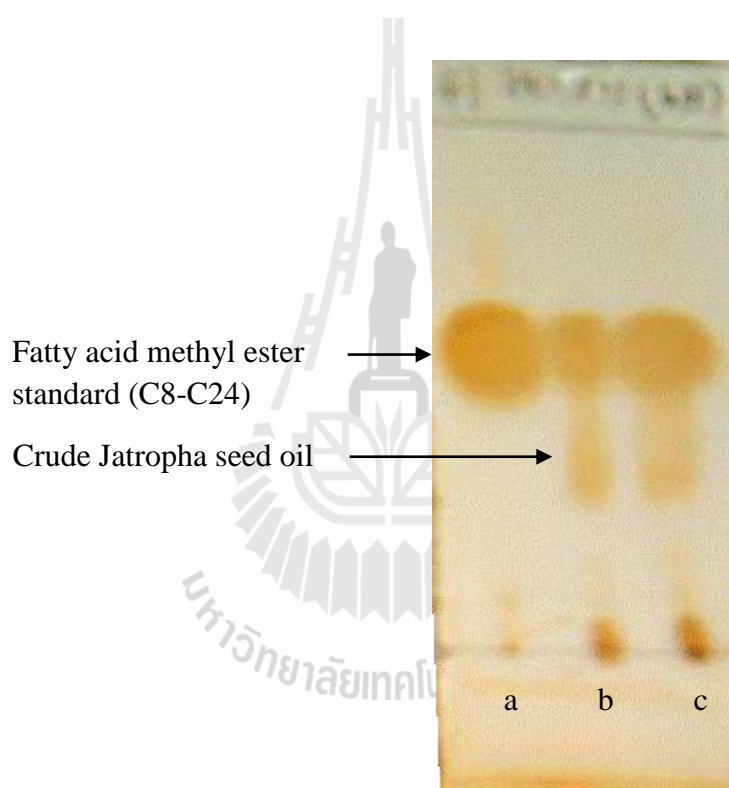


Figure 5.4 TLC plate showing spot a, methyl ester standard, spot b and c, liquid from transesterification of Jatropha seed oil with 4K/MCM-41(A)-500. Reaction condition: methanol to oil molar ratio, 40:1; reaction time, 6 h; temperature, 65 °C.

With ultrasonic condition, transesterification of Jatropha seed oil over 4K/MCM-41(A)-500 resulted in spots of methyl ester and Jatropha crude oil on TLC plate as shown in Figure 5.5. The spot of Jatropha seed oil was less intense than that of the sample from 4K/MCM-41(A)-500 under reflux condition and the reaction was also incomplete.

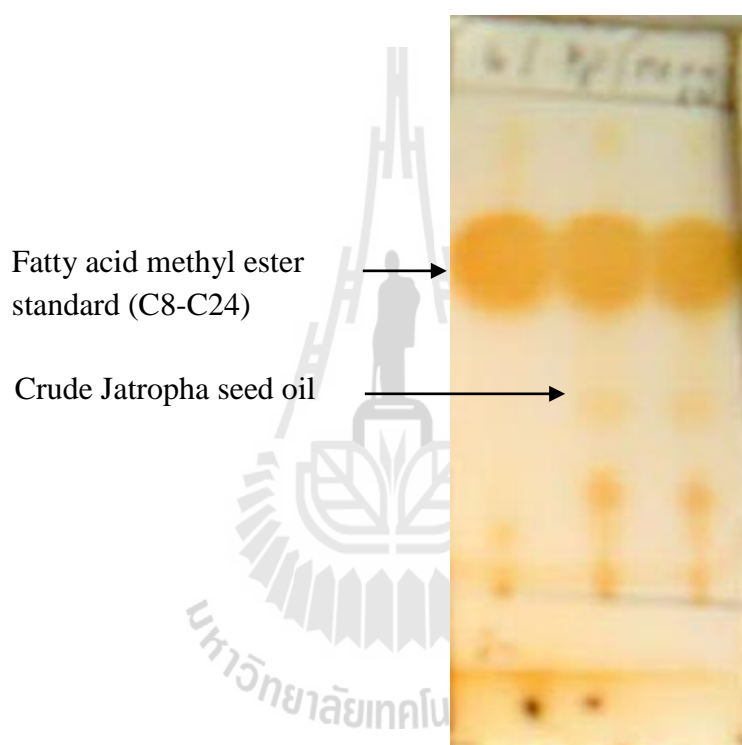


Figure 5.5 TLC plate of liquid from transesterification of Jatropha seed oil with 4K/MCM-41(A)-500 under ultrasonic condition, spots b and c compared to methyl ester standard, spot a. Reaction condition: methanol to oil molar ratio, 40:1; reaction time, 2 h.

With reflux condition, transesterification of Jatropha seed oil over 8K/MCM-41(A) was incomplete at the reaction time of 3 h. Figure 5.6 shows the spot of Jatropha crude oil that was still observed on the plate. With ultrasonic condition, both spots of methyl ester and Jatropha crude oil occurred after the reaction, however, the lesser intense of oil spot was observed (Figure 5.7).

These results suggested that transesterification with sonication was more efficient than that with refluxing method under the shorter reaction time.

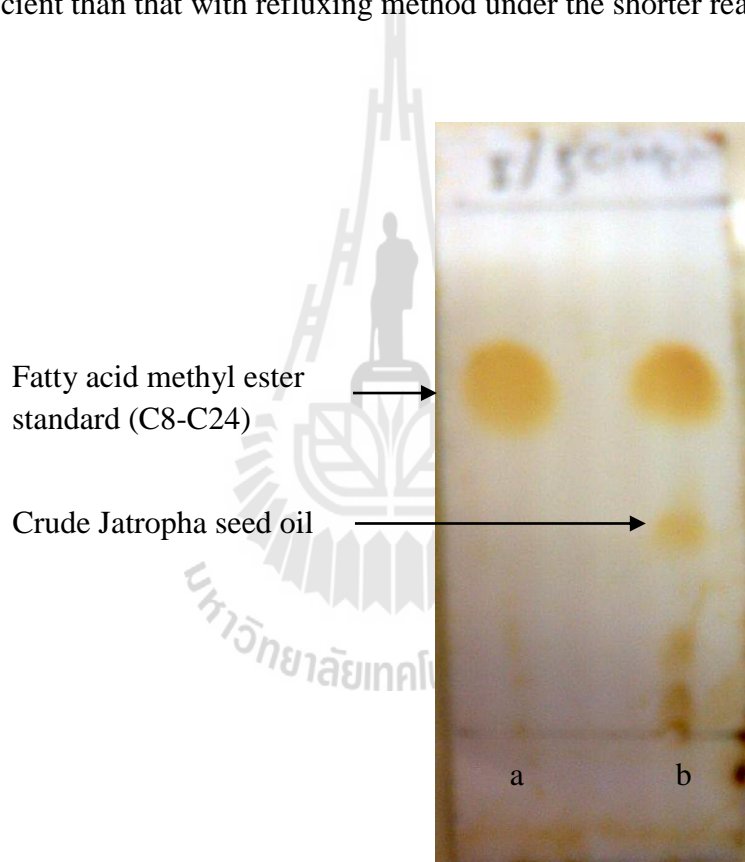


Figure 5.6 TLC plate of liquid from transesterification of Jatropha seed oil with 8K/MCM-41(A)-500 under reflux condition, spot b compared to methyl ester standard, spot a. Reaction condition: methanol to oil molar ratio = 40:1, reaction time = 3 h, temperature = 65 °C.

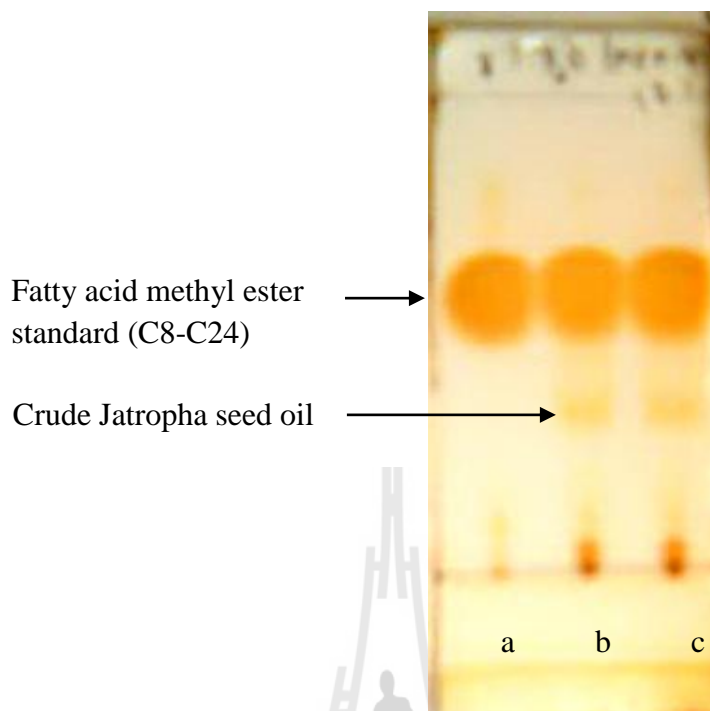


Figure 5.7 TLC plate of liquid from transesterification of Jatropha seed oil with 8K/MCM-41(A)-500 under ultrasonic condition, spots b and c compared to methyl ester standard, spot a. Reaction condition: methanol to oil molar ratio = 40:1, reaction time = 2 h.

5.3.2.2 xK/MCM-41 catalysts calcined at 400 °C

TLC was used to follow the progress of transesterification over xK/MCM-41 catalysts calcined at 400 °C. The results after transesterification for 3 h on these catalysts are shown in Figure 5.8. The reaction not complete for all of the catalysts. Only a spot of the crude oil was observed with 4K/MCM-41, whereas, spots of the crude oil and an unknown compound were present for 8K/MCM-41 and 12K/MCM-41 catalysts. The xK/MCM-41 were not the efficient catalysts for transesterification.

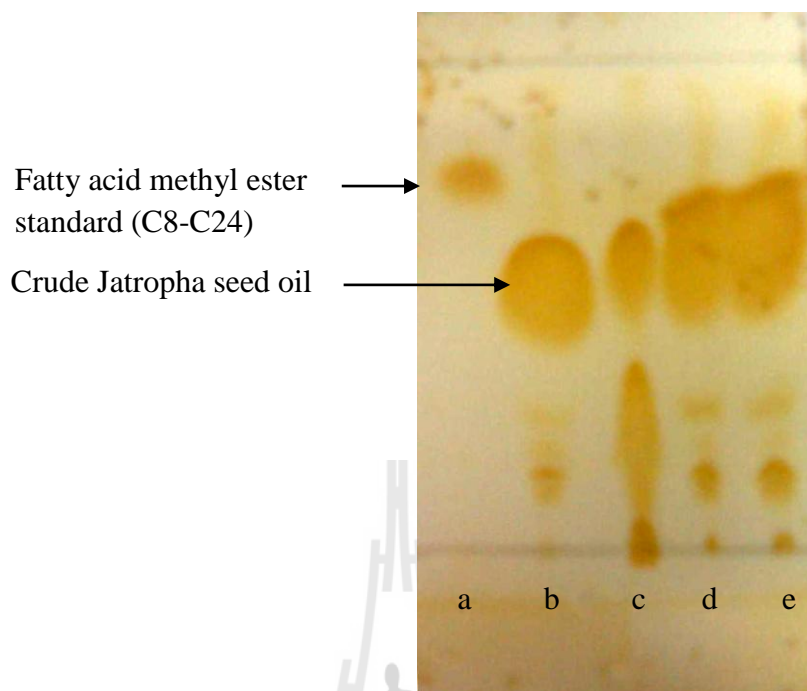


Figure 5.8 TLC plate represents spot a, methyl ester standard; spots b, c, d and e, liquid from the reaction with 4-, 8- and 12K/MCM-41 catalysts, respectively. The reaction conditions were methanol to oil molar ratio of 16:1, reaction time of 3 h and reaction temperature of 65 °C.

With 12K/RH-SiO₂, a more intense spot of methyl ester and a lighter spot of crude Jatropha oil were observed, Figure 5.9. This indicated that 12K/RH-SiO₂ provided a higher conversion than those of xK/MCM-41 under similar reaction condition. This higher conversion could be attributed to more K₂O on the external surface of RH-SiO₂ compared to those on the MCM-41 in which the impregnated K could be trapped within the collapsed structure. Besides, the leaching of K₂O during the transesterification might occur resulting in the reaction proceeding through the homogeneous catalysis pathway (Benjapornkulaphong, Ngamchanussivichai, and Bunyakia, 2009; Rashtizadeh, Farzaneh, and Ghandi, 2010).

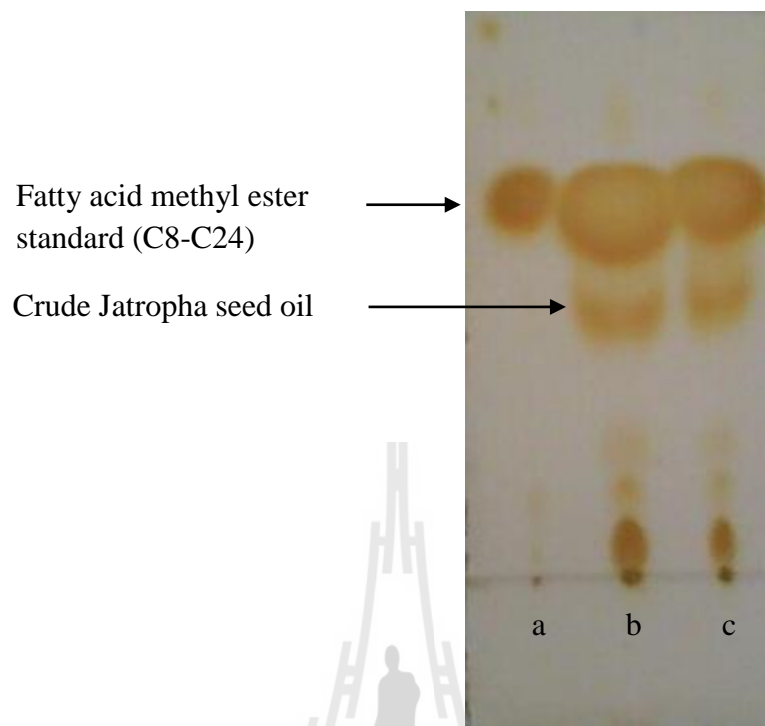


Figure 5.9 Result from transesterification over the 12K/RH-SiO₂ catalyst. Spot a is methyl ester standard. Spots b and c are liquid from the reaction condition was 16:1 methanol to oil molar ratio, 3 h reaction time and 65 °C reaction temperature.

5.3.3 Basic properties measurement

5.3.3.1 Pyrrole-TPD

The TPD profiles of desorbed pyrrole on the MCM-41, xK/MCM-41 and 12K/RH-SiO₂ are shown in Figure 5.10. The desorption peak of the MCM-41 occurred at 150 °C. After K loading, the desorption peaks of the xK/MCM-41 were slightly shift to the higher desorption temperature about 220 °C. It indicated that the stronger base strength was generated. However, the desorption temperature and the amount of desorbed pyrrole from each catalyst after K loading were about the same might be the acidic nature of MCM-41 and low amount of basic sites created because of the collapse of the MCM-41 structure. Similar behavior was observed on 12K/RH-SiO₂.

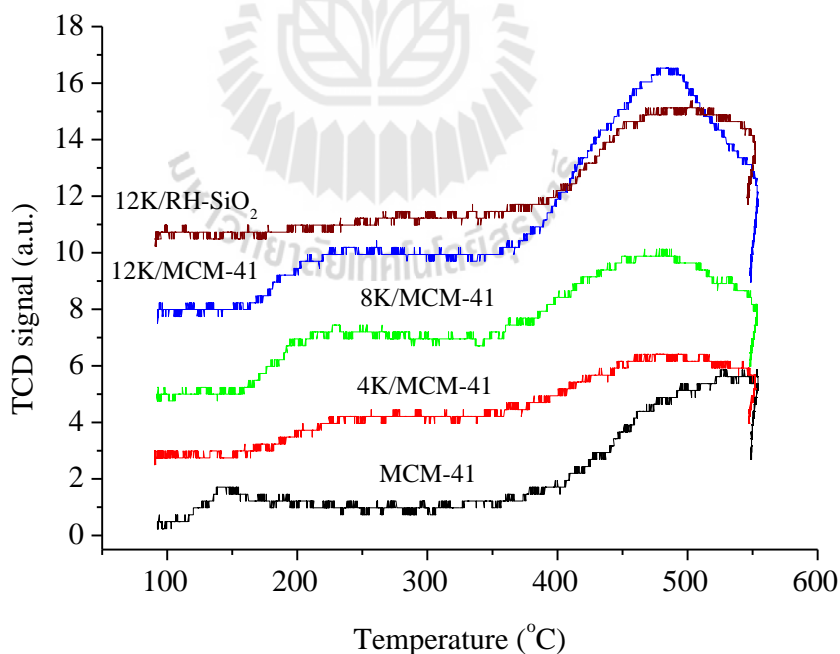


Figure 5.10 Desorption profiles of pyrrole on the MCM-41, xK/MCM-41 with 4, 8 and 12 wt% loading of K and 12K/RH-SiO₂.

5.3.3.2 Catalytic activity in conversion of MBOH

Figure 5.11 shows conversion of MBOH over the parent MCM-41 and xK/MCM-41 catalysts. These catalysts provided low MBOH ca. 0.7-0.8 mol%. It indicated that an increase in K content cannot produce an increase in activity and selectivity for xK/MCM-41. The transformation of MBOH over the parent MCM-41 agreed with that reported in a literature (Conesa, Hidalgo, Luque, Campelo, and Romero, 2006).

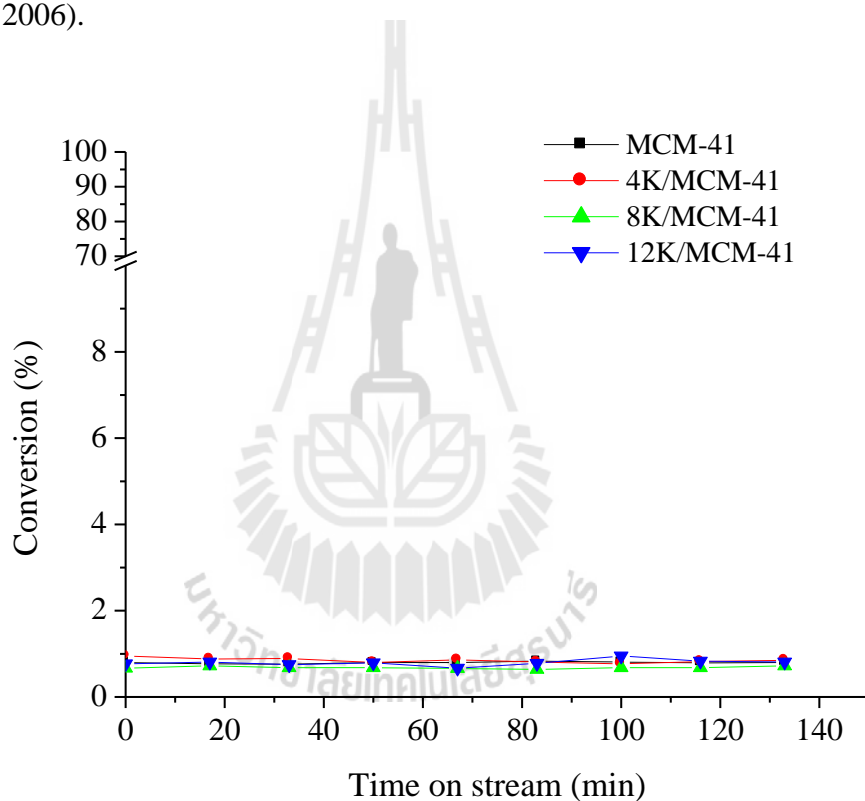


Figure 5.11 Conversion of MBOH over the parent MCM-41 and xK/MCM-41 catalysts. The reaction temperature was 120 °C and the amount of catalyst was 0.020 g.

The conversions of MBOH over 12K/MCM-41, 12K/RH-SiO₂ and 12K/NaY catalysts were compared in Figure 5.12. The highest conversion was obtained with 12K/NaY because 12K/NaY catalyst had more basic sites than 12K/MCM-41 and 12K/RH-SiO₂ catalysts as the result of NaY structure preservation after K loading.

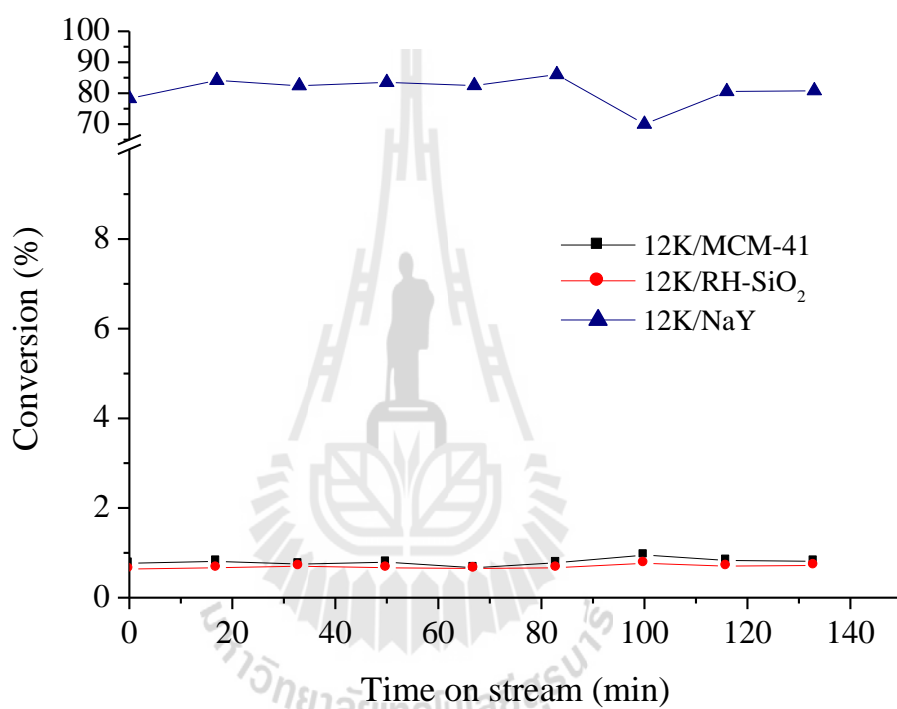


Figure 5.12 Conversion of MBOH test reaction over 12K/MCM-41, 12K/RH-SiO₂ and 12K/NaY catalysts.

5.4 Conclusions

The impregnation of a potassium buffer solution on MCM-41 did not provide the preservation of the mesoporous structure of MCM-41. Basicity characterization using pyrrole-TPD and transformation of MBOH revealed that the catalysts had low amount of base generated after K loading. All catalysts based on MCM-41 as a support were therefore inefficient for transesterification.

5.5 References

- Artkla, S., Grisdanurak, N., Neramittagapong, S. and Wittayakun, J. (2008). Characterization and catalytic performance on transesterification of plam olein of potassium oxide supported on RH-MCM-41 from rice husk silica. **Suranaree Journal of Science and Technology**. 15: 133-138.
- Benjapornkulaphong, S., Ngamchanussivichai, S. and Bunyakia, K. (2009). Al₂O₃-supported alkali and alkai earth metal oxides for transesterification of palm oil and coconuts. **Chemical Engineering Journal**. 145: 468-474.
- Chen, C.-Y., Li, H.-X. and Davis, M. E. (1993). Studies on mesoporous materials I. Synthesis and characterization of MCM-41. **Microporous Materials**. 2: 17-26.
- Conesa, T. D., Hidalgo, J. M., Luque, R. Campelo, J. M. and Romero, A. A. (2006). Influence of the acid–base properties in Si-MCM-41 and B-MCM-41 mesoporous materials on the activity and selectivity of ϵ -caprolactam synthesis. **Applied Catalysis A: General**. 299: 224-234.
- Corma, A., Iborra, S., Miquel, S. and Primo, J. (1998). Catalysts for the Production of Fine Chemicals. **Journal of Catalysis**. 173: 315-321.

- Jiménez-Morales, I., Santamaría-González, J., Maireles-Torres, P. and Jiménez-López, A. (2011). Calcined zirconium sulfate supported on MCM-41 silica as acid catalyst for ethanolysis of sunflower oil. **Applied Catalysis B: Environmental**. 103: 91-98.
- Kawi, S. and Shen, S-C. (2000). Effects of structural and non-structural Al species on the stability of MCM-41 materials in boiling water. **Materials Letters**. 42: 108-112.
- Rashtizadeh, E., Farzaneh, F. and Ghandi, M. (2010). A comparative study of KOH loaded on double aluminosilicate layers, microporous and mesoporous materials as catalyst for biodiesel production via transesterification of soybean oil. **Fuel**. 89: 3393-3398.
- Sercheli, R., Vargas, R. M. and Schuchardt, U. (1999). Alkylguanidine-Catalyzed Heterogeneous Transesterification of Soybean Oil. **Journal of the American Oil Chemists Society**. 76: 1207-1210.
- Selvam, P., Bhatia, S. K. and Sonwane, C. G. (2001). Recent Advances in Processing and Characterization of Periodic Mesoporous MCM-41 Silicate Molecular Sieves. **Industrial & Engineering Chemistry Research**. 40: 3237-3261.
- Shylesh, S., Samuel, P. P. and Singh, A. P. (2007). Synthesis of hydrothermally stable aluminium-containing ethane-silica hybrid mesoporous materials using different aluminium sources. **Microporous and Mesoporous Materials**. 100: 250-258.
- Xie, W., Peng H. and Chen, L. (2006). Transesterification of soybean oil catalyzed by potassium loaded on alumina as a solid-base catalyst. **Applied Catalysis A: General**. 300: 67-74.

Zhao, X. S., Lu Max, G. Q. and Millar, G. J. (1996). Advance in Mesoporous Molecular Sieve MCM-41. **Industrial & Engineering Chemistry Research**. 35: 2075-2090.



CHAPTER VI

CONCLUSIONS

6.1 Summary

Research was directed towards the development of heterogeneous base catalysts to be employed in transesterification of Jatropha seed oil. A buffer solution of acetic acid/potassium acetate was impregnated onto NaY and MCM-41 in the process of the catalyst preparation to obtain the catalysts with 4, 8 and 12 wt% of K loading. Potassium nitrate solution was also used as a catalyst precursor.

Transesterification was performed in a batch reactor using Jatropha seed oil obtained from the seeds of *Jatropha curcas* planted in Nakhon Ratchasima and methanol as the reactants. Reaction parameters including the molar ratio of methanol to oil, the amount of the catalyst and the reaction time were varied to obtain the optimum yield of biodiesel. Thin layer chromatography was used to follow the progress of the reaction and gas chromatography was used to determine the amount of free fatty acid methyl esters.

In the reaction using potassium supported on NaY, 12K/NaY was the most active catalyst providing the highest biodiesel yield of 73.4% under the optimum reaction condition: 16:1 methanol to oil molar ratio, 4 wt% catalyst, 65 °C reaction temperature and 3 h reaction time. The surface area of the catalyst, the basic strength and the amount of basic sites played the important roles in the catalysis process as revealed from the studies by nitrogen adsorption-desorption, temperature programmed

desorption of pyrrole and a conversion of 2-methyl-3-butyn-2-ol. Leaching of active species (K species) from the catalyst was found and this would affect the catalytic cycle.

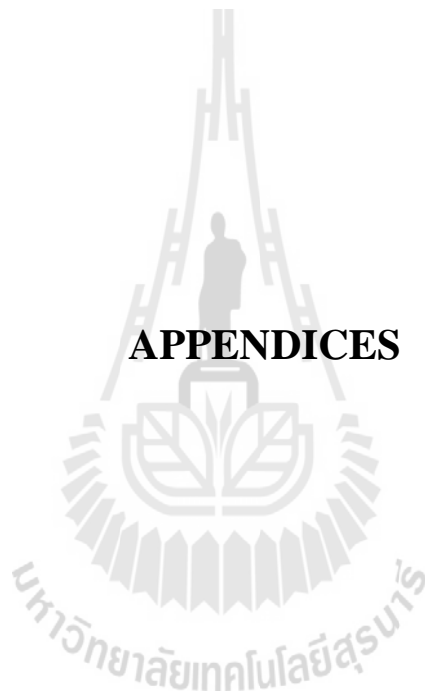
The xK/MCM-41 catalysts were not as active as the xK/NaY catalysts because the collapse of MCM-41 structure occurred after K loading and less basicity was generated on the support.

The developed 12K/NaY catalyst showed the potential to be an alternative catalyst for biodiesel production from *Jatropha* seed oil. The advantages of the catalyst over homogeneous catalysts such as NaOH and KOH commonly used in transesterification are for example, the catalyst can be separated more easily from the product, the catalyst can be recycled, the catalyst can be applied in a continuous process and the process is environmental friendly, as the water is not used to clean the product.

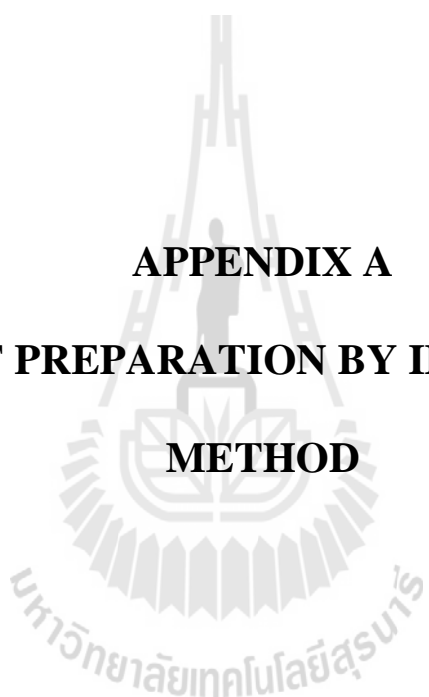
6.2 Future work

Further studies of the 12K/NaY catalyst should be concerned with leaching of the active species. Means to reduce leaching should be studied in order that the catalyst can be recycled many times as possible. A larger scale operation and a continuous operation should be investigated. Performance of the developed catalyst should be evaluated with various types of vegetable oils. Other compounds to be used as a catalyst precursor should be explored.

APPENDICES



APPENDIX A
CATALYST PREPARATION BY IMPREGNATION
METHOD



A.1 Catalyst with 4, 8 and 12 wt% of K loading on NaY

Preparation of solutions

1. 0.8186 M of potassium acetate buffer solution ($\text{CH}_3\text{COOK}/\text{CH}_3\text{COOH}$):

4.0169 g of CH_3COOK was dissolved in DI water and transferred to 50 mL volumetric flask and 2.34 mL of CH_3COOH was added. The solution was made up to the volume with DI water.

2. 1.6372 M of potassium acetate buffer solution ($\text{CH}_3\text{COOK}/\text{CH}_3\text{COOH}$):

8.0337 g of CH_3COOK was dissolved in DI water and transferred to 50 mL volumetric flask and 4.69 mL of CH_3COOH was added. The solution was made up to the volume with DI water.

3. 2.4558 M of potassium acetate buffer solution ($\text{CH}_3\text{COOK}/\text{CH}_3\text{COOH}$):

12.0506 g of CH_3COOK was dissolved in DI water and transferred to 50 mL volumetric flask and 7.03 mL of CH_3COOH was added. The solution was made up to the volume with DI water.

Impregnation Procedure

For the catalyst with 4 wt% of K loading, 2.4 g of NaY was weighed into a crucible and 3 mL of 0.8186 M of potassium acetate buffer solution was added dropwise on NaY. The resulting mixture was dried in an oven at 30 °C for 4 h and at 80 °C overnight before calcination at 400 °C for 3 h. For the preparation of the catalyst with 8 and 12 wt% of K loading, 3 mL of 1.6372 M and 2.4558 M of potassium acetate buffer solution were loaded on 2.4 g of NaY. The same drying and calcination conditions were used.

A.2 Catalyst with 4, 8 and 12 wt% of K loading on MCM-41

Preparation of solutions

1. 0.1321 M of potassium acetate buffer solution ($\text{CH}_3\text{COOK}/\text{CH}_3\text{COOH}$):

0.6482 g of CH_3COOK was dissolved in DI water and transferred to 50 mL volumetric flask and 0.38 mL of CH_3COOH was added. The solution was made up to the volume with DI water.

2. 0.2642M of potassium acetate buffer solution ($\text{CH}_3\text{COOK}/\text{CH}_3\text{COOH}$):

1.2964 g of CH_3COOK was dissolved in DI water and transferred to 50 mL volumetric flask and 0.76 mL of CH_3COOH was added. The solution was made up to the volume with DI water.

3. 0.3963 M of potassium acetate buffer solution ($\text{CH}_3\text{COOK}/\text{CH}_3\text{COOH}$):

1.9446 g of CH_3COOK was dissolved in DI water and transferred to 50 mL volumetric flask and 1.13 mL of CH_3COOH was added. The solution was made up to the volume with DI water.

Impregnation procedure

For the catalyst with 4 wt% of K loading, 1.033 g of MCM-41 was weight into a crucible and 8 mL of 0.1321 M of potassium acetate buffer solution was added dropwise on MCM-41. The resulting mixtures was dried in an oven at 30 °C for 4 h and at 80 °C overnight before calcination at 400 °C for 3 h. The same procedure was used for preparation of the catalysts with 8 and 12 wt% of K loading using 8 mL of 0.2642 M and 0.3963 M of potassium acetate buffer solution, respectively.

A.3 Catalyst with 12 wt% of K loading on RH-SiO₂

Preparation of solution

1.2278 M of potassium acetate buffer solution (CH₃COOK/CH₃COOH):

6.0248 g of CH₃COOK was dissolved in DI water and transferred to 50 mL volumetric flask and 3.51 mL of CH₃COOH was added. The solution was made up to the volume with DI water.

Impregnation procedure

0.8 g of RH-SiO₂ was weight into a crucible and 2 mL of 1.2278 M of potassium acetate buffer solution was added dropwise on NaY. The resulting mixture was dried in an oven at 30 °C for 4 h and at 80 °C overnight before calcination at 400 °C for 3 h.

A.4 Catalyst with 12 wt% of KNO₃ loading on NaY

Solution

2.4552 M of potassium nitrate solution (KNO₃):

2.4823 g of KNO₃ was dissolved in DI water and transferred to 10 mL volumetric flask and DI water was filled to make up the volume.

Impregnation procedure

0.8 g of NaY was weight into a crucible and 1 mL of 2.4552 M of Potassium nitrate solution was added dropwise on NaY. The resulting mixture was dried in an oven at 30 °C for 4 h and at 80 °C overnight before calcination at 400 °C for 3 h.

APPENDIX B
DETERMINATION OF METHYL ESTERS BY GAS
CHROMATOGRAPHY

มหาวิทยาลัยเทคโนโลยีสุรนารี

B.1 Preparation of standard solutions for GC analysis

1.1 Preparation of stock standard solution of methyl esters

Methyl ester standards as shown in Table B.1 were weighed and dissolved in hexane. The solution was made up in a 5 mL volumetric flask.

Table B.1 Composition of stock standard solution of methyl esters.

Methyl ester	Weight (mg)	Concentration (ppm)
C16:0	20	4,000
C16:1	10 (11.4 μ L)	2,000
C18:0	20	4,000
C18:1	50 (57.2 μ L)	10,000
C18:2	50 (56.2 μ L)	10,000
C20:0	11.5	2,000

1.2 Preparation of stock standard solution of methyl heptadecanoate (C17:0) and methyl linolenate (C18:3)

1.2.1 Preparation of 2,000 ppm C17:0

10 mg of C17:0 was weighed, dissolved in hexane, placed into 5 mL volumetric flask and made up to the volume by hexane.

1.2.2 Preparation of 2,000 ppm C18:3

10 mg of C18:3 was weighed, dissolved in hexane, placed into 5mL volumetric flask and made up to the volume by hexane.

1.2.3 Preparation of 1,000 ppm C17:0 and C18:3 solution

500 μL of 2,000 ppm of C17:0 and C18:3 were added into 1 mL vial, capped with the a septum-lined cap and mixed.

1.3 Preparation of 2,000 ppm of methyl linolenate (C18:3)

10 mg of C18:3 was weighed and dissolved in hexane, placed into 5 mL volumetric flask and made up to the volume with hexane.

1.4 Preparation of 20,000 ppm methyl nonadecanoate (C19:0) as internal standard (0.1g/5mL)

100 mg of C19:0 was weighed and dissolved in chloroform and transferred to 5 mL volumetric flask. Chloroform was added to make up the volume of the solution.

B.2 Preparation of calibration curve for GC analysis

2.1 Standard solutions of C16:0, C16:1, C18:0, C18:1, C18:2 and C20:0

A set of five 1 mL of volumetric flasks was labeled No. 1- 5. 0.8, 0.5, 0.2, 0.1 and 0.05 mL of the stock standard solution were added into the labeled 1 mL of volumetric flasks, respectively. 50 μL of C19:0 as the internal standard was added into all flasks and hexane was added to make up the volume of the solution. The prepared solutions were transferred to 1 mL vial and capped with the septum cap. Table B.2 presents methyl esters concentration in standard solutions.

Table B.2 Concentration of the standard solution for calibration curve.

Standard solution	Concentration of Methyl ester standard (ppm)					
	C16:0	C16:1	C18:0	C18:1	C18:2	C20:0
1	3,200	1,600	3,200	8,000	8,000	1,600
2	2,000	1,000	2,000	5,000	5,000	1,000
3	800	400	800	2,000	2,000	400
4	400	200	400	1,000	1,000	200
5	80	40	80	200	200	40

2.2 Calibration curve of stock standard solution of 1,000 ppm of C17:0 and C18:3

A set of three 1 mL of volumetric flasks was labeled No. 1- 3. 0.2, 0.1 and 0.05 mL of the stock standard solution was added into the labeled 1 mL of volumetric flasks, respectively. 50 μ L of C 19:0 was added into each flask and hexane was added to make up the solution volume. The prepared solutions were transferred to 1 mL of vial and capped with the septum cap. The methyl ester concentrations of the solutions are shown in Table B.3

Table B.3 Concentration of the standard solution of C17:0 and C18:3 for calibration curve.

Standard Solution for calibration curve	Concentration of Methyl ester standard, ppm	
	C17:0	C18:3
1	400	400
2	200	200
3	100	100

B.3 Preparation of a sample for GC analysis

50 μL of a sample (the upper phase liquid from transesterification) was added into 1 mL volumetric flask. About 500 μL of hexane was added into the flask and 50 μL of C 19:0 as the internal standard was spiked into the solution. Hexane was filled up to the marked line. The prepared sample was transferred to 1 mL of vial and capped with the septum cap.

B.4 Chromatographic conditions

Instrument:	Gas Chromatograph (GC-HP6890-Series)
Detector:	Flame Ionization Detector (FID)
Column type:	HP-INNOWax Polyethylene Glycol, 30 m \times 0.32 mm ID, 0.15 μm film
Injection Temperature:	220 $^{\circ}\text{C}$
Detector Temperature:	250 $^{\circ}\text{C}$

Temperature program: 140 °C isothermal for 3 minutes. Then increase temperature to 240 °C at a rate of 10 °C/minute. Hold at 240 °C for 7 minutes.

Injection volume: 1 μ L

B.5 GC chromatogram and retention time of methyl ester standard

Table B.4 The retention time of each methyl ester standard.

Methyl ester	Retention time (min)
C16:0	11.973
C16:1	12.239
C17:0	13.083
C18:0	14.160
C18:1	14.398
C18:2	14.921
C19:0	15.257
C19:0	15.685
C20:0	16.389

B.6 Calibration curve for fatty acid methyl ester standard

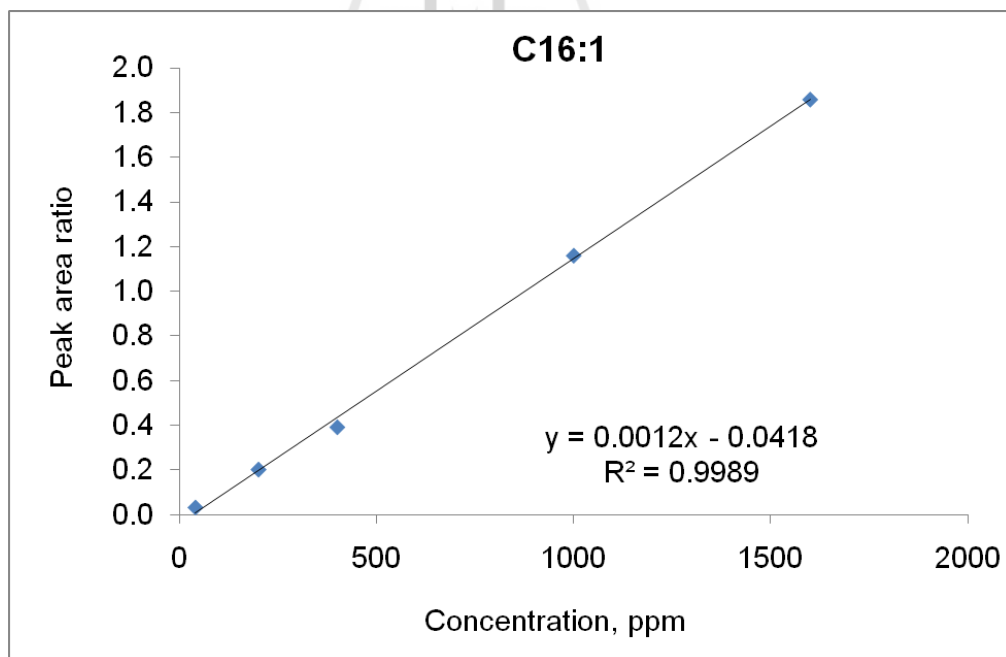
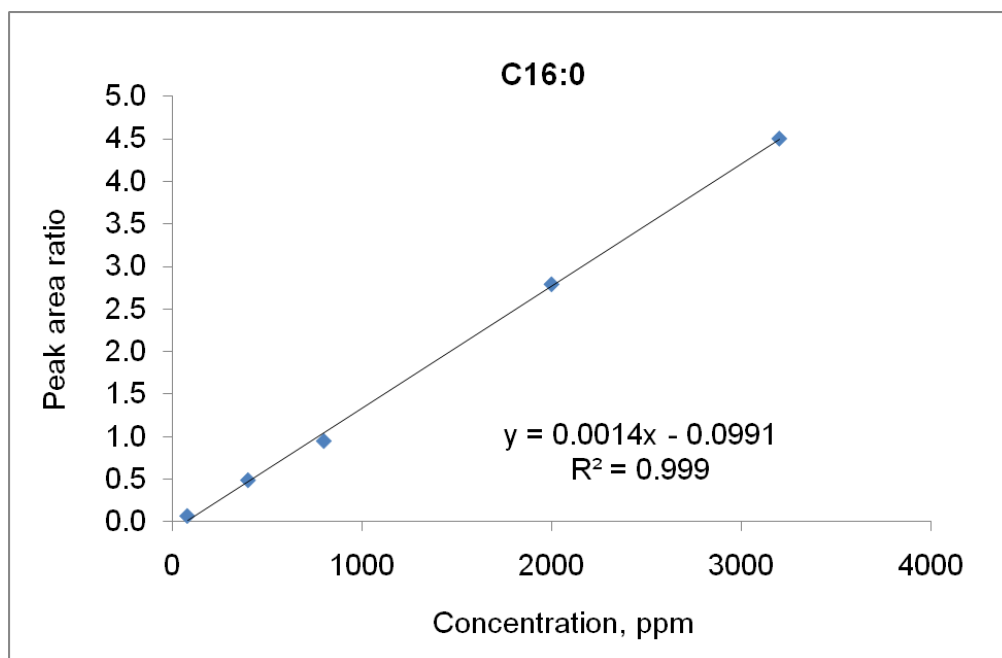


Figure B.1 Calibration curve of fatty acid methyl esters.

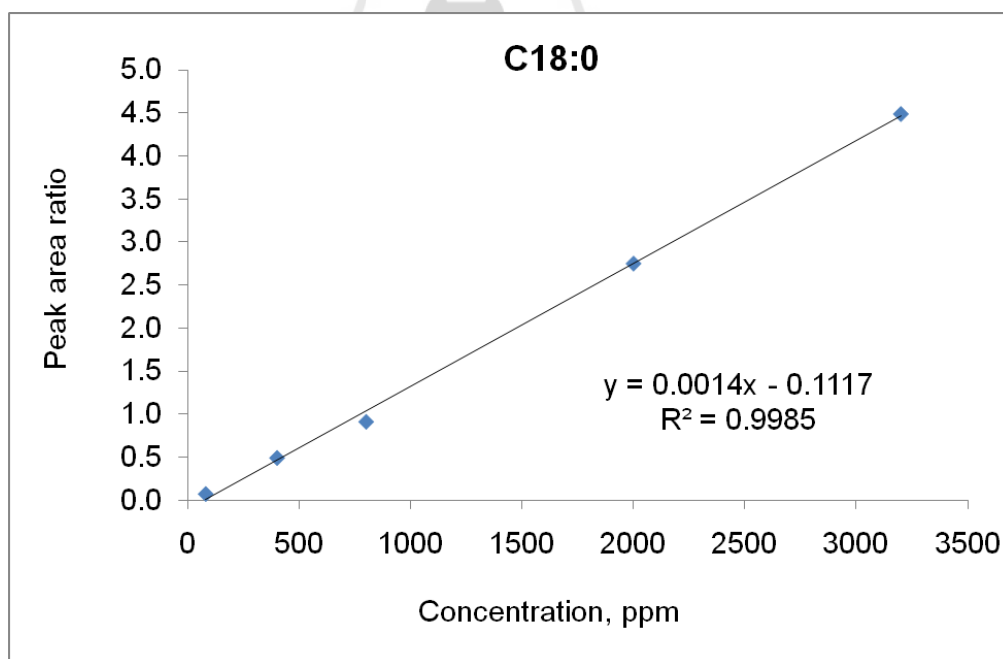
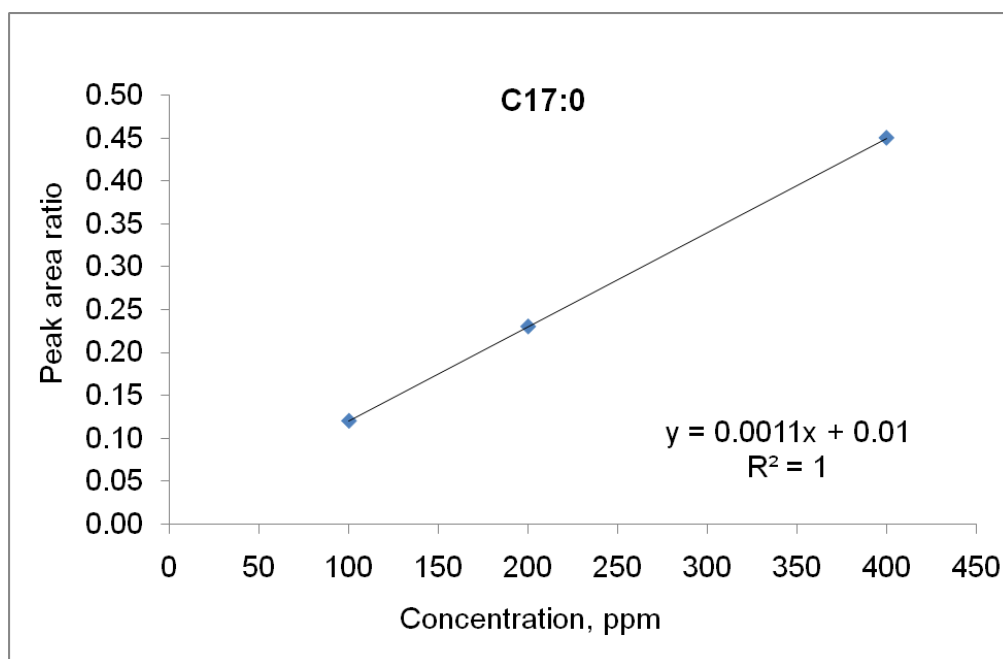


Figure B.1 (continued)

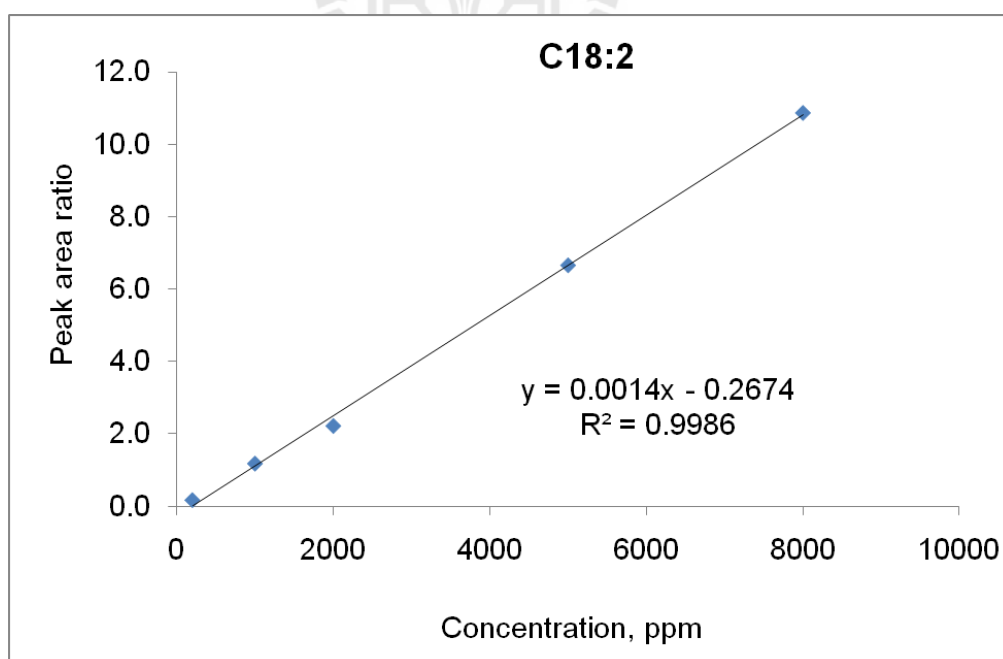
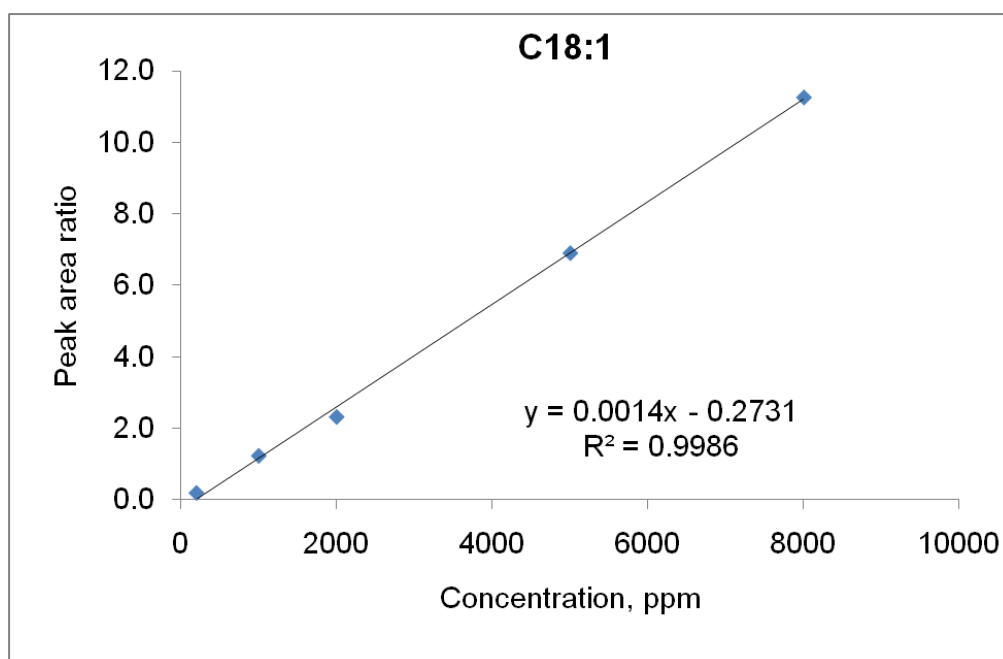


Figure B.1 (continued)

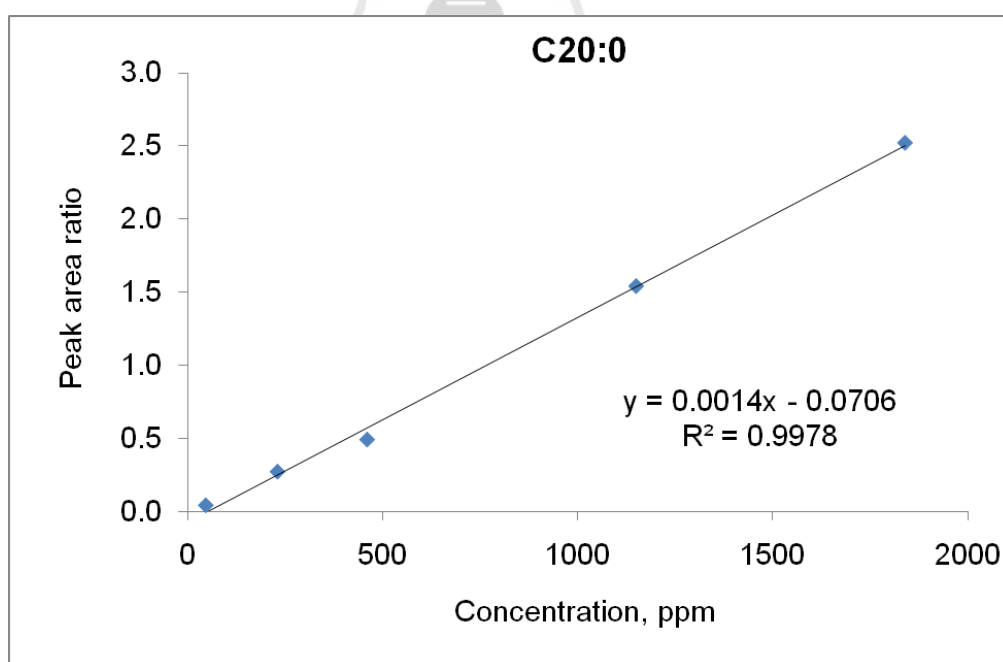
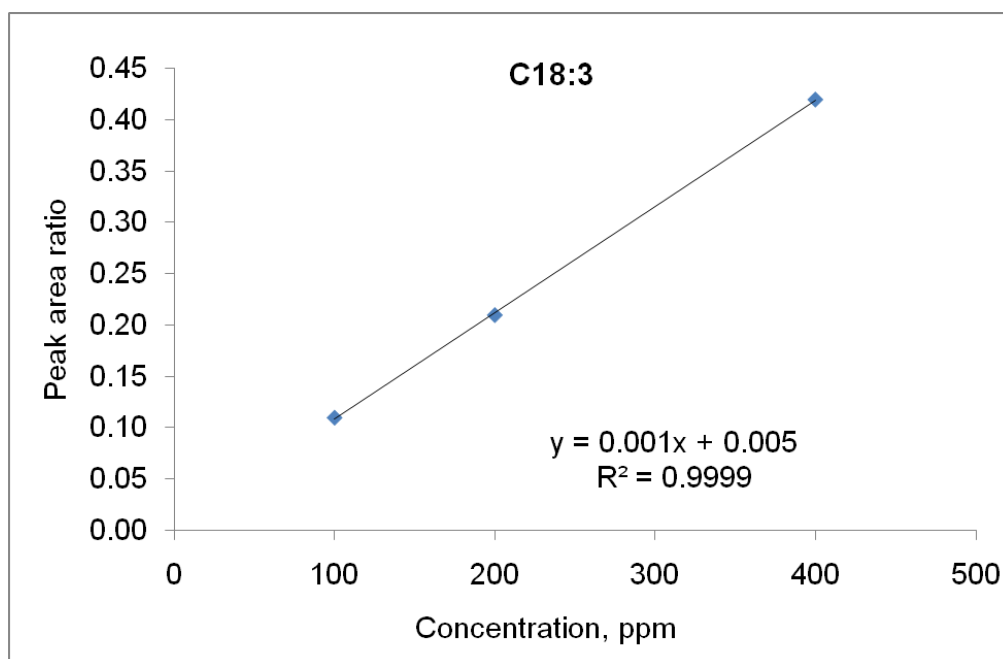


Figure B.1 (continued)

B.7 Catalyst leaching test for the transesterification

7.1 Chromatographic conditions

Instrument:	Gas Chromatography (HP5890-Series II)
Detector:	Flame Ionization Detector (FID)
Column type:	fused silica column (15 m x 0.25 mm, with a 0.25 μm film made up of 5% diphenylpolysiloxane and 95% dimethylpolysiloxane, Marcherey-Nagel)
Injection Temperature:	300 $^{\circ}\text{C}$
Detector Temperature:	360 $^{\circ}\text{C}$
Temperature program:	The initial temperature is 130 $^{\circ}\text{C}$, then increase temperature to 200 $^{\circ}\text{C}$ at a rate of 15 $^{\circ}\text{C}/\text{minute}$ and hold for 2 minutes. Next, increase temperature to 340 $^{\circ}\text{C}$ at a rate of 10 $^{\circ}\text{C}/\text{minute}$.
Injection volume:	0.5 μL

7.2 GC chromatogram and retention time of each methyl ester standard

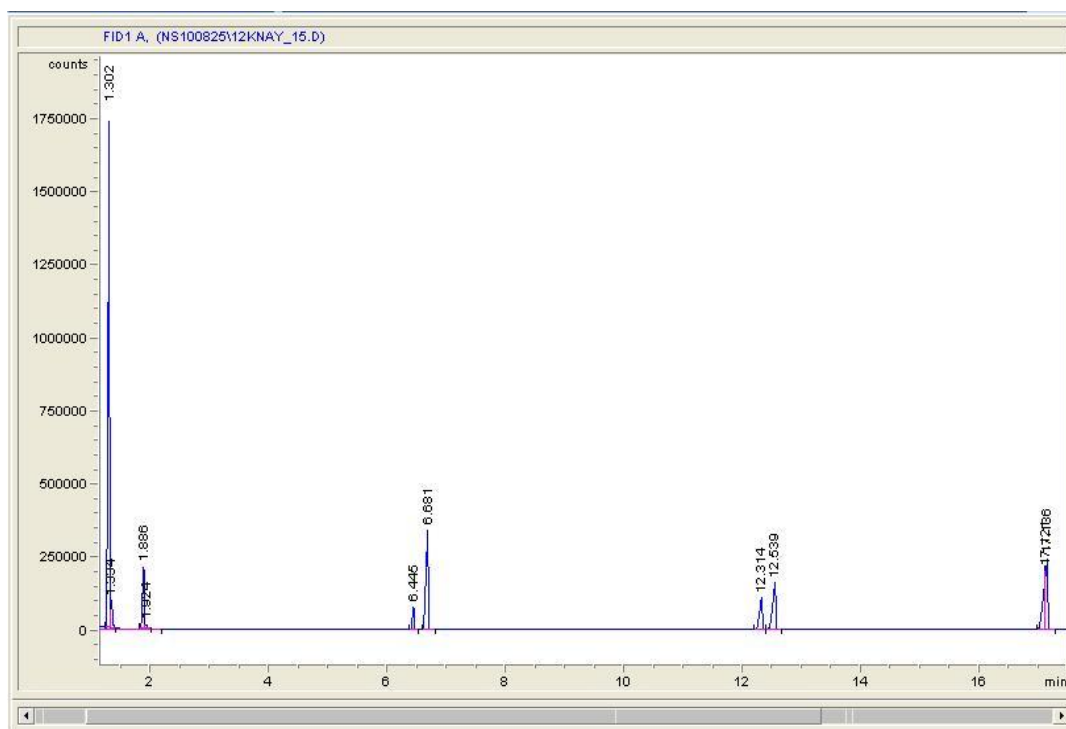


Figure B.2 GC chromatogram of products from transesterification of glycerol trioctanoate with 12K/NaY catalyst.

Table B.5 The retention time of compounds.

Retention time (min)	compound
1.3	Octanic acid methyl ester
1.9	Glycerol (trimethylsilyl)
6.5	Glycerol mono-octanoate (trimethylsilyl)
6.7	Glycerol mono-octanoate (trimethylsilyl)
12.4	Glycerol di-octanoate (trimethylsilyl)
12.6	Glycerol di-octanoate (trimethylsilyl)
17.3	Glycerol tri-octanoate

APPENDIX C
CATALYTIC ACTIVITY IN CONVERSION OF
2-METHYL-3-BUTYN-2-OL

มหาวิทยาลัยเทคโนโลยีสุรนารี

Table C.1 Summary of the results from the transformation of 2-methyl-3-butyn-2-ol over NaY at 120 °C.

Time (min)	MBOH	MBYNE		Prenal		HMB		MIPK		Acetone		Acetylene	
	Conversion	yield	Selectivity	yield	Selectivity	yield	Selectivity	yield	Selectivity	yield	Selectivity	yield	Selectivity
0	3.15	0.67	21.16	0.00	0.00	0.02	0.72	0.01	0.39	1.36	43.20	1.09	34.53
16	3.35	0.59	17.50	0.00	0.00	0.02	0.61	0.00	0.00	1.43	42.75	1.31	39.14
32	3.26	0.53	16.24	0.00	0.00	0.02	0.71	0.00	0.00	1.42	43.66	1.29	39.39
49	2.66	0.44	16.46	0.00	0.00	0.06	2.27	0.00	0.00	1.17	44.03	0.99	37.24
65	2.98	0.46	15.58	0.00	0.00	0.03	1.00	0.00	0.00	1.31	43.90	1.18	39.52
82	3.09	0.45	14.42	0.00	0.00	0.06	1.85	0.00	0.00	1.39	44.78	1.20	38.95
98	2.64	0.40	15.20	0.00	0.00	0.03	1.28	0.00	0.00	1.18	44.64	1.03	38.88
115	2.55	0.38	15.02	0.00	0.00	0.04	1.63	0.00	0.00	1.15	45.04	0.98	38.30
132	2.79	0.41	14.58	0.00	0.00	0.04	1.36	0.00	0.00	1.25	44.64	1.10	39.42

Amount of catalyst was 0.02 g.

Table C.2 Summary of the results from the transformation of 2-methyl-3-butyn-2-ol over 4K/NaY catalyst at 120 °C.

Time (min)	MBOH	MBYNE		Prenal		HMB		MIPK		Acetone		Acetylene	
	Conversion	yield	Selectivity	yield	Selectivity	yield	Selectivity	yield	Selectivity	yield	Selectivity	yield	Selectivity
0	55.82	0.36	0.65	0.02	0.03	0.02	0.04	0.00	0.00	26.78	47.98	28.64	51.31
16	56.54	0.31	0.54	0.02	0.03	0.02	0.04	0.01	0.02	28.19	49.86	27.99	49.51
33	58.63	0.31	0.53	0.02	0.03	0.02	0.04	0.00	0.00	27.82	47.45	30.46	51.95
50	56.92	0.30	0.52	0.02	0.03	0.03	0.04	0.02	0.04	26.83	47.15	29.72	52.21
67	41.43	0.86	2.08	0.04	0.11	0.02	0.04	0.02	0.04	18.49	44.64	21.99	53.08
84	53.01	0.51	0.96	0.03	0.05	0.02	0.03	0.03	0.06	24.99	47.15	27.44	51.75
101	53.78	0.46	0.85	0.03	0.06	0.06	0.10	0.04	0.07	27.02	50.24	26.17	48.67
118	55.10	0.41	0.75	0.02	0.03	0.02	0.04	0.01	0.02	26.03	47.24	28.61	51.92
135	58.91	0.34	0.59	0.02	0.03	0.02	0.04	0.00	0.00	27.41	46.52	31.12	52.83

Amount of catalyst was 0.02 g.

Table C.3 Summary of the results from the transformation of 2-methyl-3-butyn-2-ol over 8K/NaY catalyst at 120 °C.

Time (min)	MBOH	MBYNE		Prenal		HMB		MIPK		Acetone		Acetylene	
	Conversion	yield	Selectivity	yield	Selectivity	yield	Selectivity	yield	Selectivity	yield	Selectivity	yield	Selectivity
0	57.87	0.43	0.75	0.00	0.00	0.04	0.08	0.00	0.00	26.43	45.68	30.96	53.49
17	76.84	0.23	0.30	0.00	0.00	0.01	0.01	0.00	0.00	34.32	44.67	42.27	55.02
33	78.19	0.18	0.23	0.00	0.00	0.01	0.02	0.00	0.00	35.98	46.02	42.01	53.73
50	81.82	0.17	0.20	0.00	0.00	0.02	0.02	0.00	0.00	38.26	46.76	43.38	53.02
67	83.49	0.17	0.20	0.00	0.00	0.02	0.02	0.00	0.00	37.44	44.85	45.85	54.93
83	81.15	0.15	0.19	0.00	0.00	0.02	0.02	0.00	0.00	37.44	46.14	43.54	53.65
100	83.96	0.14	0.16	0.00	0.00	0.02	0.02	0.00	0.00	39.49	47.03	44.32	52.78
116	84.35	0.16	0.19	0.00	0.00	0.03	0.04	0.00	0.00	37.90	44.94	46.26	54.84
133	82.21	0.14	0.17	0.00	0.00	0.02	0.03	0.00	0.00	37.83	46.01	44.22	53.79

Amount of catalyst was 0.02 g.

Table C.4 Summary of the results from the transformation of 2-methyl-3-butyn-2-ol over 12K/NaY catalyst at 120 °C.

Time (min)	MBOH	MBYNE		Prenal		HMB		MIPK		Acetone		Acetylene	
	Conversion	yield	Selectivity	yield	Selectivity	yield	Selectivity	yield	Selectivity	yield	Selectivity	yield	Selectivity
0	78.29	0.20	0.26	0.01	0.01	0.02	0.02	0.01	0.01	38.25	48.86	39.80	50.84
16	84.16	0.18	0.22	0.01	0.01	0.02	0.02	0.01	0.01	38.77	46.07	45.17	53.67
32	82.42	0.15	0.18	0.01	0.01	0.02	0.03	0.00	0.00	36.24	43.97	46.01	55.82
49	83.47	0.14	0.17	0.00	0.01	0.02	0.03	0.01	0.01	37.02	44.35	46.28	55.44
66	82.45	0.16	0.19	0.01	0.01	0.02	0.03	0.01	0.01	38.66	46.88	43.60	52.88
82	86.04	0.13	0.16	0.00	0.01	0.02	0.03	0.01	0.01	39.64	46.07	46.23	53.73
99	69.98	0.31	0.44	0.02	0.02	0.01	0.02	0.01	0.01	32.19	46.01	37.44	53.50
116	80.56	0.25	0.31	0.01	0.01	0.01	0.01	0.01	0.01	36.04	44.74	44.24	54.92
133	80.82	0.18	0.23	0.01	0.01	0.01	0.02	0.01	0.01	35.82	44.32	44.79	55.41

Amount of catalyst was 0.02 g.

Table C.5 Summary of the results from the transformation of 2-methyl-3-butyn-2-ol over 8K/NaY catalyst at 120 °C.

Time (min)	MBOH	MBYNE		Prenal		HMB		MIPK		Acetone		Acetylene	
	Conversion	yield	Selectivity	yield	Selectivity	yield	Selectivity	yield	Selectivity	yield	Selectivity	yield	Selectivity
0	32.84	1.59	4.84	0.00	0.00	0.03	0.08	0.03	0.10	14.79	45.03	16.41	49.96
17	44.47	0.86	1.93	0.00	0.00	0.05	0.12	0.05	0.10	20.41	45.91	23.10	51.94
33	43.63	0.68	1.55	0.00	0.00	0.03	0.06	0.01	0.02	20.39	46.75	22.52	51.62
50	47.91	0.56	1.17	0.00	0.00	0.03	0.05	0.03	0.06	22.73	47.44	24.56	51.28
66	48.09	0.50	1.03	0.00	0.00	0.03	0.06	0.00	0.00	21.85	45.43	25.72	53.47
83	47.52	0.46	0.96	0.00	0.00	0.03	0.06	0.00	0.00	22.80	47.97	24.24	51.00
99	49.97	0.42	0.83	0.00	0.00	0.03	0.06	0.00	0.00	22.85	45.74	26.66	53.37
116	45.66	0.39	0.85	0.00	0.00	0.03	0.07	0.02	0.04	21.82	47.79	23.40	51.25
132	48.65	0.33	0.68	0.00	0.00	0.07	0.14	0.05	0.10	23.10	47.48	25.10	51.60

Amount of the catalyst was 0.01 g.

Table C.6 Summary of the results from the transformation of 2-methyl-3-butyn-2-ol over 12K/NaY catalyst at 120 °C.

Time (min)	MBOH	MBYNE		Prenal		HMB		MIPK		Acetone		Acetylene	
	Conversion	yield	Selectivity	yield	Selectivity	yield	Selectivity	yield	Selectivity	yield	Selectivity	yield	Selectivity
0	41.84	0.15	0.35	0.00	0.00	0.02	0.05	0.00	0.00	20.15	48.16	21.52	51.45
17	51.99	0.12	0.24	0.00	0.00	0.02	0.04	0.00	0.00	25.02	48.13	26.82	51.95
33	56.24	0.11	0.2	0.00	0.00	0.03	0.05	0.00	0.00	26.56	47.22	29.54	52.53
49	57.09	0.09	0.16	0.00	0.00	0.03	0.05	0.00	0.00	26.75	46.86	30.22	52.93
66	55.27	0.08	0.15	0.00	0.00	0.03	0.06	0.00	0.00	25.89	46.84	29.27	52.95
82	54.40	0.08	0.14	0.00	0.00	0.03	0.06	0.00	0.00	26.26	48.28	28.02	51.51
99	56.72	0.07	0.12	0.00	0.00	0.03	0.06	0.00	0.00	27.44	48.38	29.18	51.44
115	56.02	0.07	0.13	0.00	0.00	0.03	0.06	0.00	0.00	26.81	47.86	29.10	51.95
132	58.06	0.07	0.13	0.00	0.00	0.03	0.06	0.03	0.05	27.42	47.22	30.51	52.54

Amount of the catalyst was 0.01 g.

Table C.7 Summary of the results from the transformation of 2-methyl-3-butyn-2-ol over 12K/NaY-1 catalyst at 120 °C.

Time (min)	MBOH	MBYNE		Prenal		HMB		MIPK		Acetone		Acetylene	
	Conversion	yield	Selectivity	yield	Selectivity	yield	Selectivity	yield	Selectivity	yield	Selectivity	yield	Selectivity
0	9.19	1.02	11.06	0.00	0.00	0.04	0.41	0.01	0.15	3.85	41.84	4.28	46.54
16	7.65	0.83	10.82	0.00	0.00	0.05	0.67	0.01	0.17	3.26	42.64	3.50	45.69
33	6.98	0.71	10.13	0.00	0.00	0.07	1.06	0.01	0.13	3.00	42.96	3.19	45.71
49	6.67	0.65	9.68	0.00	0.00	0.06	0.97	0.00	0.00	2.87	43.04	3.09	46.31
66	5.80	0.58	9.98	0.00	0.00	0.05	0.83	0.00	0.00	2.54	43.78	2.63	45.41
82	5.53	0.53	9.50	0.00	0.00	0.05	0.97	0.00	0.00	2.45	44.38	2.50	45.15
98	5.47	0.51	9.37	0.00	0.00	0.07	1.34	0.00	0.00	2.40	43.85	2.49	45.43
114	5.12	0.50	9.80	0.00	0.00	0.07	1.28	0.00	0.00	2.25	43.94	2.30	44.98
130	13.14	1.58	12.06	0.00	0.00	0.03	0.26	0.03	0.19	5.47	41.59	6.03	45.90

Amount of the catalyst was 0.02 g.

Table C.8 Conversion of 2-methyl-3-butyn-2-ol over 12K/NaY-2 catalyst at 120 °C.

Time (min)	MBOH Conversion
0	1.42
16	1.40
33	1.39
49	1.45
66	1.31
82	1.41
98	1.43
114	1.07
130	1.29

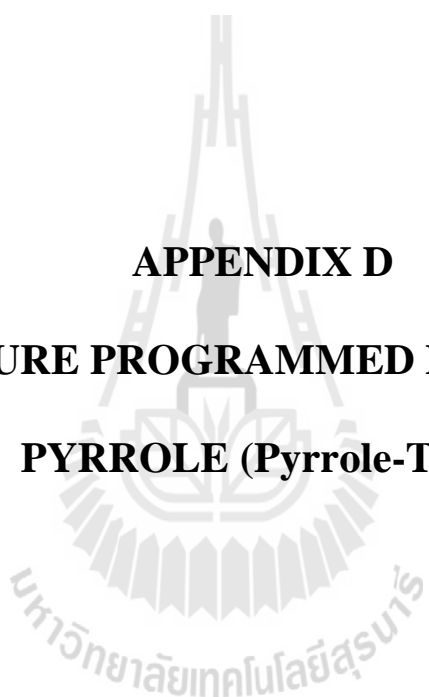
Amount of the catalyst was 0.02 g.

Table C.9 Conversion of 2-methyl-3-butyn-2-ol over MCM-41, xK/MCM-41 with 4, 8 and 12 wt% K loading and 12K/RH-SiO₂ at 120 °C.

Time (min)	MBOH Conversion				
	MCM-41	4K/MCM-41	8K/MCM-41	12K/MCM-41	12K/RH-SiO ₂
0	0.76	0.95	0.67	0.77	0.64
16	0.77	0.88	0.72	0.81	0.67
32	0.76	0.89	0.68	0.75	0.70
49	0.80	0.80	0.68	0.79	0.67
65	0.80	0.86	0.66	0.67	0.65
82	0.83	0.81	0.64	0.78	0.67
98	0.81	0.77	0.68	0.95	0.77
115	0.79	0.82	0.68	0.83	0.70
132	0.80	0.85	0.72	0.81	0.72

Amount of the catalyst was 0.02 g.

APPENDIX D
TEMPERATURE PROGRAMMED DESORPTION OF
PYRROLE (Pyrrole-TPD)



TEMPERATURE PROGRAMMED DESORPTION OF PYRROLE (Pyrrole-TPD)

Procedure for preparation of calibration curve for pyrrole

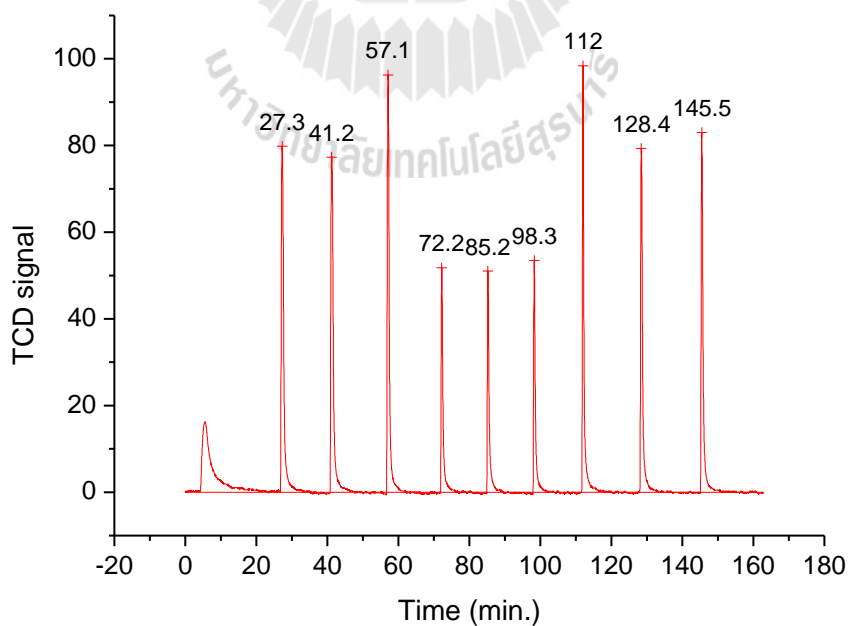
The apparatus for the study with pyrrole-TPD is shown in Figure D.1. The glass wool was placed in the U-shape sample. After that, desorption of temperature was set at 110 °C. A 0.5, 0.8 or 1.0 μL of pyrrole was injected into the U-shape sample tube and thermal conductivity detector (TCD) was used to detect the amount of the desorbed pyrrole.



Figure D.1 The apparatus for the study of TPD-pyrrole.

Table D.1 Peak area of pyrrole.

Volume of pyrrole (μL)	Peak area	Average of peak area
0.5	31.478	31.197
0.5	30.972	
0.5	31.142	
0.8	50.136	52.039
0.8	52.636	
0.8	53.347	
1.0	65.707	64.708
1.0	65.460	
1.0	62.958	

**Figure D.2** Chromatogram of pyrrole peak with different injected volumes.

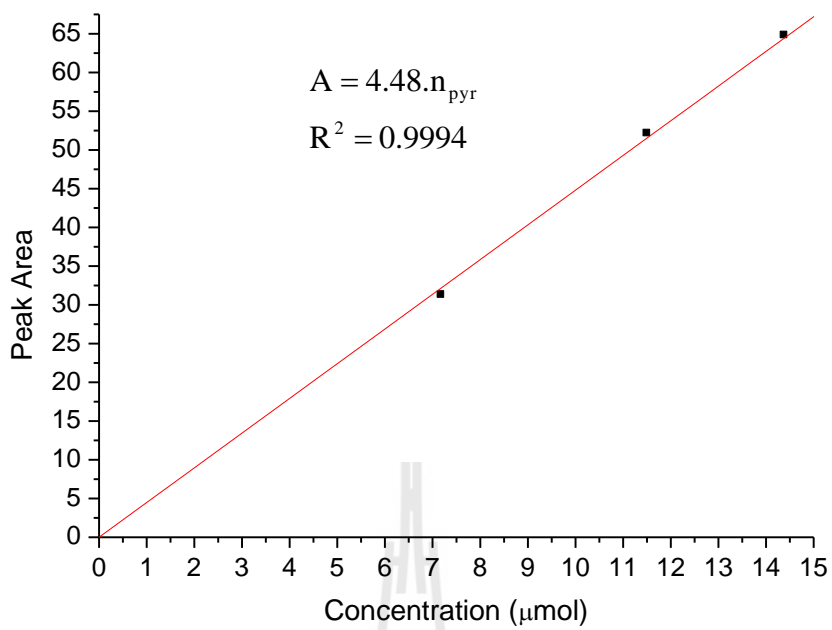
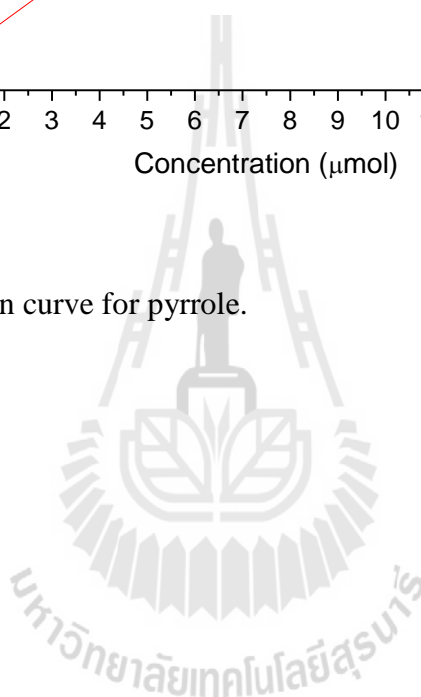


Figure D.3 Calibration curve for pyrrole.



CURRICULUM VITAE

NUTTINEE SUPAMATHANON

Born: 26 March, 1975 in Nakhon Ratchasima, Thailand

Education:

- 1994-1998 B. Sc. (Analytical Chemistry)
Rajamangala Institute of Technology, Pathum Thani, Thailand
- 2001-2005 M. Sc. (Chemistry) Suranaree University of Technology, Thailand

Experience:

- 1998-2001 Chemist, QA. Section
JVC Components (Thailand) Co, Ltd, Nakhon Ratchasima, Thailand
- 2005-2007 Lecturer, Nakhon Ratchasima Rajabhat University
- June-August 2010 Research at Industrial Chemistry, Institute of Pure and Applied Chemistry, Carl von Ossietzky University of Oldenburg, Oldenburg, Germany

Publications:

Supamathanon, N., Wittayakun, J., Prayoonpokarach, S. (2011). Properties of Jatropha seed oil from Northeastern Thailand and its transesterification catalyzed by potassium supported on NaY zeolite. **Journal of Industrial and Engineering Chemistry**, 17: 182-185.